ARPA No. 6207
Contract No. C-104-65

52

WORLDWIDE COLLECTION AND EVALUATION OF EARTHQUAKE DATA

Terminal Report

31 August 1967

140

ARPA No. 6207
Contract C-104-65

WORLDWIDE COLLECTION AND EVALUATION OF EARTHQUAKE DATA

Terminal Report

Project Manager
Ray L. Fisher

Telephone

Dallas, Texas
1-214-238-4284

31 August 1967

Prepared for

UNITED STATES DEPARTMENT OF COMMERCE
ENVIRONMENTAL SCIENCE SERVICES ADMINISTRATION
COAST AND GEODETIC SURVEY
Washington Science Center
Rockville, Maryland, 20852

Work Sponsored by
ADVANCED RESEARCH PROJECTS AGENCY
Project VELA UNIFORM

Contractor
TEXAS INSTRUMENTS INCORPORATED

This research was supported through the

UNITED STATES DEPARTMENT OF COMMERCE
ENVIRONMENTAL SCIENCE SERVICES ADMINISTRATION
COAST AND GEODETIC SURVEY

Under Contract C-104-65(Neg)

And was sponsored by the

ADVANCED RESEARCH PROJECTS AGENCY
Department of Defense

ARPA No. 6207

TABLE OF CONTENTS

LIST OF APPENDIXES

LIST OF ILLUSTRATIONS

LIST OF TABLES

BLANK PAGE

SECTION I

INTRODUCTION AND SUMMARY

This report presents and discusses work performed and results obtained under Contract C-104-65 from 28 April through 15 October 1966. During that period, the hypocenter and magnitude programs were tested and then used to process January 1964 data at the computer facilities of the Environmental Science Services Administration (ESSA), Suitland, Maryland, using the CDC 6600 computer. Results of this processing are shown in Appendix A.

Other results obtained in the reporting period are given in Section II and in the appendixes. Results presented in Section II can be summarized as follows:

- The relationship between m_b and M_s, restrained to a slope of 0.63, is given by $m_b = 0.63\ M_s + 1.77$ as compared to Richter's (1958) $m_b = 0.63\ M_s + 2.5$
- Magnitudes comparable to m_b but based on long-period P amplitudes average approximately 0.7 units higher than m_b
- Vertical-component surface-wave magnitudes average about 0.5 units higher than M_s
- The ratio of maximum P to P_n amplitudes is a function of distance, with maxima generally falling in the range of 300 to 750 km, although considerable variation is evident from station to station. These observed differences lead to the conclusion that m_b is currently unreliable when based on data recorded less than 1000 km from the source

- Nonlinear or "exact" confidence regions may be computed from use of the last equations in Section II, subsection B

- Chengmai, Thailand, is the most capable single-element station studied, having a theoretical capability to record all events of $m_b \geq 4.5$ to more than 100°. Another 14 stations indicate capabilities to record events from $m_b = 4.5$ to 5.0 at similar distances: five of these are Arctic or Antarctic stations; three are located in the Western United States; three are on the Indian subcontinent; two are in Africa; and the other is in Shiraz, Iran

- Analysis of magnitude residuals indicates that patterns of residuals do exist; these patterns might be used to infer source mechanisms and, possibly, as a further criterion for discriminating between earthquakes and explosions

Results included in the appendixes can be summarized as follows:

- Approximately half of the 344 January 1964 revised hypocenters are changed appreciably from the USC&GS preliminary locations

- Depth determination remains a considerable problem and requires continued investigation

- The number of earthquakes occurring in the vicinity of Istanbul, Turkey, increases much more slowly with decreasing magnitude than the number near Shiraz, Iran; Quetta, Pakistan; or Shillong, India. However, more larger earthquakes occurred near Istanbul than near the other stations in the time period studied

- Nearly 3-1/2 times as many pP phases are identified after application of array processing than can be identified from the single-channel presentation, based on the sample investigated

- Application of digital filters provides better signal enhancement than does analog filtering

- Studies of energy attenuation based on automated calculation of energy from digital data indicate considerable error in the Q curves used in magnitude calculation

- Empirical fits to observed energy attenuation as a function of distance lead to a relationship of the form

$$E = K_1 r^{-2} \cos(e_o) e^{-2K_2 r}$$

where K_1 and K_2 are constants, r is epicentral distance, and e_o is angle of incidence

- Assuming that the shape of power spectra is independent of distance, as shown by LeBlanc and Howell (1965), a set of crustal filters is developed to describe in the frequency domain the effect of crustal structure beneath several stations

These results, combined with those previously published, lead to the following conclusions:

- A hypocenter program capable of high accuracy should include the means of correcting travel-time tables on the basis of both station and source region
- High-quality well-distributed stations yield better results than do large numbers of average stations concentrated in one or two quadrants
- Generally, magnitudes computed at distances of less than 1000 km are inaccurate and should not be used as estimates of event size or be combined with teleseismic data to obtain average values
- Short-period P-wave magnitudes now in use can be considered accurate to only about $\pm$ 0.5 units; attempts to compare m_b with other magnitudes must consider this scatter
- Variations in seismic activity represent more than simple differences in level; the ratio of the numbers of large and small earthquakes also varies considerably from place to place

Considering the results and conclusions, the following recommendations are made:

- More studies of crustal structure are needed in areas of prevalent seismic activity as well as near seismograph stations; such studies will benefit both hypocenter and magnitude determinations

- There should be more use of tape recording — preferably direct digital recording
- The "world-array" processing concept should be applied to more data and to an even broader range of problems than those discussed in this report
- Automated techniques for "energy" or magnitude determination should be considered as alternates to current methods
- The method for obtaining first approximations of hypocenter coordinates developed under this contract should be investigated more fully
- The method for assessing epicenter accuracy (described in Special Report No. 5) should be developed and applied more fully
- The USC&GS should provide continuing year-to-year assessments of seismic activity on regional and worldwide bases
- The USC&GS should develop as complete a file of seismic data as possible in a format adopted as "standard" on at least a national, and preferably on an international, basis

These recommendations, if followed, would provide considerable steps toward solving several problems in earthquake seismology.

BLANK PAGE

SECTION II

PRESENTATION OF RESULTS

A. MAGNITUDE STUDIES

1. Magnitude Calculation

a. Definitions

Various methods for computing seismic event magnitudes have been developed over the years, beginning with Richter's (1935) local magnitude scale (M_L). Gutenberg (1945, a, b, c) extended magnitude determination to 20-sec-period surface waves and the body phases P, PP, and S. Båth (1952) extended magnitude computation to vertical-component surface waves and broadened the period range over which surface-wave calculations could be made. Gutenberg and Richter later (1956) revised bodywave magnitude calculation and the relationship between surface-wave magnitudes (M_s) and what Gutenberg termed "unified magnitude" (m).

The USC&GS (1963) adopted a form of Gutenberg's unified magnitude (m_b) and began reporting values of this magnitude in its Preliminary Determination of Epicenter cards in April 1963. This latter magnitude (m_b) is calculated by

$$m_b = \log \frac{A}{T} + Q \qquad (1)$$

where

A = maximum amplitude of P_n or P in the first few cycles, measured in microns, as recorded by short-period vertical-component seismographs

T = dominant period of the measured P wave

Q = depth-distance factor as given by Gutenberg and Richter (1956) for the distance range 5° to 110° and extrapolated to 2° for surface-focus events, assuming an inverse cube attenuation of signal

Texas Instruments Incorporated has used all of the preceding methods of magnitude calculation. Taking into account previously observed variations in similar magnitudes computed from data recorded by long-period and short-period instruments, the following 10 magnitudes were computed, here possible, from 1964 data:

$M_1 = m_b$

M_2 = short-period vertical-component P-wave magnitude differing from m_b only at short distances ($\Delta \leq 10°$) where the amplitude used is the maximum P amplitude (not necessarily P_n)

M_3 = long-period vertical-component P-phase magnitude

M_4 = short-period vertical-component PP-phase magnitude

M_5 = long-period vertical-component PP-phase magnitude

M_6 = short-period horizontal-component S-phase magnitude

M_7 = long-period horizontal-component S-phase magnitude

$M_8 = M_L$

M_9 = vertical-component surface-wave magnitude

$M_{10} = M_s$

b. Method

The first seven magnitudes are computed from bodywave data computed from equations similar to (1):

$$M_i = \log \frac{A_i}{T_i} + Q_1 \qquad i = 1\text{-}7 \qquad (2)$$

where

$\frac{A_i}{T_i}$ = vertical-component amplitude (peak-trough/2) of P or PP phase, corrected for instrument response, divided by the dominant period (μ/sec) for i = 1 to 5; for i = 6 and 7, the vector amplitude of SH is used

Q_i = depth-distance factor; for i = 1 to 3, PZ values are used; for i = 4 and 5, PPZ values are used; for i = 6 and Z, SH values are used; all values are as given by Gutenberg and Richter (1956)

The eighth magnitude is an adaptation of Richter's (1935) local magnitude scale M_L. It is computed by

$$M_8 = \log\left(A \cdot \frac{V_{wa}}{V_t}\right) - \log A_o \qquad (3)$$

where

A = maximum short-period horizontal trace motion

V_{wa} = response of standard Wood-Anderson seismograph at period T

V_t = response of short-period seismograph recording the data at period T

$-\log A_c$ = Richter's (1935) distance factor extrapolated from 600 km to 10°

Separate magnitudes are computed for each horizontal component and the mean taken.

The ninth and tenth magnitudes are computed from surface-wave data in the period range of 17 sec ≤ T ≤ 23 sec, using the following equations, adapted from Båth (1952) and Gutenberg (1945a):

$$M_9 = a\left[\log A + \frac{1}{2}\log\frac{20}{T} + 24.13\,\Delta\,(K_T - K_{20}) + b - \log B\right] + C \qquad (4)$$

and

$$M_{10} = \log A + \frac{1}{2}\log\frac{20}{T} + 24.13\,\Delta^\circ\,(K_T - K_{20}) - \log B$$

where

A = maximum amplitude of surface waves (vector sum of both horizontal-component amplitudes for M_{10}) in μ

T = period of surface waves measured (17 sec ≤ T ≤ 23 sec) - log B = distance factor

Δ = epicenter-to-station distance in degrees

$(K_T - K_{20})$ = difference in extinction coefficients of surface waves of T-sec and 20-sec periods

h = depth of focus in km

a = 0.8 for h ≤ 40 km, 0.5 for 40 km < h ≤ 300 km

b = 0.0082 h for h ≤ 100 km, 0.85 for 100 km < h ≤ 300 km

c = 1.42 for h ≤ 40 km, 3.55 for 40 km < h ≤ 300 km

Values of M_{10} are calculated only for events occurring at depths ≤ 35 km and M_9 for events occurring at depths ≤ 300 km.

A computer program described in Semiannual Technical Report No. III (Texas Instruments, 1966) was written to compute earthquake magnitudes. This program computes each of the 10 magnitudes for each station recording a particular event (where data permit). The mean and standard deviation of each magnitude type for each event also is computed where data permit. Values of event mean magnitudes ($m_b = M_1$ and $M_s = M_{10}$) are given in Appendix A with results of hypocenter determinations.

2. Comparison of Magnitude Scales

a. General

In the previously cited technical report by Texas Instruments, various magnitudes were compared. From the standpoint of frequency of calculation, it was determined that short-period P-wave magnitudes were most valuable since, in the study of 1963 seismicity (Texas Instruments, 1964b), more than 2-1/2 times as many short-period P-wave magnitudes were computed than all other types combined. The internal variation was greatest, however, for the short-period P-phase magnitudes than for all others except short-period S-phase magnitudes.

Variations in the short-period P-phase magnitude could be reduced perhaps by revising the depth-distance factors (Q tables). However, it has been observed that the m_b magnitudes do not appear to behave properly for large events; furthermore, data for computing m_b for rather large earthquakes are difficult to obtain since the dynamic range of the seismographs is often exceeded, precluding measurement of period and amplitude. To alleviate this situation and to provide consistent magnitude data for both the smallest and largest events recorded, it is desirable to use an alternate magnitude scale which may be converted to m_b values.

b. m_b and M_s (M_l and M_{10})

In Technical Report No. III (1966), the better 1963 magnitude data were investigated to obtain a relationship between m_b and M_s. Actually, two relationships were found. When m_b was considered independent, the relationship was determined to be

$$M_s = 0.93\, m_b + 0.565 \qquad (5)$$

When M_s was considered independent, the derived relationship was

$$m_b = 0.439\, M_s + 2.825 \qquad (6)$$

Neither relationship was in good agreement with Richter's (1958) relationship:

$$M_s = 1.59\, m_b - 3.96$$

or

$$m_b = 0.63\, M_s + 2.5 \qquad (7)$$

Visual inspection of the data used to determine the m_b - M_s relationship indicated that a line with the same slope as the Richter relationship appeared to fit the data as well as the relationships given by Equations (5) and (6). Consequently, a new relationship was derived, assuming a slope of 1.59. Resulting from this was the relationship

$$M_s = 1.59\, m_b - 2.82$$

or

$$m_b = 0.63\, M_s + 1.77 \qquad (8)$$

Figure II-1 shows the three derived relationships and the data used in their derivation.

c. m_b and Long-Period P-Phase Magnitudes (M_1 and [illegible])

Linear regression of M_3 (long-period P-wave magnitude) on M_1 (m_b), using 1963 data, obtained the relationship

$$M_3 = 0.83\, M_1 + 1.67 \qquad (9)$$

Since the slope was nearly unity, the differences between M_3 and m_b were investigated to determine average differences for each seismograph station and the mean difference for the total data. Table II-1 lists the corrections to be applied to M_3 values for each station to obtain an estimated m_b and the mean correction for all stations. Using this mean value, M_3 may be related to m_b by

$$M_3 = m_b + 0.72 \qquad (10)$$

Figure II-2 shows the relationships given by Equations (9) and (10) and the data used in their derivation.

It is doubtful that significant differences in internal consistency would be noted in converting M_3 values to the m_b scale by any of the three following methods:

- To average M_3 values computed at all stations and to convert to m_b using Equation (8)
- To average all M_3 values for the event and to convert to m_b using Equation (9)
- To apply the corrections listed in Table II-1 to the M_3 values computed from each station's data and then to average

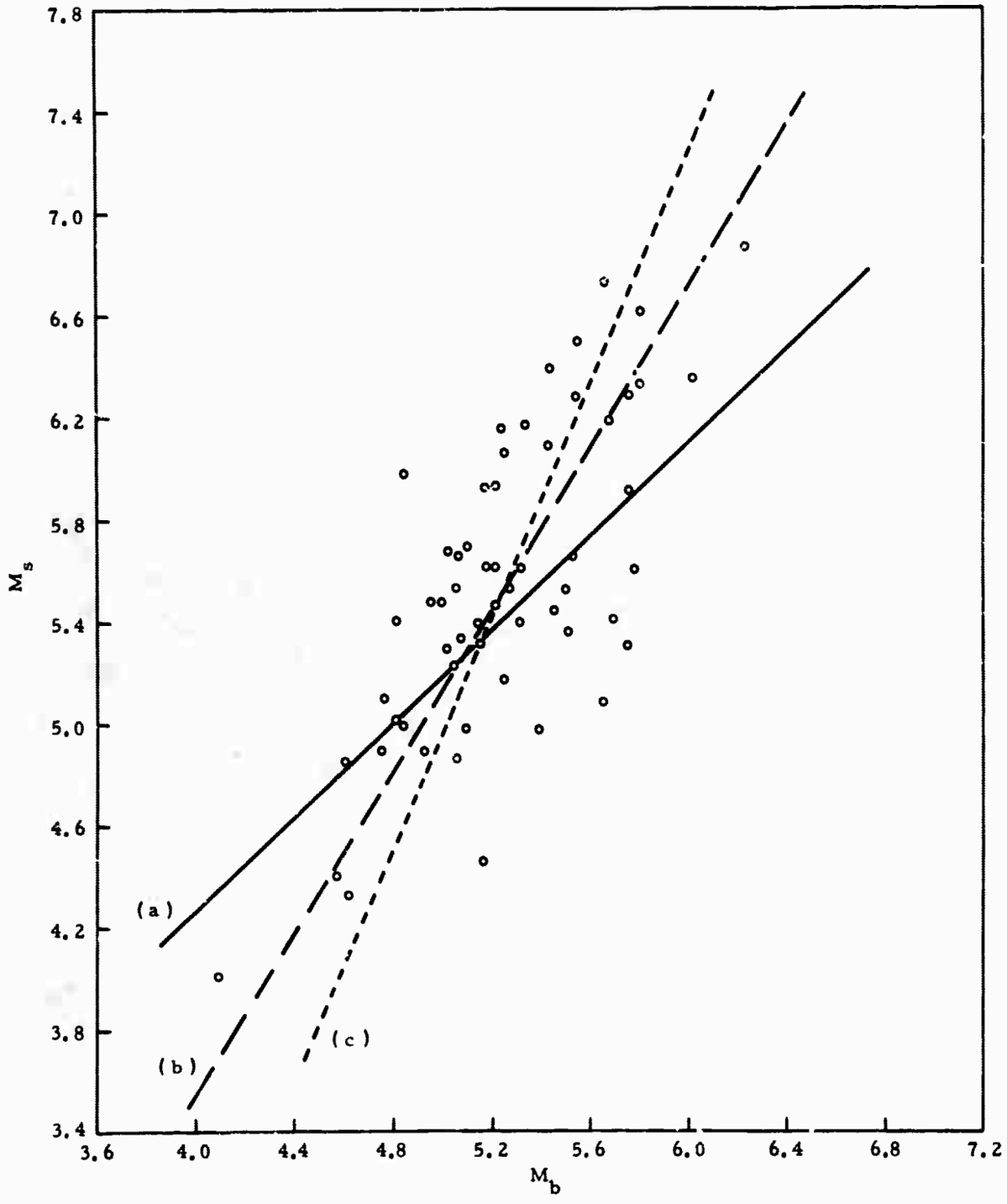

Figure II-1. m_b Vs M_s. Curve a = $M_s = 0.93\ m_b + 0.565$; curve b = $M_s = 1.59\ m_b - 2.82$; curve c = $m_b = 0.439\ M_s + 2.82$

Table II-1

AVERAGE DIFFERENCES BETWEEN LONG-PERIOD P-PHASE MAGNITUDES (M_3) AND $m_b(M_1)$ AND BETWEEN VERTICAL-COMPONENT SURFACE-WAVE MAGNITUDES (M_9) AND M_s (M_{10})

Station	(M_3-M_1)	σ	N	(M_9-M_{10})	σ	N
AAE	0.61	0.20	8	0.62	0.01	2
AAM	0.13	—	1	0.35	0.27	4
ADE	0.68	0.39	13	0.60	0.17	14
AFI	0.97	—	1	0.02	0.12	5
ALE	1.16	0.57	8	0.48	0.20	8
ALQ	1.22	0.48	9	0.61	0.22	21
ANT	1.04	0.49	3	0.70	—	1
ARE	0.98	0.91	9	0.61	0.18	5
ATU	1.01	0.33	11	0.59	0.23	4
BAG	0.58	0.64	22	0.32	0.12	7
BEC	0.35	0.55	4	0.50	0.15	7
BHP	1.29	0.17	5	0.57	0.28	4
BKS	0.65	0.56	23	0.02	0.32	24
BLA	0.49	0.39	4	0.43	0.17	6
BOG	0.33	0.36	10	0.56	0.10	5
BUL	0.72	—	1	0.51	0.17	4
CAR	0.93	0.39	7	0.82	0.04	4
CHG	1.32	0.73	5	—	—	-
CMC	0.64	0.46	5	0.45	0.10	2
COP	0.81	0.38	9	0.35	0.23	10
COR	0.29	0.20	2	0.43	0.46	6
CTA	0.78	0.40	4	0.83	0.14	6
DUG	0.70	0.24	3	0.36	0.56	3
FLO	1.14	0.26	2	0.58	0.28	9
GDH	0.79	0.23	4	0.62	0.41	10
GOL	0.83	0.52	21	0.51	0.27	29
GSC	0.93	0.43	4	—	—	-
GUA	0.61	0.32	11	0.24	0.26	3
HKC	1.01	0.30	3	0.77	—	1
HNR	0.61	0.39	17	0.51	0.15	7
IST	0.61	0.31	12	0.63	0.07	3

Table II-1 (Contd)

Station	(M_3-M_1)	σ	N	(M_9-M_{10})	σ	N
KEV	0.82	0.05	2	0.43	0.18	10
KIP	0.97	0.61	4	0.31	0.13	4
KON	0.76	0.36	6	0.10	0.10	2
LAH	0.63	—	1	—	—	–
LON	0.38	0.44	3	0.53	—	1
LPB	1.17	0.55	5	0.38	0.18	4
LPS	0.35	—	1	—	—	–
LUB	0.99	—	1	0.66	0.14	3
MAL	0.39	—	1	0.46	0.27	7
MAN	0.18	—	1	—	—	–
MBC	1.10	0.70	11	0.27	0.21	13
MDS	0.31	—	1	0.37	—	1
MNN	0.86	—	1	0.56	0.12	3
MUN	0.66	0.36	12	0.47	0.22	10
NDI	0.87	0.43	3	—	—	–
NNA	0.78	0.58	4	—	—	–
NUR	0.73	0.62	15	0.65	0.27	17
PMG	0.72	0.66	30	0.53	0.19	16
PRE	0.49	0.39	5	0.63	0.22	14
PTO	0.45	—	1	—	—	–
QUE	1.09	0.62	8	0.46	0.21	18
RAB	0.80	0.61	16	0.36	0.04	3
RES	1.02	0.30	8	0.34	0.15	6
RIV	0.81	0.33	3	0.51	0.22	13
SCP	1.06	0.52	8	0.44	0.08	4
SHI	0.78	0.75	15	0.39	0.09	6
SHL	0.87	0.63	14	0.57	0.19	7
STU	0.82	0.42	18	0.41	0.16	7
TAU	1.17	—	1	0.78	0.25	4
TOL	0.68	0.55	11	0.58	0.26	16
TRN	0.94	0.19	4	0.20	0.09	3
VAL	0.25	0.31	5	0.43	0.40	2
WES	0.38	0.22	4	0.60	0.32	16
WIN	0.76	0.12	3	0.50	—	1
Average	0.72	0.57		0.48	0.29	

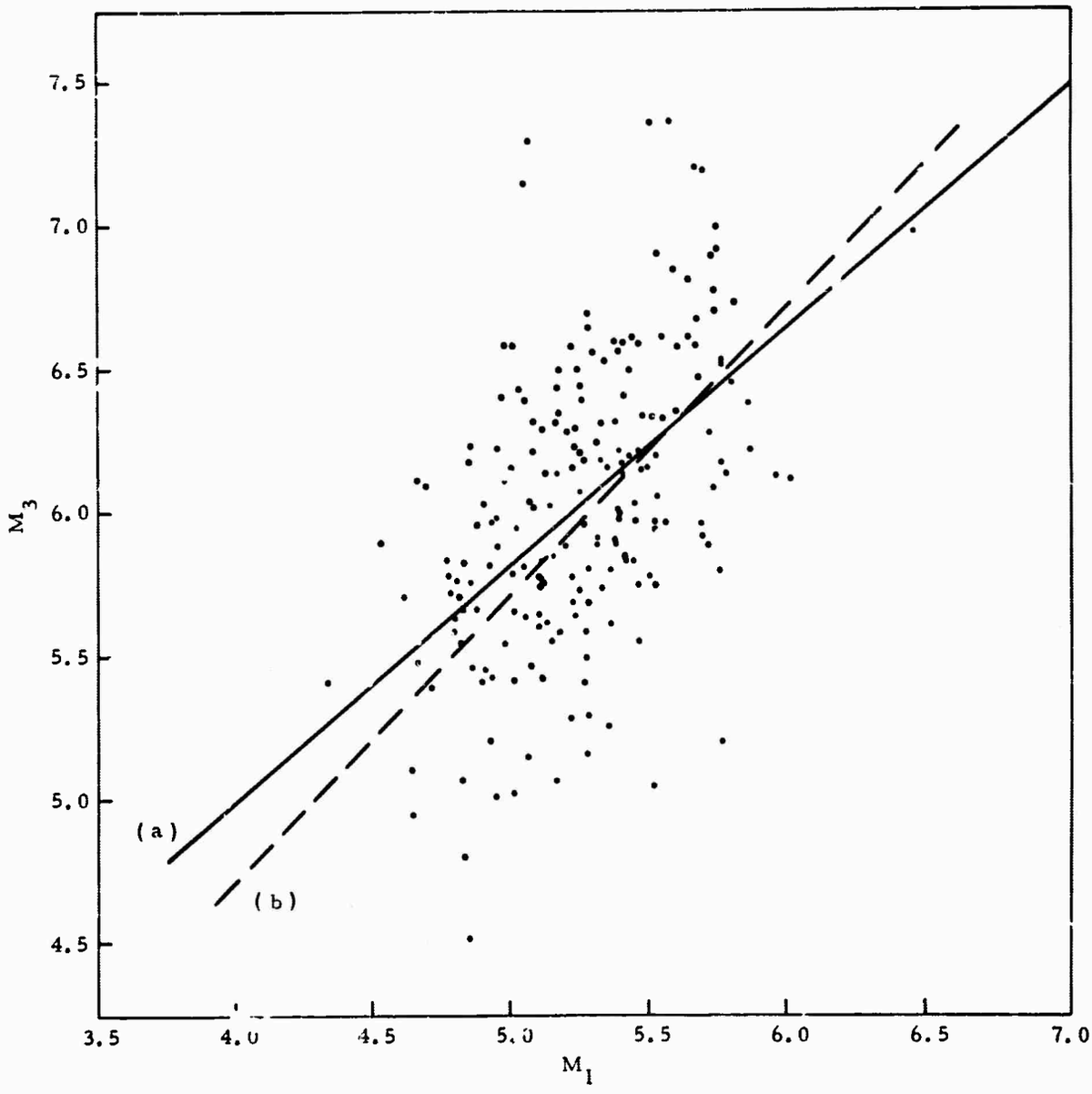

Figure II-2. Long-Period P-Wave Magnitudes M_3 Vs m_b (M_1). Curve a = $M_3 = 0.83\ m_b + 1.67$; curve b = $M_3 = m_b + 0.72$

As shown in Table II-2, however, there appears to be some correlation between geographical location and the difference between M_3 and m_b. Thus, the third approach may be the best method for approximating m_b from long-period P-wave magnitudes.

3. Horizontal- and Vertical-Component Surface-Wave Magnitudes (M_{10} and M_9)

Vertical-component surface-wave magnitudes generally are higher than horizontal-component surface-wave magnitudes. This may result from deletion of Båth's (1952) path correction in Equation (4). The correction was assumed to be 0, since no prior information was available for the stations used.

In Texas Instruments Technical Report No. III, the results of a linear regression of M_9 on M_{10} were reported as

$$M_9 = 0.764\, M_{10} + 1.728$$

However, the M_9 scale was originally defined in such a way to make it equal to the M_s scale. Therefore, the differences between M_9 and M_s calculations have been tabulated, and mean corrections of M_9 to obtain M_s values have been determined. The results are shown in Table II-1.

The mean difference of all M_9 and M_s values also has been determined. However, a comparison of the standard deviations for the data of individual stations and for the total mean correction indicates that the individual corrections are probably preferable. Also, Figure II-3 indicates considerable geographical dependence for the station corrections.

Figure II-3. Geographical Distribution of Vertical-Component Surface-Wave Magnitude Deviation from M_S Values

4. Comparison of P_n and Maximum P Amplitudes, $\Delta < 9°$

As discussed earlier, the m_b scale is a somewhat specialized form of Gutenberg and Richter's (1956) unified magnitude scale. However, the definition of the USC&GS m_b differs in one respect from the Gutenberg and Richter P-phase magnitude: P_n amplitudes rather than maximum P amplitudes are used.

At distances of less than about 1000 km or 9°, considerable variation in magnitudes computed by the two methods has been observed. Since the two magnitudes differ only in the amplitude used, comparison results in an analysis of P_n and maximum P-amplitude variations.

Using data accumulated in the 1963 study (Texas Instruments, 1964b), variations between M_1 and M_2 values for the following stations have been analyzed:

- Istanbul, Turkey (IST)
- Shiraz, Iran (SHI)
- Quetta, West Pakistan (QUE)
- Shillong, India (SHL)
- Chengmai, Thailand (CHG)
- Port Moresby, New Guinea (PMG)
- Nana, Peru (NNA)
- Arequipa, Peru (ARE)
- Antofagasta, Chile (ANT)

Both M_1 and M_2 magnitudes were computed a total of 1566 times at all stations. About 50 percent of the time, the analysts measured the same amplitude and period for both magnitude calculations. At least two interpretations of this fact may be made:

- About half the time, P_n is the maximum P phase at distances ≤ 1000 km
- Often, the P_n phase is not measurable

The experience of Texas Instruments in analyzing earthquake and explosion data over the past 6 years indicates that, at most distances for most stations, P_n is not the maximum P amplitude. Thus, the second interpretation is preferred.

Of the 62 events within 1000 km of Istanbul which were analyzed, three had epicenters located by the USC&GS; for the remainder, only the epicentral distance determined from the S-P interval was known. M_1 and M_2 magnitudes were equal for 30 of the 62 events (48 percent). Figure II-4 shows the differences in magnitudes for the other 32 events. At distances of approximately 1° to 2°, maximum P amplitudes averaged about three times the P_n amplitudes. From approximately 2° to 3°, maximum P amplitudes were about twice as large as P_n (on the average). Little data are available beyond 3° distance, but there are indications that the ratio of maximum P-to-P_n amplitudes increased to approximately 5 around a distance of 5°. At greater distances, the ratio approaches unity.

At Shiraz, Iran, only 25 of the 99 analyzed events had $M_1 = M_2$. The majority of the other 74 events were at 1° to 2° from the station, and considerable scatter was noted from these data. However, an average ratio of approximately 3 to 4 is indicated for the distance range of 1° to 2°. The ratio appears to increase to approximately 10 near 4° and slowly decrease to near 0 at 9° (1000 km), as shown in Figure II-5.

The two magnitudes were equal for approximately one-third of the analyzed events near Quetta. The computed ratios for the remainder of these events exhibited a distinctly different pattern from the previous two, as shown in Figure II-6. In this case, maximum P amplitudes average about three times the P_n amplitudes from approximately 1° to 3°. The ratio decreases to about 2 at a distance of 4° and approaches 0 at approximately 5°. At about 6.5°, however, the average ratio sharply jumps to a value of approximately 9 and decreases to about 2 again near 7.5°. Little data are available at greater distances, but the ratio does not seem to approach 1.0 at 9° as was expected.

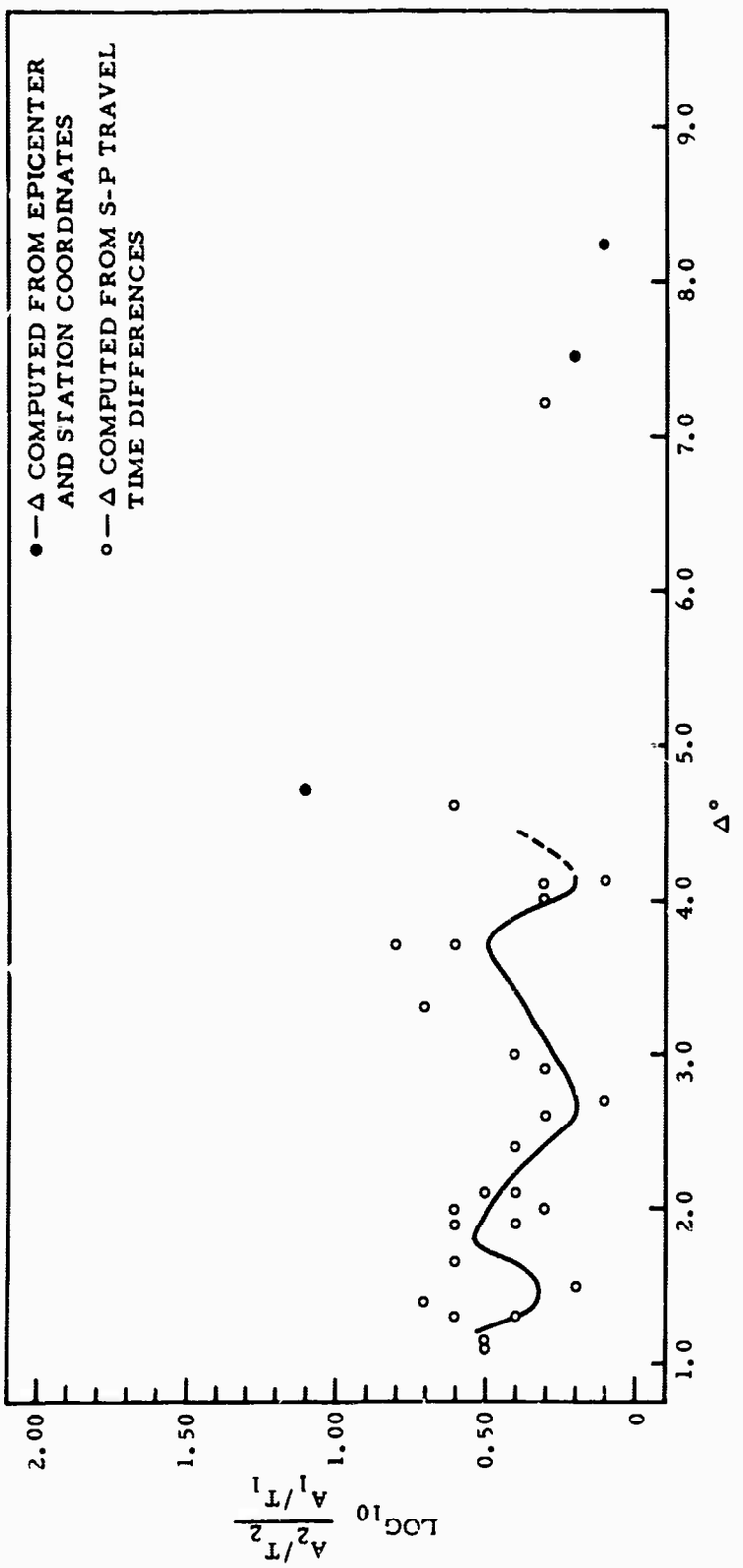

Figure II-4. Comparison of Maximum P and P_n Amplitudes in Vicinity of Istanbul, Turkey

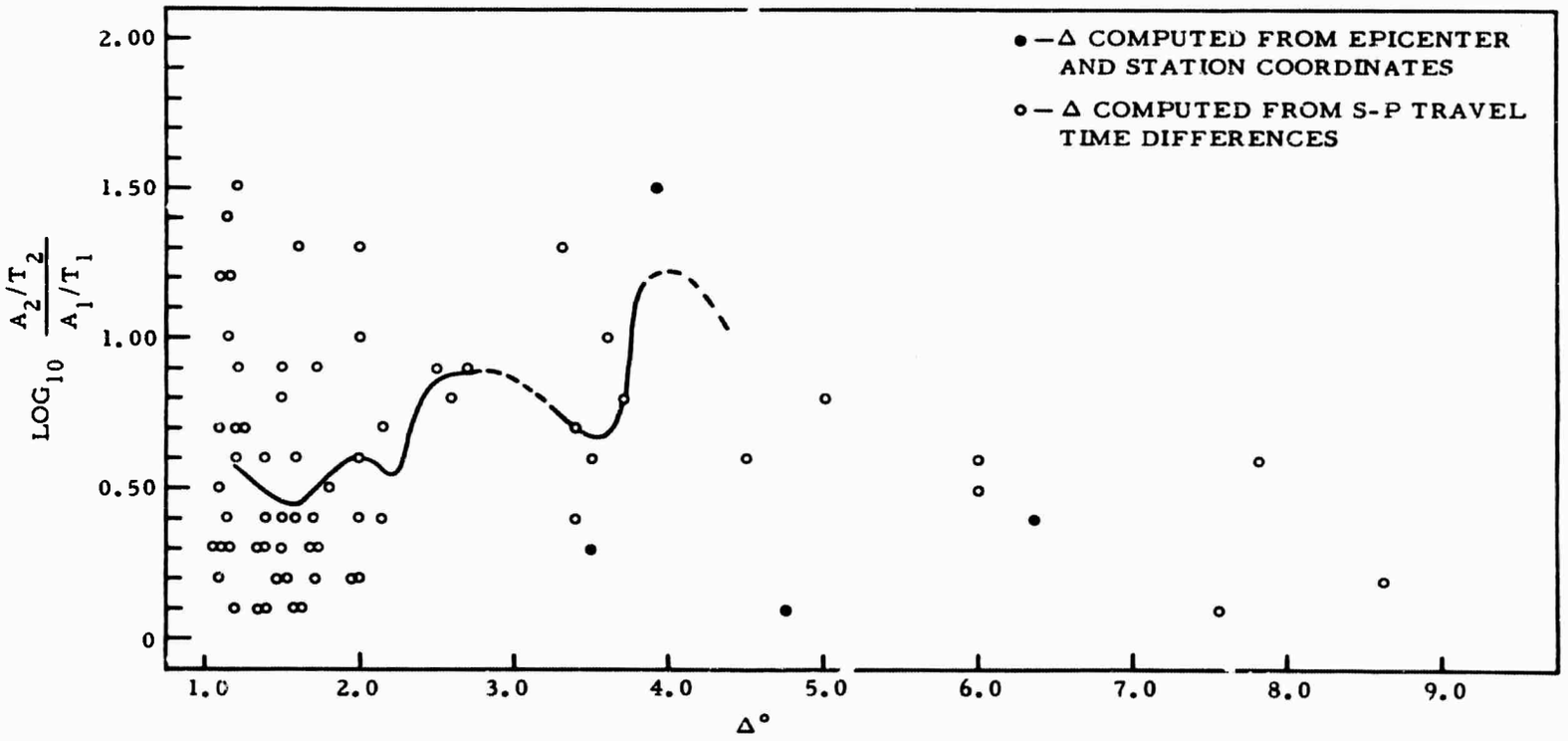

Figure II-5. Comparison of Maximum P and P_n Amplitudes in Vicinity of Shiraz, Iran

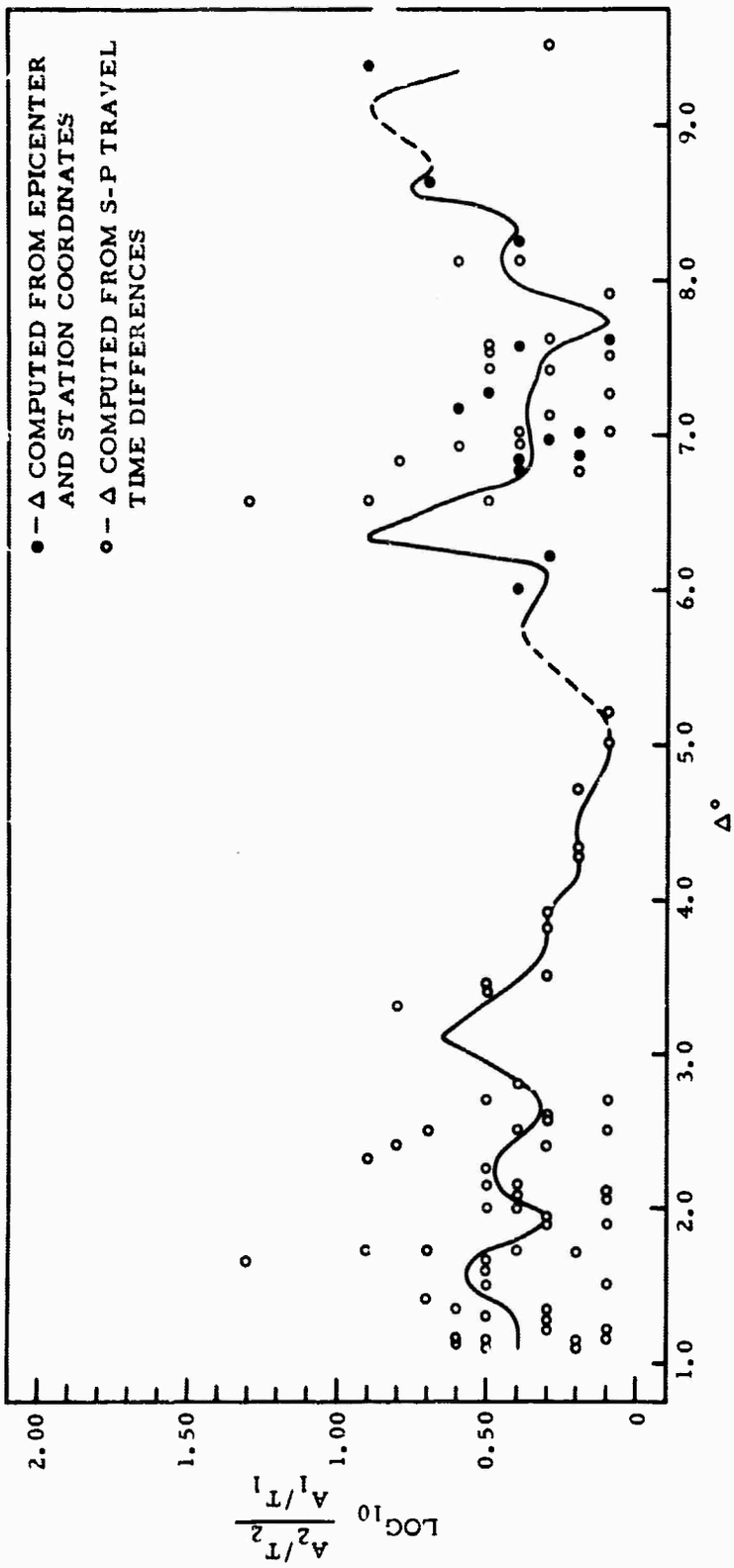

Figure II-6. Comparison of Maximum P and P_n Amplitudes in Vicinity of Quetta, Pakistan

Insufficient data were obtained for valid analyses of P_n and maximum P amplitudes at Shillong, India, and at Chengmai, Thailand, as two-thirds of the events at Shillong and half of the events at Chengmai had equal magnitudes on each scale. From the little data available, however, the average amplitude ratio for both stations can be estimated to be approximately 2 for most of the distance range.

Over 400 events at Port Moresby, New Guinea, were analyzed in this study. Since the noise level at this station is high, it is not surprising to find that nearly half of the events had equal magnitudes on both scales. Considerable scatter was noted over the entire distance range, even for events with known epicenters. This scatter complicated the determination of any clear pattern of amplitude ratios. High ratios appeared prevalent from approximately 3° to 5° (maximum P up to 12 times P_n amplitudes). From about 6° to 8°, most events were located by the USC&GS; the average ratio over this range was approximately 4. Relatively high amplitude ratios were observed to 9°. Figure II-7 shows the distribution of amplitude ratios with distance.

Slightly over 40 percent of the analyzed events near Nana, Peru, had equal magnitudes on both scales. The pattern here seems to have been increasing ratios to an average value of about 4 at a distance of 3° and near this level to approximately 7°, as shown in Figure II-8. Data were sparse at the greater distances.

More than half of the 500 analyzed events near Arequipa, Peru, had equal magnitudes on both scales. The average amplitude ratio was 2 to 3 at 1° to 7°, with an indication of an approach to unity near 9°, as indicated in Figure II-9.

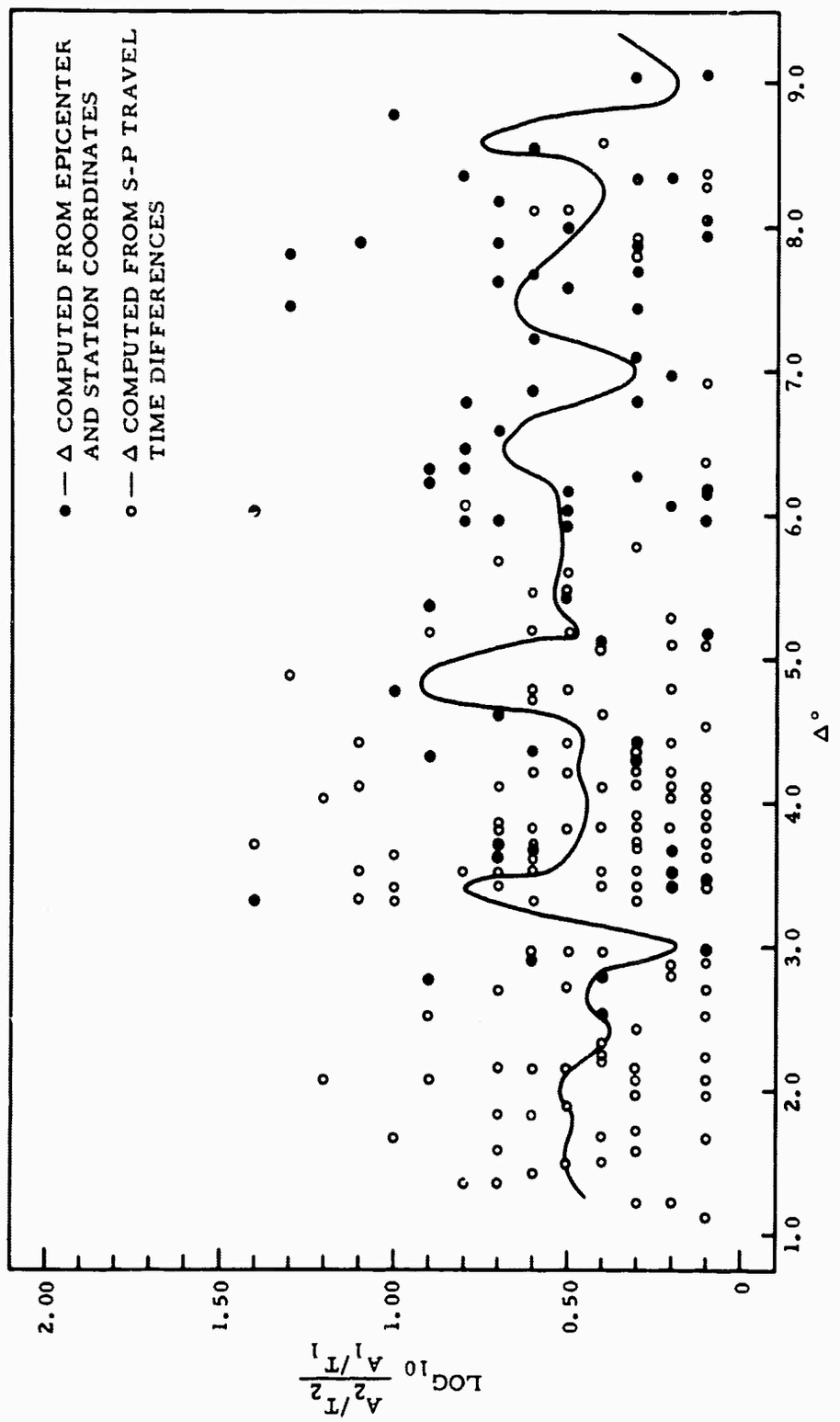

Figure II-7. Comparison of Maximum P and P_n Amplitudes in Vicinity of New Guinea

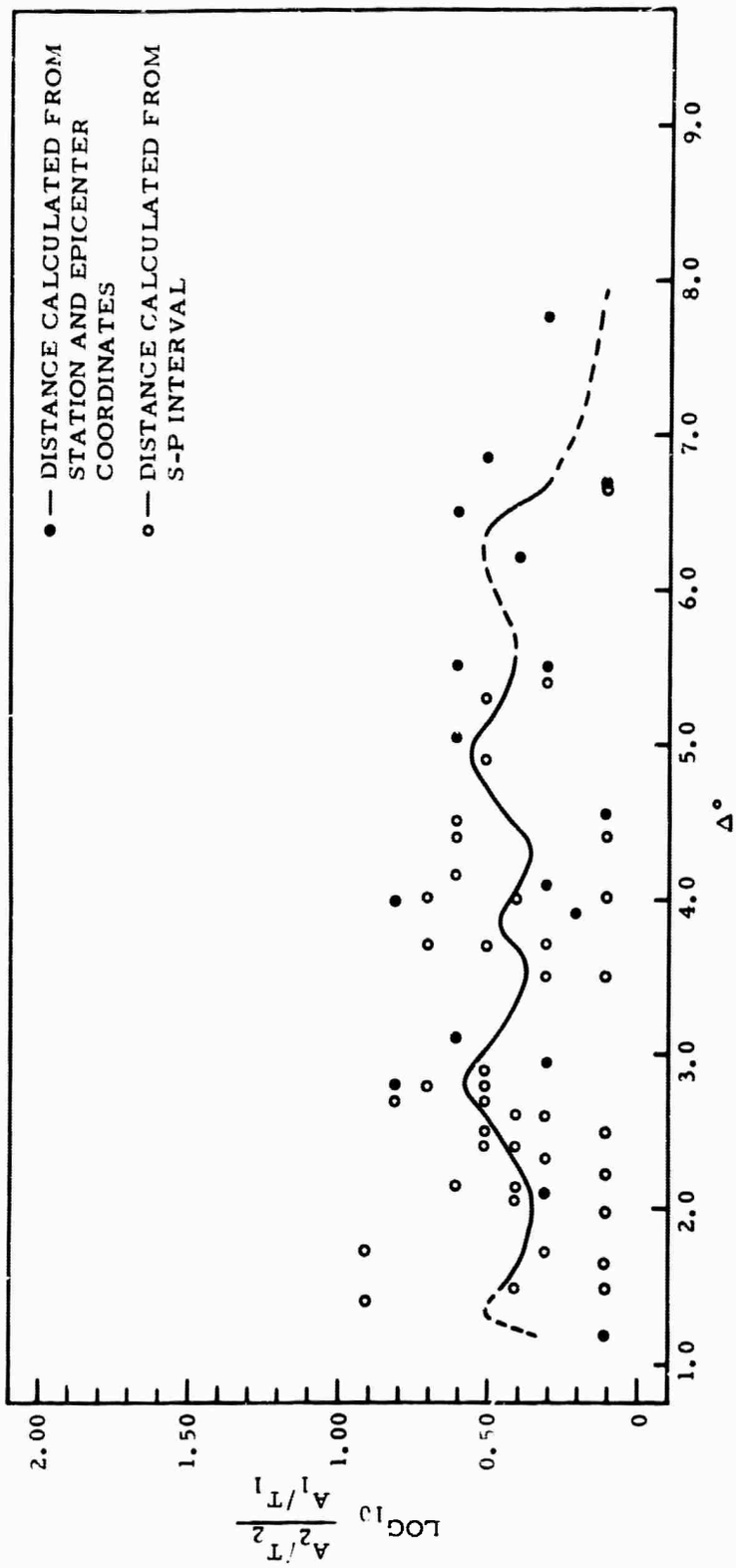

Figure II-8. Comparison of Maximum P and P_n Amplitudes in Vicinity of Nana, Peru

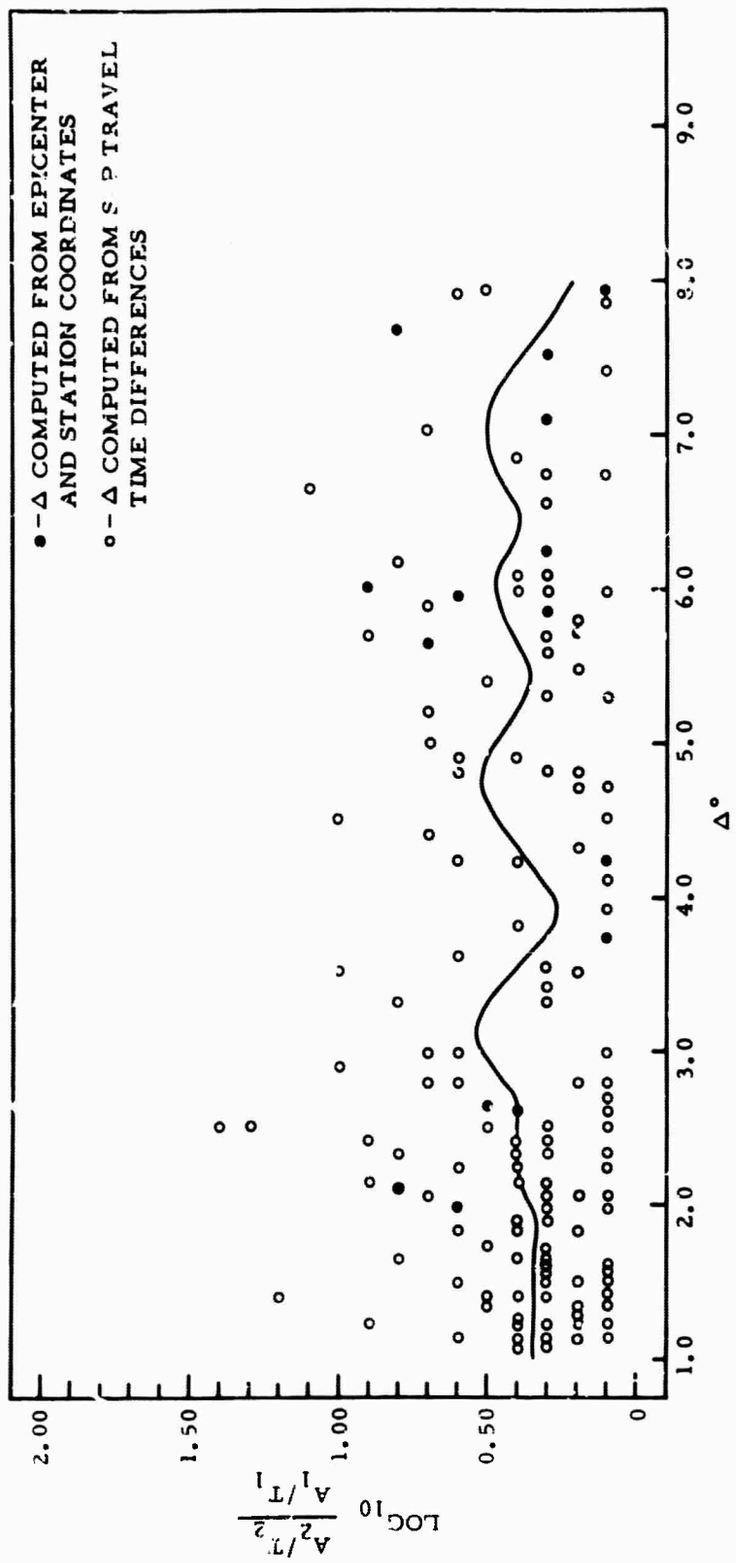

Figure II-9. Comparison of Maximum P and P_n Amplitudes in Vicinity of Arequipa, Peru

Data near Antofagasta, Chile, were from events in a narrow distance range of approximately 1.5° to 3°. The average amplitude ratio was about 2.5 to 3 over this distance interval. Of the events analyzed in this area, 75 percent had equal magnitudes on both scales. This probably resulted from high noise levels and low instrument gain which decreases the probability of P_n detection.

In summary, maximum P amplitudes at most stations appear to be at least twice as large as P_n amplitudes. High amplitude ratios often occur from 3° to 5° distances. Variations in patterns from station to station indicate that parameters other than distance affect propagation patterns for various branches of P. Some of these parameters might include azimuth, source region, crustal structure, travel-time curves, and source mechanism. Investigation of the effects of these parameters is needed before reliable magnitudes can be computed at short distances.

B. EXACT CONFIDENCE REGIONS

1. Definitions and Assumptions

a. Propagation of Seismic Waves

For the purposes of mathematical characterization, the physical, or spatial, earth is defined as follows:

- The spatial earth, denoted by W, is a compact, convex continuum with the usual 3-dimensional metric and has the geometric and topological properties of the closure of the interior of an oblate spheroid except that there is a positive real number t such that, for any boundary point p, the distance from p to the center of W may differ from the analytic value by an amount, the absolute value of which is less than or equal to t

- The surface of the spatial earth, denoted by B(W), is the boundary set of W

Regarding the temporal continuum as a copy of the real line denoted by T, the spatio-temporal earth is defined as follows:

- The spatio-temporal earth T x W is the 4-dimensional space generated by T and directed by W

Under these conditions, a seismic event occurring at time H_o and having the spatial (curvilinear) coordinates λ_o, Φ_o, and R_o can be treated just as a vector $(H_o, \lambda_o, \Phi_o, R_o) \in T \times W$. Now, let $(\omega_1, \ldots, \omega_\gamma)$ be a finite set of wave phases associated with the seismic event $(H_o, \lambda_o, \Phi_o, R_o)$ and let $\left[H_o, H_o'\right]$, denoted by T_o, be a closed interval on T. Then, the basic assumption concerning the propagation of seismic waves can be stated as follows:

(1) For each phase ω_i, there is an associated continuous monotone transformation $\Omega_i : W \times \{(H_o, \lambda_o, \Phi_o, R_o)\} \rightarrow T_o$ so that a point $\left[\lambda, \Phi, R, (H_o, \lambda_o, \Phi_o, R_o)\right] \in \Omega_i^{-1}(H)$ where $H_o \leq H \leq H_o'$ if, and only if, H is the time at which the ω_i phase arrives at (λ, Φ, R)

In accordance with the characterization given in assumption (1), the point $(H_o, \lambda_o, \Phi_o, R_o)$ which occurs in the definition of the domain of Ω_i is referred to as the parameter of the transformations. Alternately, equivalent transformations could have been developed as temporal metric functions on the space T x W; under such functions, the distance between two points $(H_o, \lambda_o, \Phi_o, R_o)$ and (H, λ, Φ, R) would simply be the absolute difference between origin time H_o and the ω_i phase arrival time H at (λ, Φ, R). However, the approach taken in the statement of the assumption, with the consequent representation of T x W as a parameter space, is better suited to the statistical development which is to follow.

It should be noted that assumption (1) does not strictly agree with empirical evidence, because travel-time curves for certain wave phases show some signs of looping. Hence, for regions in the domain corresponding to a loop in the graph of Ω_i, the assumptions that Ω_i is single-valued and monotone are unwarranted. In practice, this difficulty can probably be overcome in the case of large samples by existing routines for elimination of data differing too much from the sample mean; in the case of small or minimal samples, it may be necessary to include a procedure for eliminating observation points lying in the region of a loop as part of the process of refinement.

b. Analytic Description

The combination of tables giving wave-phase travel times, depth corrections, station corrections, and ellipticity corrections, together with rules for using these tables, can be thought of as defining, for each phase ω_i, a function $f_i: W \times (T \times W) \to T$ so that $f_i[\lambda, \Phi, R, (H_o, \lambda_o, \Phi_o, R_o)]$ is the computed time at which phase ω_i should arrive at (λ, Φ, R). Taking this view, the basic assumption regarding the analytic description of the propagation of seismic waves can be stated as follows:

(2) $\{(\lambda_j, \Phi_j, R_j): 1 \leq j \leq n\}$ is an arbitrary set of observation points (stations); therefore, ${}_ie_j$, the error residual at the j^{th} point with respect to wave phase ω_i, is given by the statement ${}_ie_j = \Omega_i[\lambda_j, \Phi_j, R_j, (H_o, \lambda_o, \Phi_o, R_o)] - f_i[\lambda_j, \Phi_j, R_j, (H_o, \lambda_o, \Phi_o, R_o)]$; the error residuals ${}_ie_j$ are independent normal variates with mean zero and variance σ^2

The importance of assumption (2) can be discussed more meaningfully in the light of the statistical theory which is to be developed; accordingly, the discussion is postponed to the conclusion of that development. It should be understood from the outset, however, that this is the central assumption. The justification of the present approach turns on the validity of this assumption.

c. Hartley's Modified Gauss-Newton Method

The procedure for nonlinear hypocenter determination to be described in the sequel employs Hartley's modification of the Gauss-Newton nonlinear estimation method. In addition to assumption (2), Hartley's method proceeds from the following definitions and assumptions. (For clarity, subscripts which serve only to associate an expression with a particular wave phase will be used from this point forward only when the distinction is critical.) Let

$$C \equiv \left(C_1, C_2, C_3, C_4\right)$$

where

$$C_1 \equiv H_o$$

$$C_2 \equiv \lambda_o$$

$$C_3 \equiv \phi_o$$

$$C_4 \equiv R_o$$

For a given set $\{(\lambda_i, \phi_i, R_i) : 1 < i < n\}$ of observation points, let

$$X_i \equiv \left\{X_{i_1}, X_{i_2}, X_{i_3}\right\}$$

where

$$X_{i_1} \equiv \lambda_i$$

$$X_{i_2} \equiv \phi_i$$

$$X_{i_3} \equiv R_i$$

and let

$$X \equiv \left(X_1, \ldots, X_n\right)$$

Now, let

$$N = (1, \ldots, n)$$

$$F = (1, 2, 3, 4)$$

$$G = (1, 2, 3)$$

Let

$$Q(X, C) = \sum_{k \epsilon N} \left[\Omega(X_k, C) - f(X_k, C)\right]^2$$

Let $i, j \epsilon F$, not necessarily distinct. Then,

$$f_i(X, C) \equiv \frac{\partial f}{\partial C_i}$$

and

$$f_{ij}(X, C) = \frac{\partial f}{\partial C_i \, \partial C_j}$$

(3) For each $i, j \epsilon F$, $f_i(X, C)$ and $f_{ij}(X, C)$ are continuous functions of C_i and C_j for all X_k where $k \epsilon N$

(4) For any nontrivial set of real numbers $\{u_i : i \epsilon F\}$ with $\Sigma_{i \epsilon F} (u_i)^2 > 0$, it is the case that

$$\Sigma_{k \epsilon N} \left(\Sigma_{i \epsilon F} \left[u_i f_i(X_k, C)\right]\right)^2 > 0$$

for all C lying in a bounded convex set S of the parameter space T x W

(5) Let $\sim S$ be the complement of the set S described in assumption (4) and let

$$Q = \lim_{\sim S} \inf Q(X, C)$$

Then, there exists a point ${}_oC$ lying in the interior of S so that

$$Q(X, {}_oC) < Q$$

As with assumption (2), the discussion of the justification for assumptions (3), (4), and (5) is best deferred to the conclusion of the description of the estimation technique. The purposes served by these latter assumptions are fairly straightforward. Assumption (3) makes possible the definition of the first and second partial derivatives of function Q with respect to C_i and C_j where i, j ϵ F; these definitions will be stated explicitly in the sequel. According to Hartley, assumption (4) is "equivalent to the well-known assumption of nondegeneracy of rank in a linear least-square problem..." and is "usually... satisfied in practical situations." The modified Gauss-Newton method is an iterative process, and the role of assumption (5) is to guarantee convergence of the iteration, given a vector ${}_oC$ of the specified sort as a starting point.

As will be seen later, assumption (4) must be strengthened to insure that the solution to which the process converges (say, C*) gives a unique, absolute minimum for Q(X, C).

2. Procedure

The following conventions are introduced so that the development might be expressed in terms of matrix algebra.

(1) Let $i, j \in F$, not necessarily distinct, and let $k \in N$. Then,

- The symbol $f^i(X, C)$ denotes the $N \times 1$ column vector having $f_i(X_k, C)$ as its k^{th} component
- The symbol $f_j(X, C)$ denotes the $N \times 4$ column vector having the element $f_j(X_k, C)$ in the k^{th} row and the j^{th} column

(2) The symbol Y denotes the $N \times 1$ column vector with the k^{th} component $Y_k = \Omega(X_k, C)$

Under definitions (1) and (2),

$$\begin{aligned} Q(X, C) &= [Y - f(X, C)]^t [Y - f(X, C)] \\ &= Y^t Y - 2Y^t f(X, C) + f(X, C)^t f(X, C) \end{aligned} \tag{11}$$

Hence, for $i \in F$,

$$\begin{aligned} Q^i(X, C) \equiv \frac{\partial}{\partial C_i} \cdot Q(X, C) &= -2Y^t f^i(X, C) + f(X, C)^t f^i(X, C) + f^i(X, C)^t f(X, C) \\ &= -2Y^t f^i(X, C) + 2f(X, C)^t f^i(X, C) \\ &= -2[Y^t - f(X, C)^t] f^i(X, C) \\ &= -2[Y - f(X, C)]^t f^i(X, C) \end{aligned} \tag{12}$$

Now, let the symbol ${}_oC$ denote the least-squares estimate of the hypocenter location determined by the existing program under the assumption of linearity.

By Taylor's theorem, $f(X, {}_oC + D_o)$ can be approximated by

$$f(X, {}_oC) + f_1(X, {}_oC)\, D_o^t$$

where D_o is the 1 x 4 vector having the i^{th} component

$$D_i^o = \frac{\delta_o C_i}{\delta v}$$

fo $0 \le v \le 1$. The error of the approximation is given by

$$\frac{1}{2}\left[f_1(X, {}_oC + v' D_o)\, D_o\right]^2$$

for some v' so that $0 \le v' \le 1$ where the exponent indicates the usual formal expansion of the operator.

Substitution of the approximation for $f(X, C)$ yields

$$\begin{aligned} Q^i(X, {}_oC) &= -2\left[Y - f(X, {}_oC) - f_1(X, {}_oC)\, D_o^t\right]^t f^i(X, {}_oC) \qquad (13) \\ &= -2\left[Y - f(X, {}_oC)\right]^t f^i(X, {}_oC) + 2\, D_o f_1(X, {}_oC)^t f^i(X, {}_oC) \\ &= Q^i(X, {}_oC) + 2 f^i(X, {}_oC)^t f_1(X, {}_oC)\, D_o^t \end{aligned}$$

The formal least-squares equations which minimize $Q(X, C)$ are given by the system $Q^i(X, C) = 0 (i = 1, \ldots, 4)$; hence, for $i = 1, \ldots, 4$,

$$2 f^i(X, {}_oC)^t f_1(X, {}_oC)\, D_o^t = -Q^i(X, {}_oC) \qquad (14)$$

By assumption (4), the determinant of the latter system is of rank 4; therefore, it is possible to solve the system for the vector D_o.

Now, let

$$Q_\alpha(v') \equiv Q(X, {}_\alpha C + v' D_\alpha)$$

for $0 \leq v' \leq 1$ where α is a nonnegative integer and let v'_α denote the value of v' for which $Q_\alpha(v')$ is a minimum on the interval $0 \leq v' \leq 1$. Hartley gives

$$v'_\alpha = \frac{1}{2} + \frac{1}{4}\left[Q_\alpha(0) - Q_\alpha(1)\right] / \left[Q_\alpha(1) - 2Q_\alpha\left(\frac{1}{2}\right) + Q_\alpha(0)\right] \qquad (15)$$

The estimate given by the α^{th} iteration of Hartley's method is defined to be the vector

$$\alpha + 1 C \equiv {}_\alpha C + v'_\alpha D_\alpha$$

If, after m steps, Hartley's method yields an estimate C* which satisfies predetermined convergence criteria, an exact 100p percent confidence region for $0 \leq p \leq 1$ can be constructed by Booker's method. As before, the linear terms of a Taylor expansion of $f(X, C)$ about C* are given by $f(X, C^*) + f_1(X, C^*) D^t_*$. Let

$$A \equiv f_1(X, C^*)\left[f_1(X, C^*)^t \; f_1(X, C^*)\right]^{-1} f_1(X, C^*)^t \qquad (16)$$

and

$$\text{Reg}(e) = \left[Y - f(X, C)\right]^t \; A\left[Y - f(X, C)\right] \qquad (17)$$

and

$$\text{Res}(e) = \left[Y - f(X, C)\right]^t \; (I - A)\left[Y - f(X, C)\right] \qquad (18)$$

Then, an exact 100p percent confidence region R_p is given by

$$R_p = \{C \subset T \times W : Reg(e)/Res(e) \leq 4\Phi(p;4, N-4)/(N-4)\} \qquad (19)$$

where $Reg(e)/Res(e)$ has the distribution $4\Phi(p;4, N-4)/(N-4)$.

C. INSTRUMENTAL PERCEPTIBILITY

Instrumental perceptibility, a measure of a seismograph station's capability to record seismic events, is based on noise measurements and theoretical variations in P-phase amplitudes with distance. Before theoretical perceptibility limits can be calculated, microseism particle velocities (amplitude/apparent period) for each station must be estimated. This is accomplished by determining the distributions of seismic noise (mμ/sec) at each station and using as the noise estimate that value for which the probability of occurrence is 0.5. Then, the observed noise at a particular station should be less than or equal to the estimated value half the time.

Solving the magnitude equation for the depth-distance factor, one obtains

$$Q = m_b - \log\left(\frac{A}{T}\right) = f(\Delta, h) \qquad (20)$$

Let h = 25 km, substitute estimated values of A/T, and let m_b = 4.0, 4.5 and 5.0; then, the distance ranges for which Q ≤ the value calculated from Equation (20) are the perceptibility limits for m_b = 4.0, 4.5, and 5.0 for each station. The results of these calculations for 44 of the analyzed stations are shown in Table II-2. These results indicate that Chengmai, Thailand, has the highest capability for recording seismic events but is followed closely by two Canadian Arctic stations, Mould Bay (MBC) and Resolute Bay (RES).

Table II-2

STATIONS' CAPABILITIES TO RECORD SEISMIC EVENTS

Station	$\frac{A}{T}$ (mμ/sec)	m_b	Instrumental Perceptibility Limits (°)
AFI	32	4.0	0 - 2.7
		4.5	0 - 4.0, 15.3 - 19.5
		5.0	0 - 6.0, 14.2 - 28.0, 39.8 - 42.5
AKU	27	4.0	0 - 2.9
		4.5	0 - 4.4, 15.2 - 20.0
		5.0	0 - 6.3, 14.1 - 29.6, 37.2 - 43.9
ALE	2.5	4.0	0 - 6.3, 14.0 - 30.0, 36.8 - 44.3
		4.5	0 - 8.0, 12.1 - 91.4
		5.0	0 - 104.2
ALQ	2.5	4.0	0 - 6.3, 14.0 - 30.0, 36.8 - 44.3
		4.5	0 - 8.0, 12.1 - 91.4
		5.0	0 - 104.2
ARE	9.5	4.0	0 - 4.1, 15.5 - 19.7
		4.5	0 - 6.1, 14.2 - 29.0, 39.0 - 43.3
		5.0	0 - 8.2, 12.0 - 85.0
ATL	9	4.0	0 - 4.1, 15.3 - 19.9
		4.5	0 - 6.2, 14.1 - 29.4, 37.8 - 43.6
		5.0	0 - 8.5, 11.6 - 86.5
ATU	35	4.0	0 - 2.7
		4.5	0 - 3.9, 15.8 - 19.3
		5.0	0 - 5.8, 14.3 - 27.6
BAG	23	4.0	0 - 3.0
		4.5	0 - 4.5, 15.2 - 20.9
		5.0	0 - 6.5, 13.8 - 31.0, 36.4 - 45.0
BOZ	7	4.0	0 - 4.5, 15.4 - 21.1
		4.5	0 - 6.2, 14.1 - 29.5, 37.5 - 43.8
		5.0	0 - 92.0
BUL	15	4.0	0 - 3.5
		4.5	0 - 5.1, 14.6 - 23.8
		5.0	0 - 7.1, 13.3 - 47.8, 49.5 - 56.0, 71.2 - 81.8
CHG	1.5	4.0	0 - 7.1, 13.3 - 47.8, 49.5 - 56.0, 71.2 - 81.8
		4.5	0 - 97.0
		5.0	0 - 106.0

Table II-2 (Contd)

Station	$\frac{A}{T}$ (mμ/sec)	m_b	Instrumental Perceptibility Limits (°)
CMC	4.5	4.0	0 - 5.2, 14.3 - 24.1
		4.5	0 - 7.2, 13.2 - 57.0, 71.0 - 82.1
		5.0	0 - 101.2
COL	6	4.0	0 - 4.7, 14.8 - 22.0
		4.5	0 - 6.7, 13.6 - 33.0, 35.0 - 46.2
		5.0	0 - 93.0
CTA	11	4.0	0 - 3.9, 15.8 - 19.3
		4.5	0 - 5.8, 14.3 - 27.6
		5.0	0 - 7.8, 12.7 - 83.8
EDM	20	4.0	0 - 3.2
		4.5	0 - 4.7, 14.8 - 21.7
		5.0	0 - 6.7, 13.7 - 32.0, 35.5 - 46.0
ESK	73	4.0	0 - 2.1
		4.5	0 - 3.0
		5.0	0 - 4.5, 15.2 - 20.9
GOL	2.5	4.0	0 - 6.3, 14.0 - 30.0, 36.8 - 44.3
		4.5	0 - 8.0, 12.1 - 91.4
		5.0	0 - 104.2
GSC	2.5	4.0	0 - 6.3, 14.0 - 30.0, 36.8 - 44.3
		4.5	0 - 8.0, 12.1 - 91.4
		5.0	0 - 104.2
IST	14	4.0	0 - 3.6
		4.5	0 - 5.2, 14.5 - 24.3
		5.0	0 - 7.2, 12.6 - 58.0, 70.5 - 82.3
JER	16	4.0	0 - 3.5
		4.5	0 - 5.0, 14.6 - 23.5
		5.0	0 - 7.0, 13.3 - 47.4, 50.0 - 55.5
KEV	25	4.0	0 - 2.9
		4.5	0 - 4.3, 15.0 - 20.3
		5.0	0 - 6.3, 14.0 - 30.0, 36.8 - 44.3
KON	12	4.0	0 - 3.8, 15.9 - 19.0
		4.5	0 - 5.6, 14.4 - 27.2
		5.0	0 - 7.6, 12.8 - 61.3, 63.0 - 83.2

Table II-2 (Contd)

Station	$\frac{A}{T}$ (mμ/sec)	m_b	Instrumental Perceptibility Limits (°)
KTG	20	4.0	0 - 3.2
		4.5	0 - 4.7, 14.8 - 21.7
		5.0	0 - 6.7, 13.7 - 32.0, 35.5 - 46.0
LON	6	4.0	0 - 4.7, 14.8 - 22.0
		4.5	0 - 6.7, 13.6 - 33.0, 35.0 - 46.2
		5.0	0 - 93.0
LPS	6	4.0	0 - 4.7, 14.8 - 22.0
		4.5	0 - 6.7, 13.6 - 33.0, 35.0 - 46.2
		5.0	0 - 93.0
MAT	66	4.0	0 - 2.2
		4.5	0 - 3.1
		5.0	0 - 4.6, 14.8 - 21.4
MBC	2	4.0	0 - 6.7, 13.7 - 32.0, 35.5 - 46.0
		4.5	0 - 92.7
		5.0	0 - 105.2
MUN	20	4.0	0 - 3.2
		4.5	0 - 4.7, 14.8 - 21.7
		5.0	0 - 6.7, 13.7 - 32.0, 35.5 - 46.0
NAI	4	4.0	0 - 5.5, 14.4 - 27.0
		4.5	0 - 7.5, 13.0 - 61.0, 64.0 - 83.0
		5.0	0 - 102.0
NDI	5	4.0	0 - 5.0, 14.6 - 23.5
		4.5	0 - 7.0, 13.3 - 47.4, 50.0 - 55.5
		5.0	0 - 96.5
NOR	7	4.0	0 - 4.5, 15.4 - 21.1
		4.5	0 - 6.2, 14.1 - 29.5, 37.5 - 43.8
		5.0	0 - 92.0
NUR	10	4.0	0 - 4.0, 15.6 - 19.5
		4.5	0 - 6.0, 14.2 - 28.0, 39.5 - 43.0
		5.0	0 - 8.0, 12.1 - 84.5
PMG	9.5	4.0	0 - 4.1, 15.5 - 19.7
		4.5	0 - 6.1, 14.2 - 29.0, 39.0 - 43.3
		5.0	0 - 8.2, 12.0 - 85.0

Table II-2 (Contd)

Station	$\frac{A}{T}$ (mu/sec)	m_b	Instrumental Per. bility Limits (°)
POO	7.5	4.0	0 - 4.4, 15.0 - 20.6
		4.5	0 - 6.4, 13.9 - 30.5, 36.6 - 44.7
		5.0	0 - 91.5
QUE	3.5	4.0	0 - 5.8, 14.3 - 27.6
		4.5	0 - 7.8, 12.5 - 83.8
		5.0	0 - 102.7
RES	2	4.0	0 - 6.7, 13.7 - 32.0, 35.5 - 46.0
		4.5	0 - 92.7
		5.0	0 - 105.2
SCH	25	4.0	0 - 2.9
		4.5	0 - 4.3, 15.0 - 20.3
		5.0	0 - 6.3, 14.0 - 30.0, 36.8 - 44.3
SCP	7.5	4.0	0 - 4.4, 15.0 - 20.6
		4.5	0 - 6.4, 13.9 - 30.5, 36.6 - 44.7
		5.0	0 - 91.5
SHI	3.5	4.0	0 - 5.8, 14.3 - 27.6
		4.5	0 - 7.8, 12.5 - 83.8
		5.0	0 - 102.7
SHL	2.5	4.0	0 - 6.3, 14.0 - 30.0, 36.8 - 44.3
		4.5	0 - 8.0, 12.1 - 91.4
		5.0	0 - 104.2
SPA	4.5	4.0	0 - 5.2, 14.3 - 24.1
		4.5	0 - 7.2, 13.2 - 57.0, 71.0 - 82.1
		5.0	0 - 101.2
STU	7.5	4.0	0 - 4.4, 15.0 - 20.6
		4.5	0 - 6.4, 13.9 - 30.5, 36.6 - 44.7
		5.0	0 - 91.5
TRI	15	4.0	0 - 3.5
		4.5	0 - 5.1, 14.6 - 23.8
		5.0	0 - 7.1, 13.3 - 47.8, 49.5 - 56.0, 71.2 - 81.8
WIN	5	4.0	0 - 5.0, 14.6 - 23.5
		4.5	0 - 7.0, 13.3 - 47.4, 50 - 55.5
		5.0	0 - 96.5

Note that the results shown in Table II-2 are theoretical; several factors influencing the amplitudes of P waves from seismic events are not considered in the perceptibility calculations. These factors include

- Energy radiation patterns from the source
- Anomalous energy attenuation
- Station environment
- Regional geology in the vicinity of the station

Amplitudes of P phases from the same event, then, may vary considerably at the same distances, depending on these factors.

D. ENERGY PROPAGATION PATTERNS

1. Objectives

The tendency of magnitudes computed at certain stations for events in the same areas to be consistently higher or lower than the average event magnitude was observed, and this suggested the possibility of determining distinct energy propagation patterns from events in given areas through investigation of station magnitude residuals.

This investigation was performed to

- Determine whether such patterns exist
- Categorize the patterns found
- Evaluate and determine the applicability of the method

2. Methods of Investigation

Magnitude values (m_b) computed by Texas Instruments (1964b) and published in USC&GS Earthquake Data Reports (1963, 1964), VELA UNIFORM Array Station Bulletins (1964, 1965), and LRSM Bulletins (1964, 1965) for the selected events are combined to determine average event magnitudes.

All magnitudes are rounded to the nearest tenth magnitude unit and, where duplicate values are found, precedence is given to bulletin or Texas Instruments values.

Defined are 10 geographical sectors in which magnitude data are grouped according to recording-station locations. The azimuthal and distance boundaries are different for Aleutian Islands events and Kurile Islands events but correspond to the same groupings of stations. The sectors are defined as follows:

(1) Canadian Arctic and Greenland
(2) Alaska and Northwest Canada
(3) Eastern United States
(4) Western United States
(5) Hawaiian Islands
(6) Southwest Pacific and Eastern Australia
(7) Southeast Asia
(8) India to Iran
(9) Turkey and Southeastern Europe
(10) Western Europe

Magnitude residuals are computed by subtracting the event mean from the individual magnitude values, and an average magnitude residual is computed for each sector if two or more residuals are determined for the sector:

$$P_j = \frac{\sum_{i=1}^{n_j} \tau_i}{n_j} \qquad (21)$$

where

P_j = mean residual in j^{th} sector

r_i = magnitude residual at i^{th} station

n_j = number of magnitudes in j^{th} sector

Values of P_j are plotted in sector boundaries shown in a polar display and events grouped from visual inspection. Values of P_j for events associated with a given pattern are usually within ±0.1 magnitude unit of the mean for the pattern.

3. Results

Table II-3 lists the events selected for the study. The first nine events in the table are located in the Rat Islands area between 50.3°N and 51.8°N and between 178.1°E and 176.[illegible]°W. The Aleutian arc in this area trends nearly east-west, with little apparent curvature.

Events 4478, 4947, 5001, and 6536 have similar patterns, as shown in Figure II-10. The pattern is characterized by relative highs in sectors 3 and 10 and relative lows in sectors 4 and 7. The difference in mean magnitude residuals between the Eastern U.S. and the Western U S. averages almost 0.6 magnitude units for the four events fitting this pattern (1-A).

Events 2945 and 2958 are grouped together as fitting patterr 1-B. This pattern is characterized by mean magnitude residuals which are slightly larger than 0 in the Arctic and Eastern United States and slightly less than 0 in the Western United States (Figure II-11). There is some evidence that a nodal plane passes just off the West Coast of the United States for both events fitting this pattern.

Table II-3

LIST OF EVENTS STUDIED

Event No.	Date	Origin Time	Latitude	Longitude	Depth (km)	CGS m_b	Pub M_s	TI m_b	TI M_s	Pattern
2212	3/24/63	21 35 24.4	51.8N	178.1W	57	5.5	5.5	5.61	6.25	
2945	4/29/63	21 44 17.1	51.4N	178.1E	60	5.6	5.7	5.02	6.66	1-B
2955	4/30/63	03 26 04.2	51.2N	178.6E	50	4.9		4.90		
2958	4/30/63	07 07 55.9	51.6N	178.4E	64	5.1		5.10	6.07	1-B
3012	5/4/63	05 56 04.1	51.8N	175.4W	69	5.5		4.89		
4478	8/18/63	18 43 16.1	50.3N	176.9W	33	5.5	5.7	5.56	5.24	1-A
4947	9/23/63	17 02 36.6	51.3N	179.2W	33	5.2		5.03	5.03	1-A
5001	9/26/63	05 28 07.3	50.4N	176.9W	30	5.3		5.09	5.57	1-A
6536	12/11/63	17 08 12.3	51.2N	179.3W	32	5.3		5.11	5.46	1-A
2098	3/16/63	08 44 48.3	46.5N	154.7E	26	6.2	7.2	5.83	6.75	19-A
2319	3/30/63	16 51 56.6	44.2N	148.0E	33	6.3	5.4	5.91	5.65	19-A
3366	5/22/63	13 56 43.0	48.6N	154.7E	22	6.3	6.3	5.73	6.09	
3429	5/25/63	08 41 09.6	42.7N	144.3E	80	5.4	6.5	5.05		19-B
5298	10/12/63	11 26 57.9	44.8N	149.0E	40		6.9	5.73	7.21	19-B
5327	10/13/63	05 17 57.1	44.8N	149.5E	60		8.1	5.45		19-D
5375	10/14/63	04 06 01.7	44.9N	150.2E	50	5.3		5.14	6.50	19-C
5396	10/14/63	13 21 45.2	44.8N	151.0E	60	5.9	6.1	5.72	6.68	19-C
5401	10/14/63	17 50 15.3	45.2N	151.3E	60	5.0	6.3	4.88		
5422	10/15/63	09 02 08.3	45.3N	150.2E	40	5.4	5.5	5.19		19-A
5423	10/15/63	09 32 08.7	45.2N	150.2E	40	5.5		5.25		
5425	10/15/63	10 47 12.6	44.6N	149.0E	50	5.4		5.38		19-B
5484	10/17/63	23 24 34.4	44.6N	149.0E	45	5.4		5.14	6.62	19-C
5520	10/19/63	02 18 37.9	46.8N	153.7E	45	5.2	6.0	4.95	6.39	19-B
5523	10/19/63	03 34 19.6	46.6N	153.8E	33	5.4	5.7	5.04		19-D
5524	10/19/63	03 47 07.7	46.8N	153.8E	25	5.2		5.17		19-B
5550	10/20/63	00 53 07.2	44.7N	150.7E	25		7.1	5.19	6.68	19-C
5578	10/20/63	09 10 43.9	44.4N	150.0E	40	5.5	5.9	5.35	6.42	19-B
5583	10/20/63	11 52 20.7	44.7N	150.2E	45	5.1	6.0	5.13	6.65	
5771	10/28/63	12 03 19.8	52.8N	159.8E	33	5.7	5.2	5.64	5.85	19-A

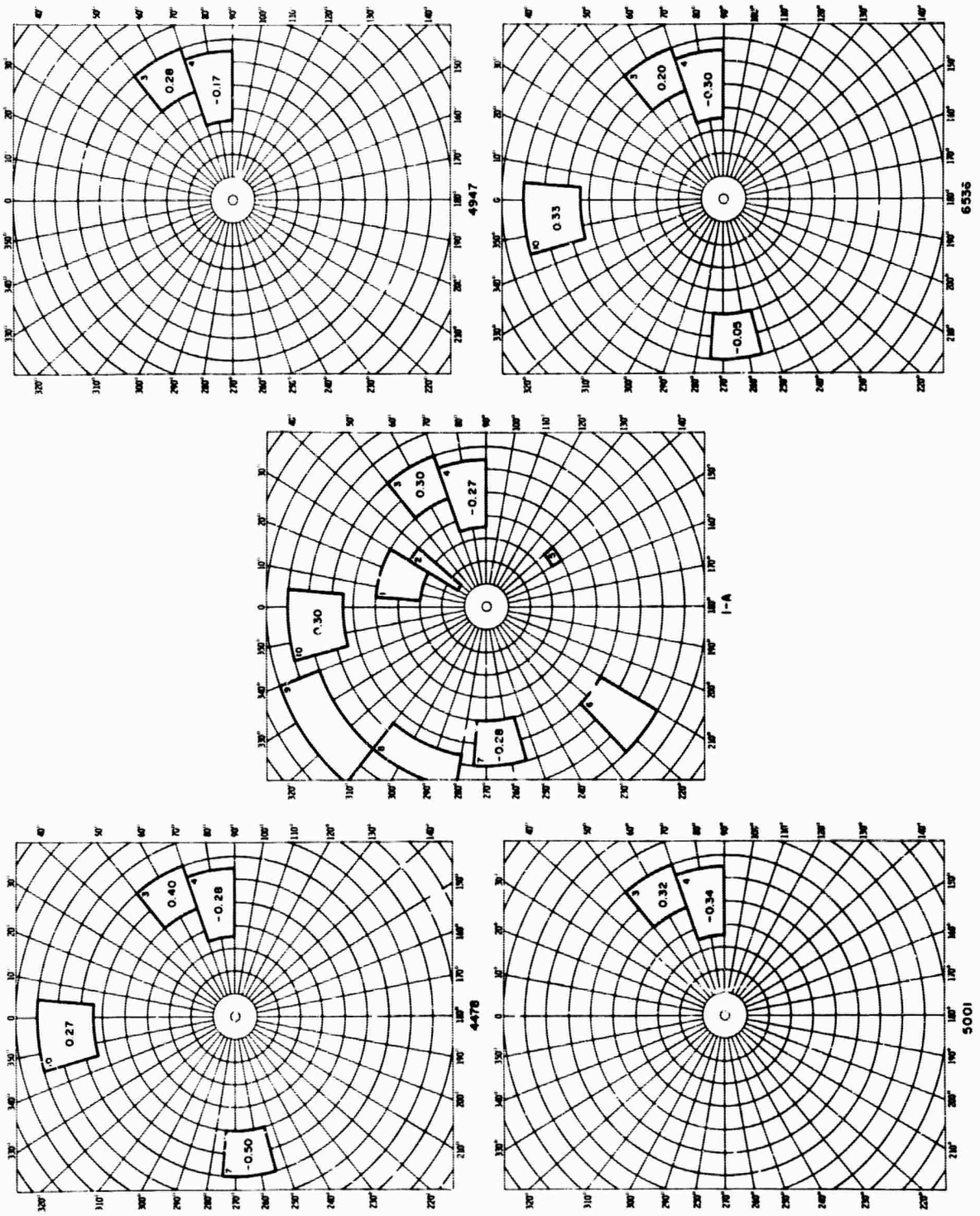

Figure II-10. Magnitude Residual Pattern 1-A and Associated Events

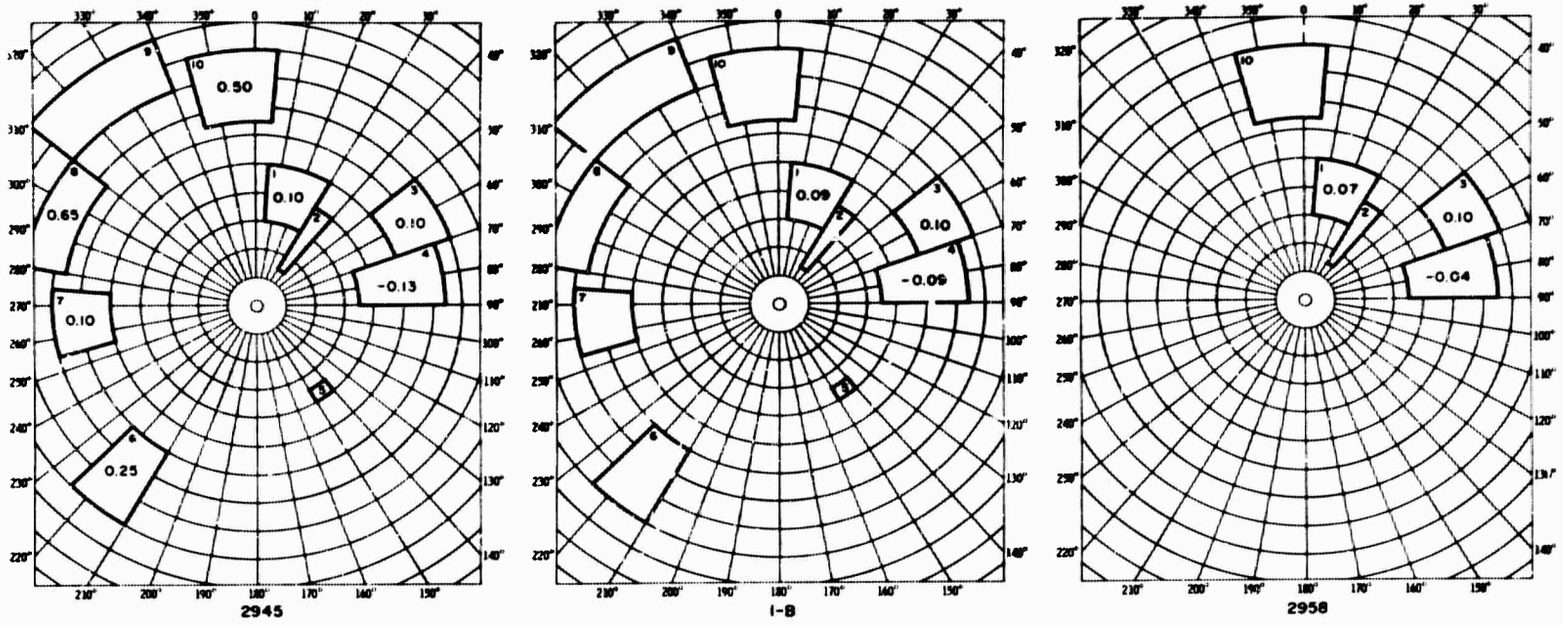

Figure II-11. Magnitude Residual Pattern 1-B and Associated Events

Three Rat Islands events have not been associated with either patterns 1-A or 1-B. Of these events, 2212 and 3012 show considerable similarity. In both cases, there appears to be a nodal plane in a northerly direction and a maximum energy propagation through the Eastern United States. The remaining event (2955) shows some similarity with pattern 1-B except for negative mean residuals in sectors 1 and 3. Figure II-12 shows the magnitude residual patterns for events 2212, 2955, and 3012.

Figure II-13 shows the locations of the Rat Islands events studied. The events fitting pattern 1-A are grouped rather closely on the eastern side of the area included in the study. Probably, all of the events are shallow. Events 5001 and 6536 have depths of 30 km and 32 km, respectively, while events 4478 and 4947 are assigned depths of 33 km which implies a negative depth encountered in the hypocenter determination.

Events 2945 and 2958 associated with pattern 1-B are also located quite near each other; focal depths of 60 km and 64 km, respectively, are determined for them. Event 2955, which is quite similar to pattern 1-B, also is located near events 2945 and 2958 and is determined to have slightly shallower depth of 50 km.

In this area, then, similarity in magnitude residual patterns may be correlated with location, depth, and time of occurrence. From Table II-3, it can be observed that all events fitting pattern 1-A occurred from August 1963 to December 1963, while events associated with or similar to pattern 1-B occurred in March and April 1963.

From Table II-3 and Figure II-14, it is evident that the Kurile Islands events occurred over a larger area than did the Rat Islands events.

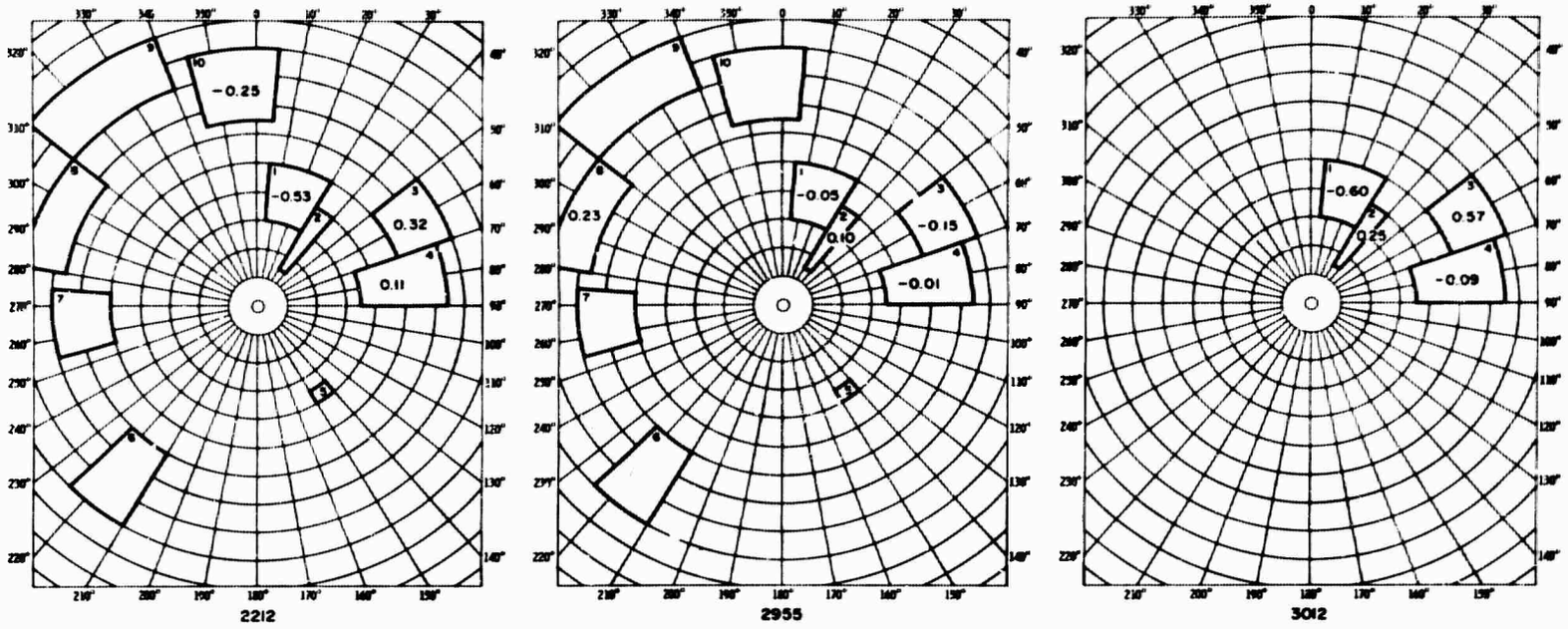

Figure II-12. Rat Islands Events Investigated but Not Classified by Magnitude Residual Pattern

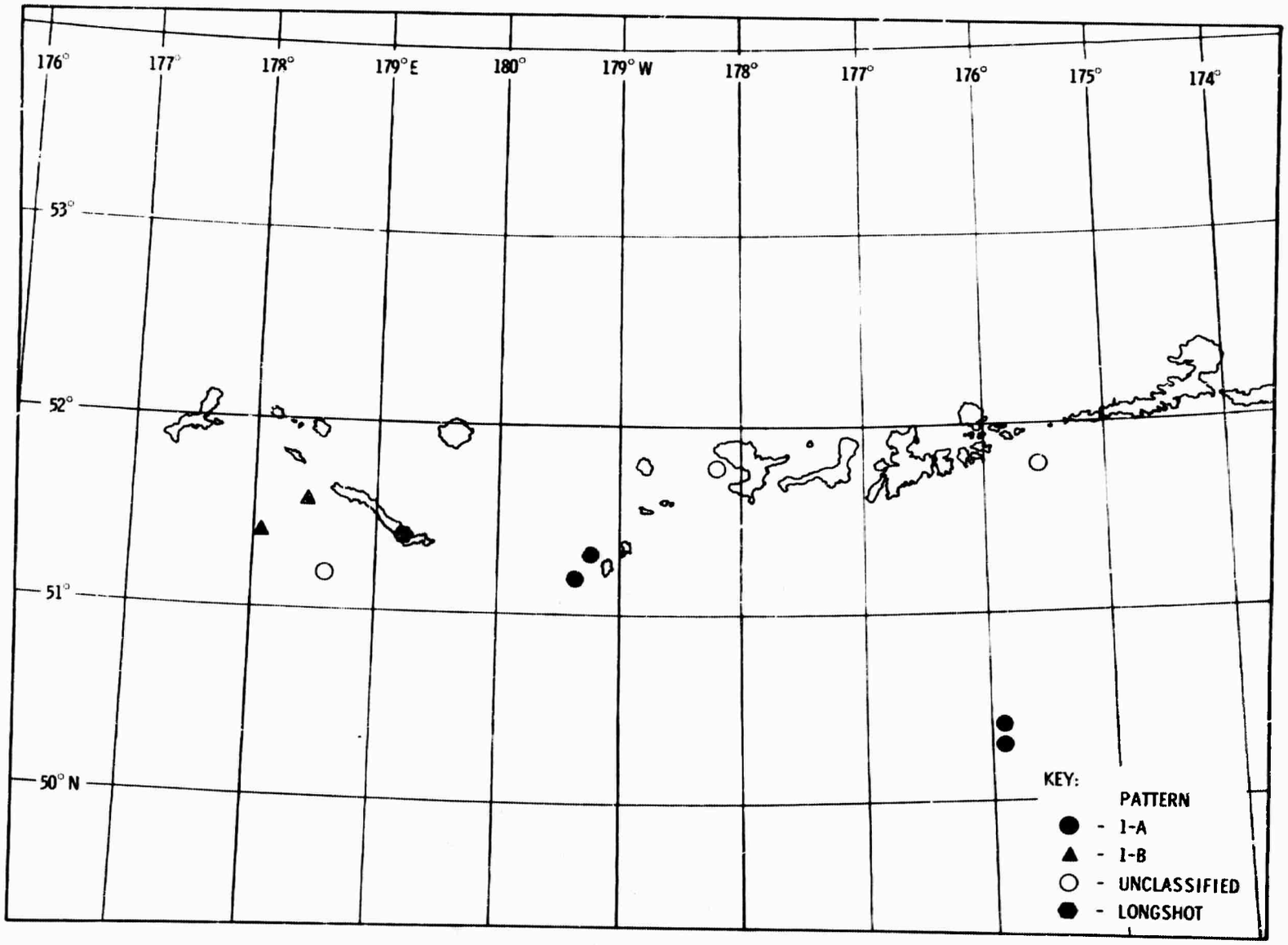

Figure II-13. Location of Rat Islands Events

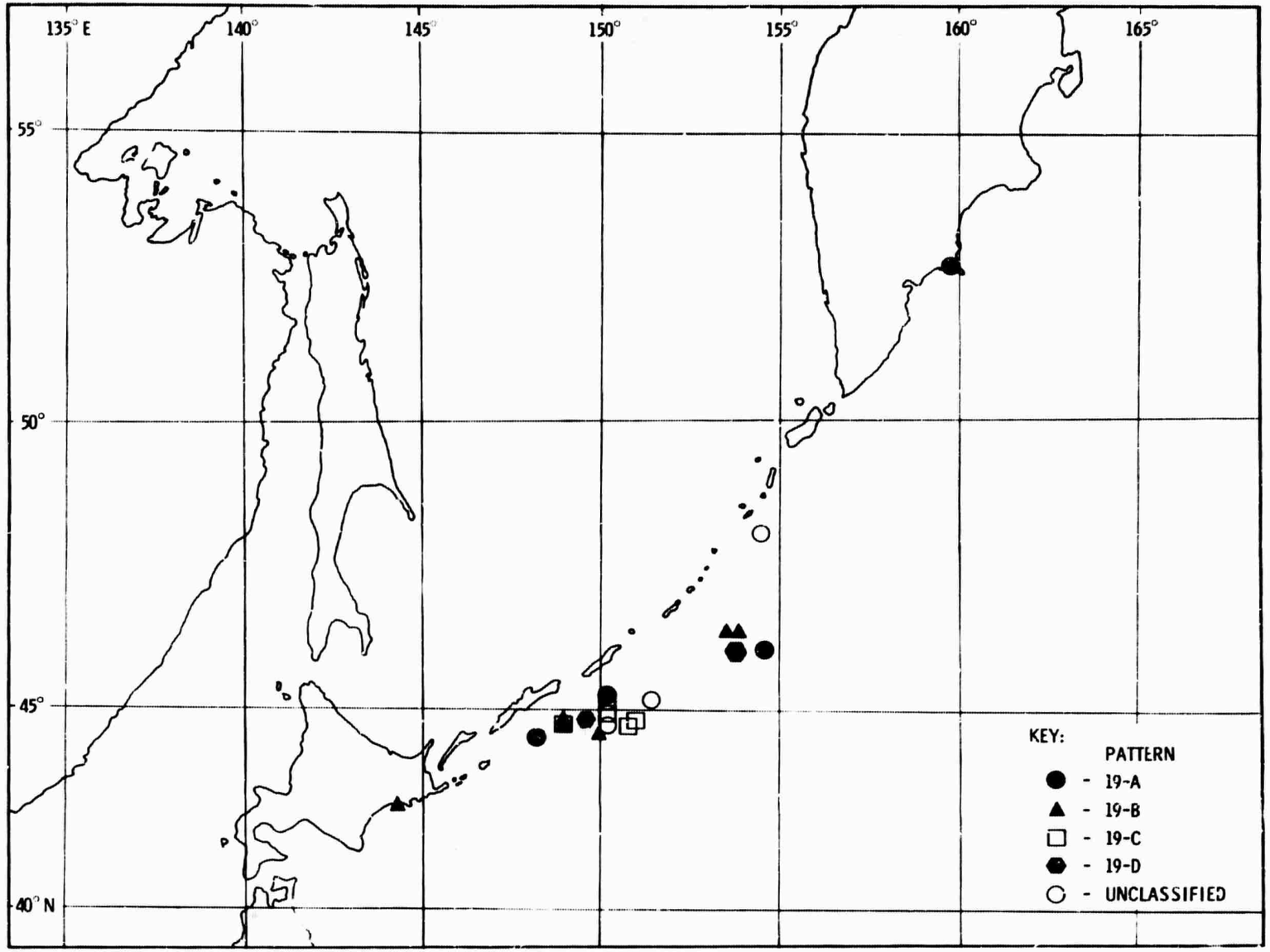

Figure II-14. Location of Kurile Islands Events

Four patterns of magnitude residuals are observed for the 20 events studied. Pattern 19-A shows no clear indication of the location of a nodal plane, but all events fitting this pattern do appear to have a maximum of P-wave energy passing through the Eastern United States. Average magnitude residuals in the Western United States and Western Europe are about equal for events classified with pattern 19-A. Events 2098, 2319, 5422, and 5771 are grouped together as fitting pattern 19-A, as shown in Figure II-15.

Events 3429, 5298, 5425, 5520, 5524, and 5578 are classified as pattern 19-B events. Again, there is no clear definition of a nodal plane for this pattern, although residuals at the westernmost stations in sector 4 indicate the nodal plane may be closer to the U.S. West Coast than in pattern 19-A. Mean magnitude residuals in sector 3 are also lower than in pattern 19-A, while the mean residual in Western Europe (sector 19) is considerably higher, indicating that a maximum of P-wave energy may be radiated in this direction. Figure II-16 shows pattern 19-B and the events associated with it.

Events 5375, 5390, 5484, and 5550 are classified as pattern 19-C events. Figure II-17 shows the pattern and the events associated with it. For this pattern, there is considerable evidence of a nodal plane passing through the Western United States. Also, a maximum of P-wave energy appears to be propagated in the direction of the Hawaiian Islands. Mean magnitude residuals in the Eastern United States and Western Europe are about the same. It is interesting to note that the difference between the mean magnitude residuals in the Eastern U.S. and the Western U.S. (sectors 3 and 4) remains nearly constant at approximately 0.3 magnitude units for all three patterns. Mean magnitude residuals in both sectors are most positive for pattern 19-A and become progressively more negative for patterns 19-B and 19-C.

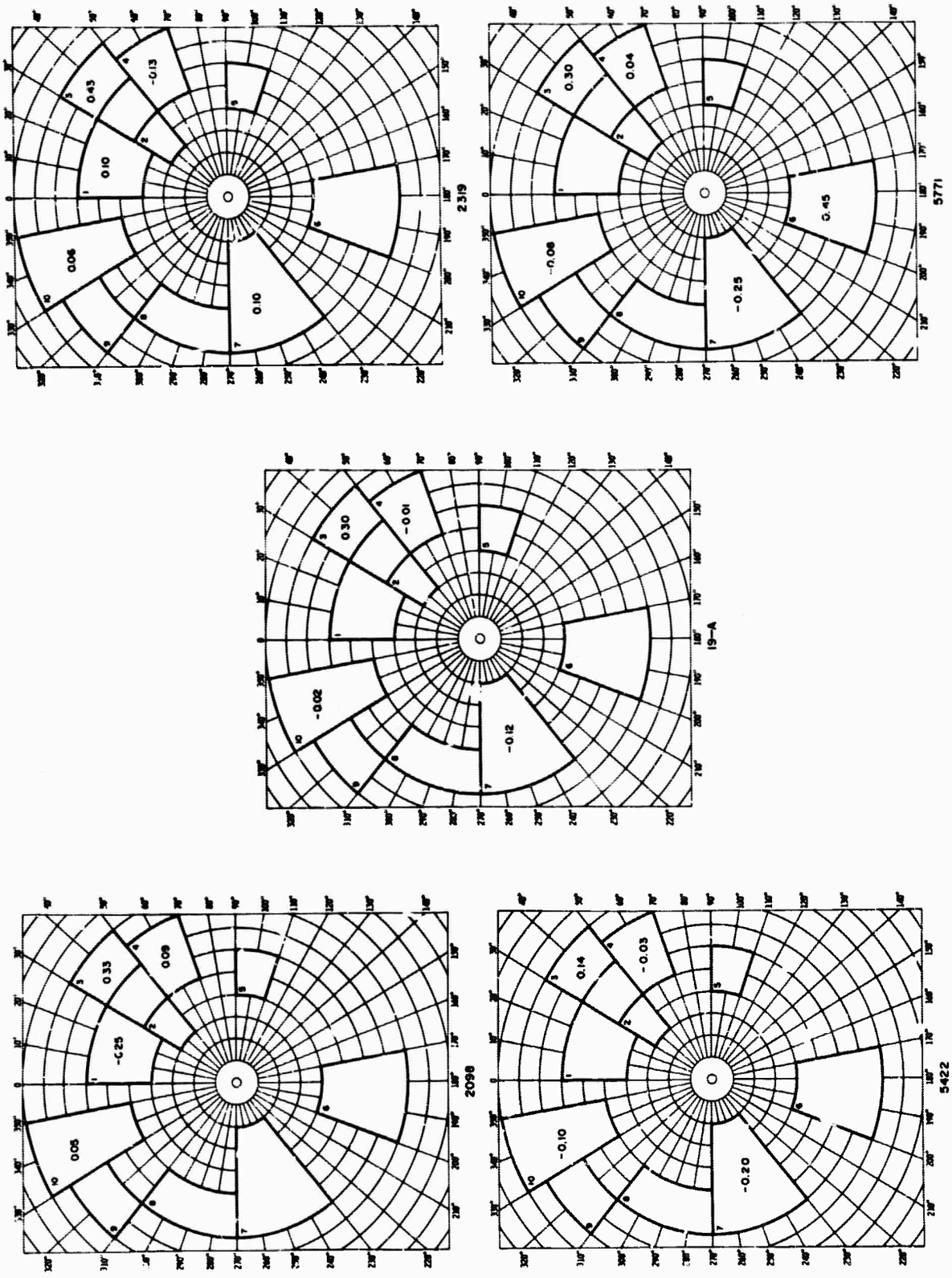

Figure II-15. Magnitude Residual Pattern 19-A and Associated Events

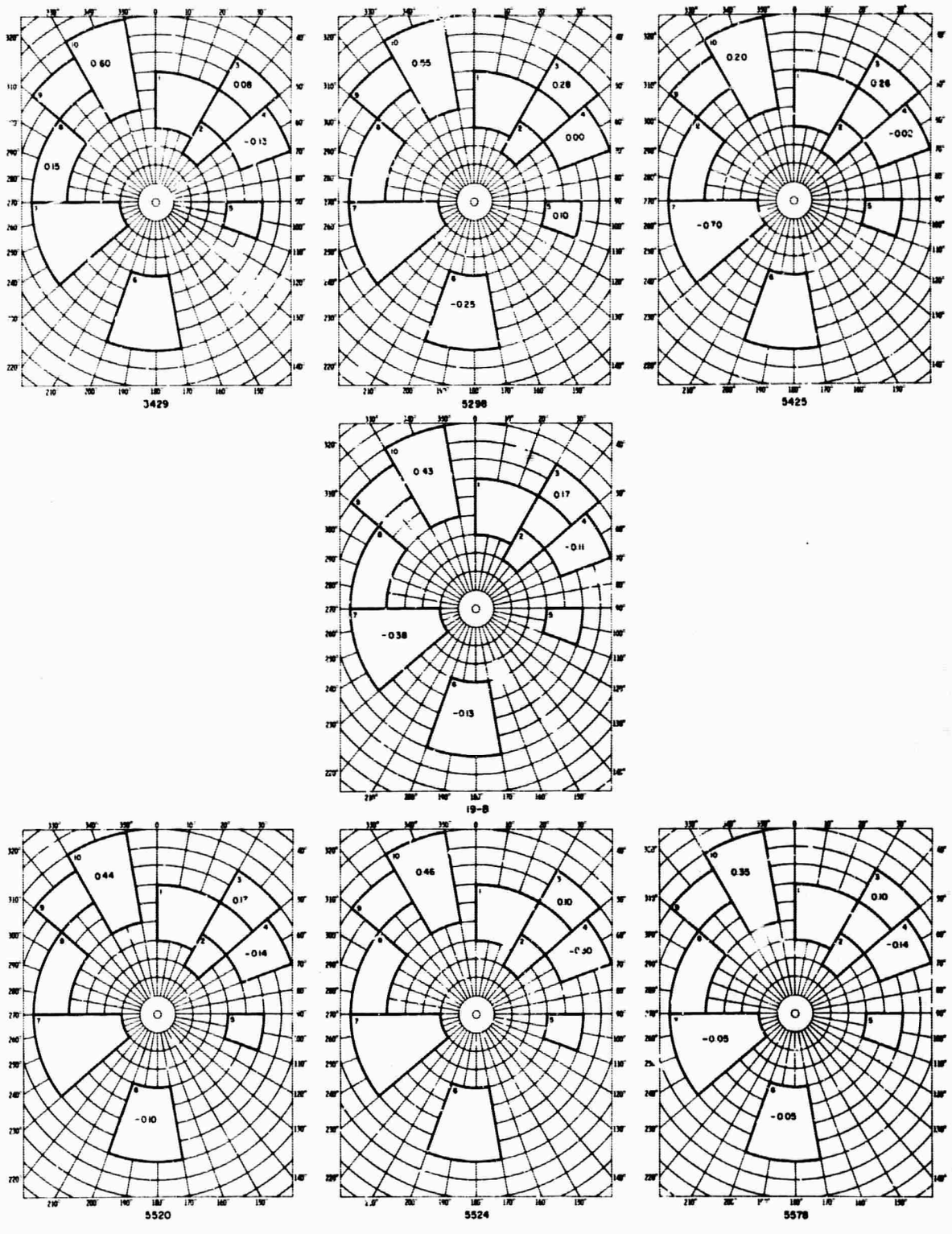

Figure II-16. Magnitude Residual Pattern 19-B and Associated Events

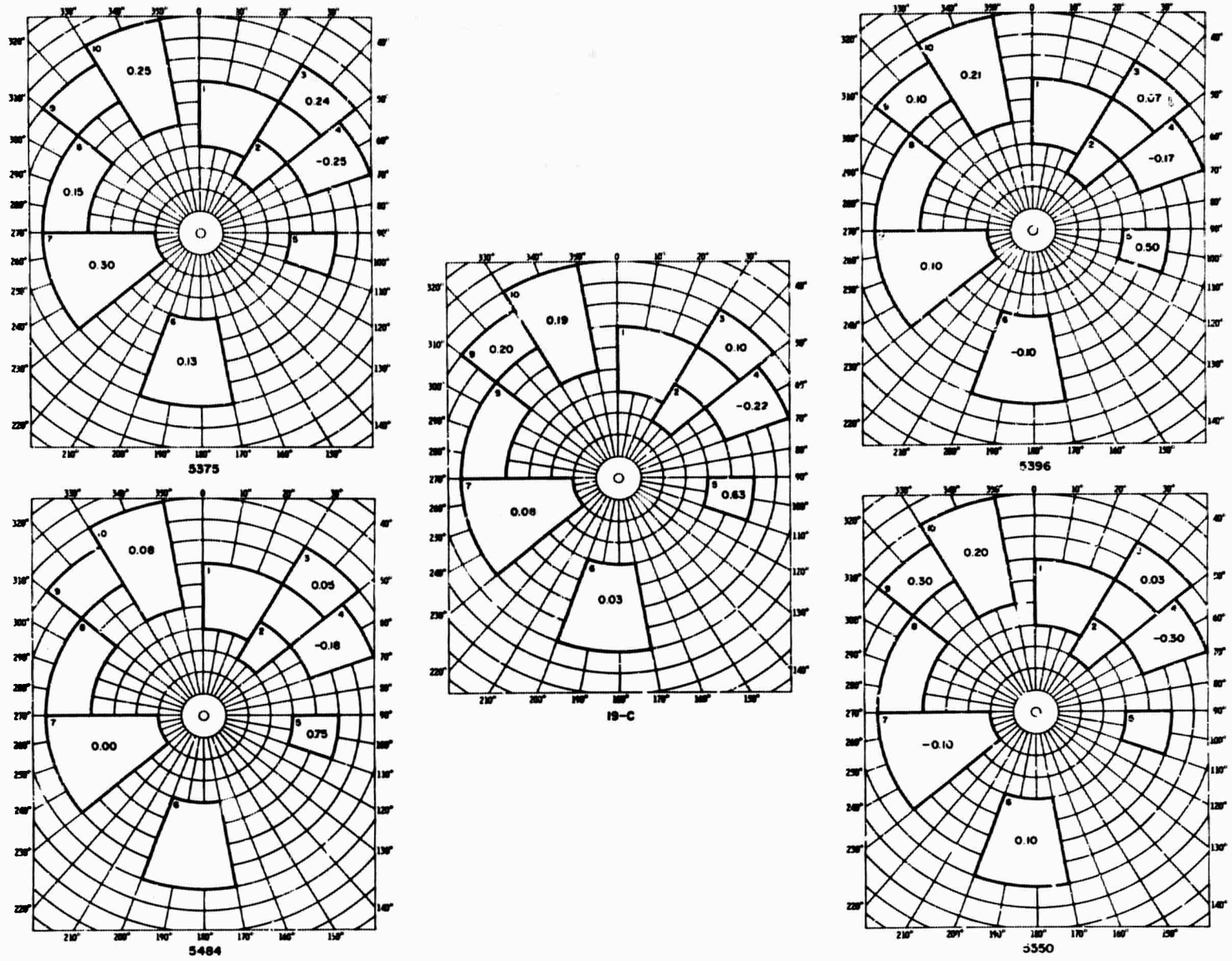

Figure II-17. Magnitude Residual Pattern 19-C and Associated Events

Events 5327 and 5523 have markedly similar magnitude residual patterns and are grouped together as pattern 19-D (Figure II-18). As in pattern 19-C, a nodal plane appears to pass through or near the Western United States (sector 4). However, the maximum of P-wave energy appears to be in the directions of the Eastern United States, Western Europe, and possibly Hawaii. The difference between mean residuals in the Eastern U.S. and the Western U.S. (sectors 3 and 4) is double those observed for patterns 19-A, -B, and -C. It may be that a focal mechanism was operating for events 5327 and 5523 that was different from that operating for the 14 events associated with the other three patterns.

The remaining four events (3366, 3401, 5423, and 5583) fit none of the four patterns observed and have patterns considerably dissimilar with one another. Observed magnitude residual patterns for these events are shown in Figure II-19.

Little correlation with event location and magnitude residual pattern is evident for the Kurile Islands events. Only those events classified with pattern 19-B are much restricted in areal extent. Even in this case, as may be seen in Figure II-14, events with different patterns are intermixed with those of pattern 19-B (with respect to location). Correlation with depth is also poor. Depths range from 26 km to 40 km for events classified with pattern 19-A, from 25 km to 80 km for pattern 19-B, from 25 km to 60 km for pattern 19-C, and 60 km and 33 km for pattern 19-D (probably restrained after a negative depth was encountered).

Time of occurrence does not appear a factor in separation into patterns either, since most events studied occurred in October 1963. Thus, while Rat Islands patterns are separated with respect to depth range, location, and time of occurrence, no such correlation can be made for Kurile Islands patterns.

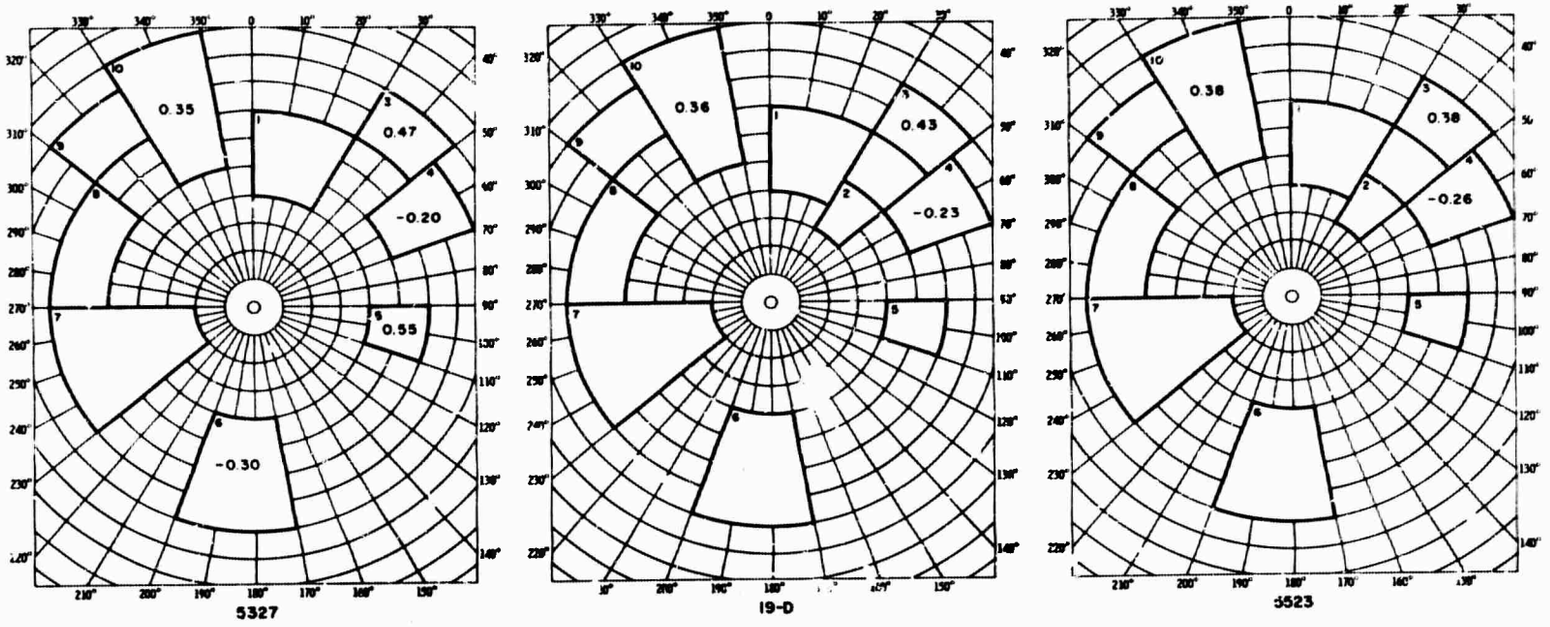

Figure II-18. Magnitude Residual Pattern 19-D and Associated Events

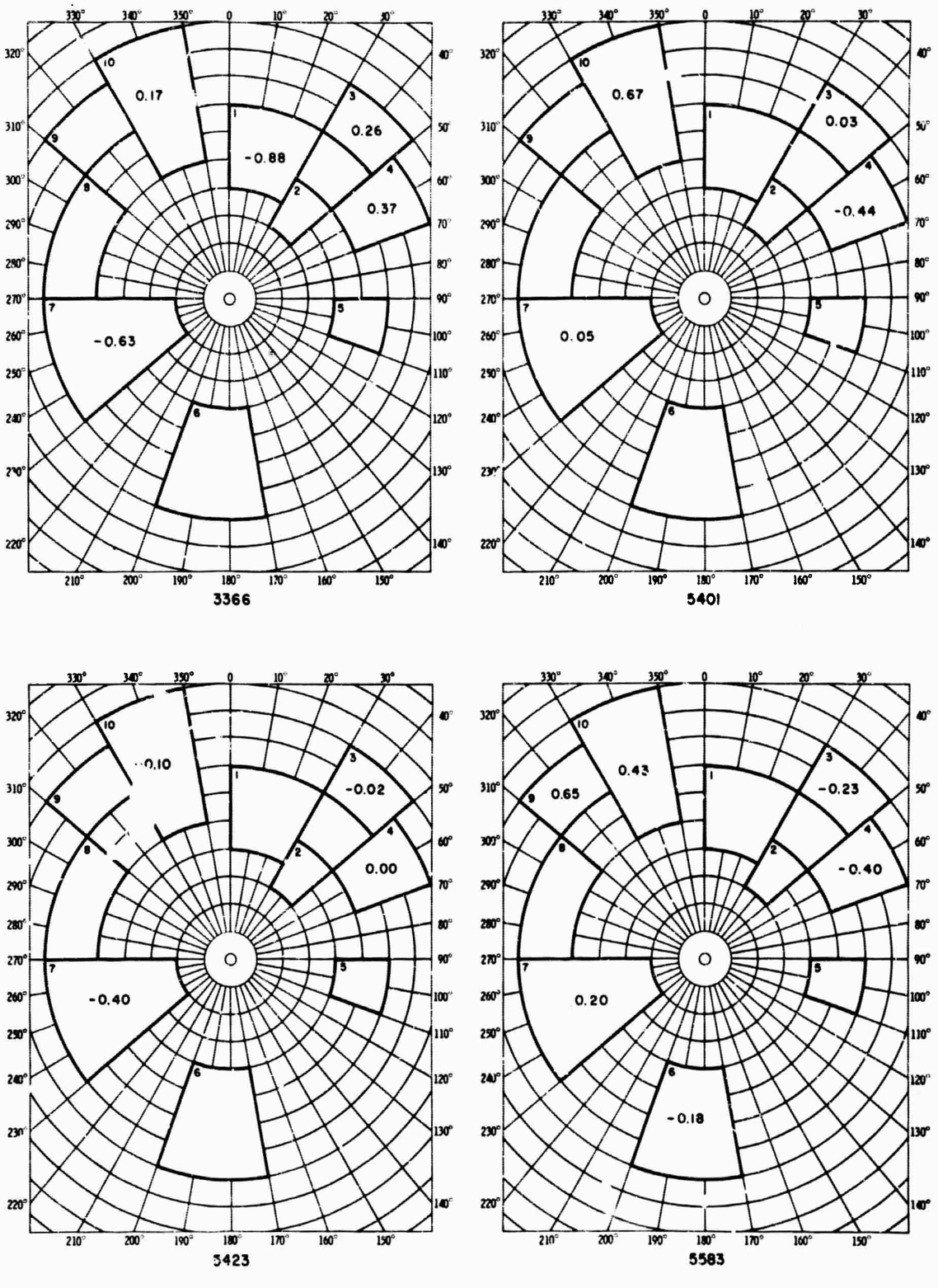

Figure II-19. Kurile Islands Events Investigated but Not Classified According to Magnitude Residual Pattern

4. Critique

This study indicates that classification of events according to patterns of magnitude residuals may be possible. Additionally, t s study shows that there may be several such patterns observed for events located in close proximity to each other. Also, these patterns may be qualitatively correlated with various focal parameter orientations and indicate possible differences in focal mechanisms. However, it must be stressed that the results obtained apply only to the two regions studied and attempts should not be made to extrapolate these results to other regions.

As a check of the effectiveness of the method, magnitude residuals from the LONGSHOT nuclear event were subjected to an analysis similar to that for the Rat Islands events. The observed pattern (Figure II-20) would not be classifed as either 1-A or 1-B. To properly assess the effectiveness of the method, more events, particularly Aleutian Islands events, need analysis of the type performed in this study. Data quality is probably as good as can be currently obtained. However, several factors influence the data:

- Possible difference in amplitude measurement criteria
- Errors in depth-distance factors used in magnitude computation
- Effects of station environment on recorded amplitudes, affecting computed magnitudes

Minimization of the effects of the factors just mentioned, plus considerably more widespread reporting of short-period P-phase amplitudes, might considerably enhance the effectiveness of the method used in this study as a means of assessing seismic-event focal mechanisms and might add a further criterion for discrimination between earthquakes and explosions.

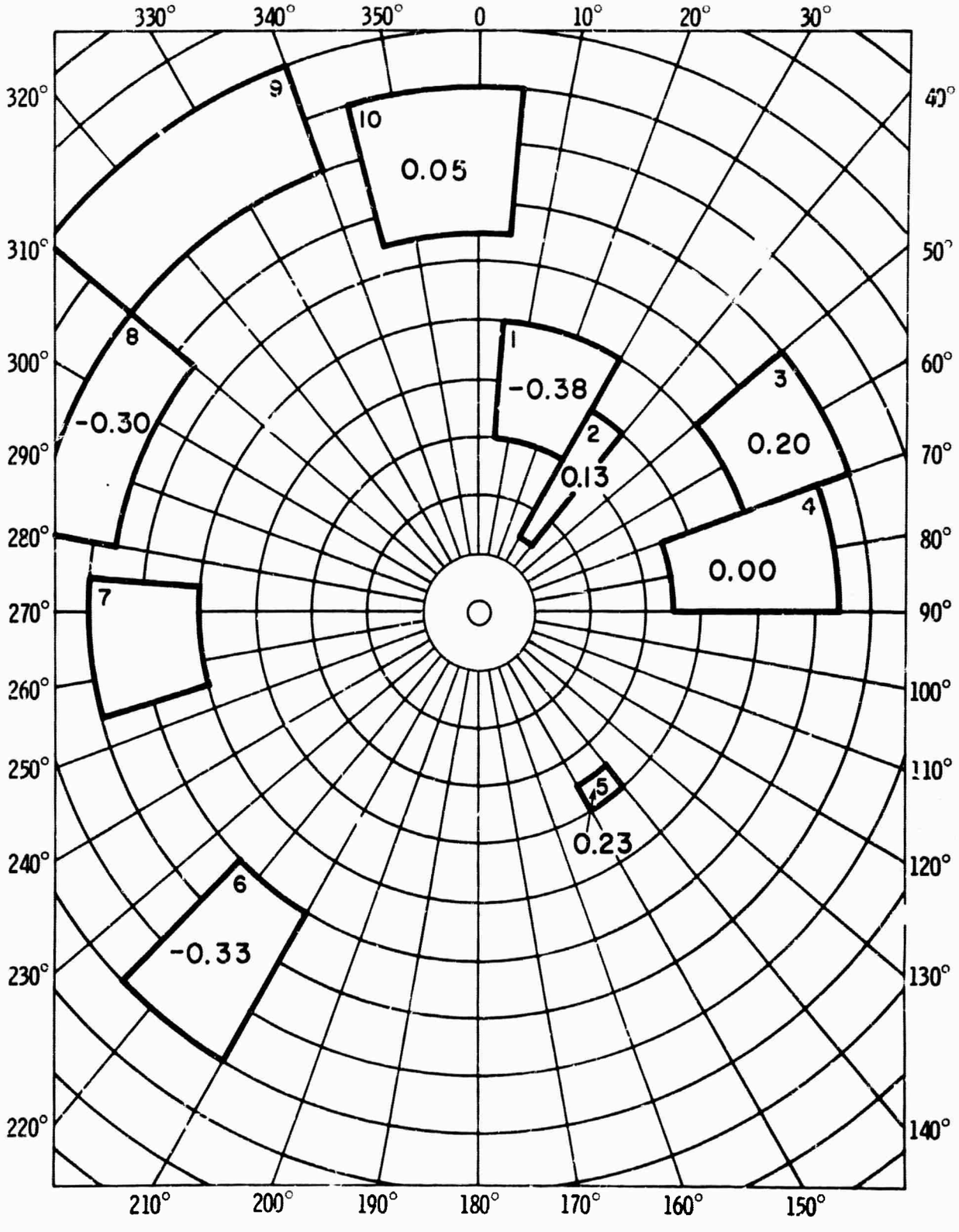

Figure II-20. Magnitude Residual Pattern Observed from LONGSHOT Nuclear Explosion

SECTION III

CRITIQUE

Data for this study were accumulated from nearly every available source. Of the highly capable seismograph stations operating in 1964, there were few, if any, from which data were not collected in one form or another for this project. Data collected by the U.S. Coast and Geodetic Survey, the International Seismological Centre at Edinburgh, Scotland, and the Seismic Data Laboratory at Alexandria, Virginia, were made available to Texas Instruments Incorporated for this study. In addition, microfilm records from 39 of the most capable Worldwide Standard Stations, from five Canadian stations, and from Matsushiro, Japan, were obtained and subjected to detailed analyses. These data were supplemented by data obtained from bulletins of various seismograph stations and networks of stations.

Considerable reliance has been placed on statistical procedures in the development of methods and the analysis of data. Such procedures, it is felt, are appropriate for studies such as this one which involve large quantities of data. Also, methods developed for the processing of array-station data have, in this study, been applied to single-station data employing the "world-array" concept. The two investigations of such application have demonstrated the feasibility of the approach when applied to records originally recorded on magnetic tape.

Conclusions reached in this study are based on well-documented results usually obtained from large quantities of data. Also, these conclusions and the results upon which they are based are, in every case, relevant to the original objectives of the study.

A lack of funds to complete the processing of all 1964 data precluded the achievement of all of the original objectives; however, the following objectives were satisfied:

- A computer program was written, tested and used for revision of January 1964 hypocenters
- The program included several innovations which represented improvements in accuracy and data-handling capability
- Studies of depth phases resulted in assessments of their reliability as depth indicators and resulted in means of increasing the capability of identifying such phases
- Relationships between magnitude scales were investigated thoroughly, and the combination of various magnitudes as an average was concluded to be statistically invalid, even though some physical meaning might be attached to such averages
- P-wave magnitudes computed from data within 1000 km of the source were found to be highly unreliable; the observed variations were likely related to crustal differences
- Patterns were observed in magnitude residuals, suggesting that such procedures be used for studying source mechanisms and possibly as a discrimination criterion

- Seismic activity near a station was found to vary considerably from place to place

In addition to achieving the specific objectives just outlined, the study obtained results which

- Demonstrated the applicability of array processing techniques to single-station data combined as a "world array"
- Established a means of easily assessing epicenter-location accuracy from the distribution of time residuals
- Allowed the computation of nonlinear or "exact" confidence regions

Thus, it is felt that the original objectives were met as well as possible within the financial limitations imposed and, in some cases, were exceeded.

SECTION IV

REFERENCES AND BIBLIOGRAPHY

Båth, Markus, 1952: Earthquake Magnitude Determination from the Vertical Component of Surface Waves, Trans., Am. Geophys. Union, v. 33, n. 1.

Booker, Aaron, 1963: Nonlinear Estimation, Iowa State Univ. of Sci. and Tech., Ames, Iowa.

Geotechnical Corporation, 1963-64: Long-Range Seismic Measurements Program, Jan.-Dec. 1963, Seis. Bull. n. 13-24, May 1963-Aug. 1964.

Geotechnical Corporation: Registration of Earthquakes at Wichita Mountains Seismological Observatory, v. 3, n. 1.

Geotechnical Corporation: Registration of Earthquakes at Blue Mountains Seismological Observatory, Cumberland Plateau Seismological Observatory, Uinta Basin Seismological Observatory, and Wichita Mountains Seismological Observatory, v. 2, n. 2 and 3.

Geotechnical Corporation: Registration of Earthquakes at Blue Mountains Seismological Observatory, Cumberland Plateau Seismological Observatory, Tonto Forest Seismological Observatory, Uinta Basin Seismological Observatory, and Wichita Mountains Seismological Observatory, v. 2, n. 4-12.

Gutenberg, B., 1945a: Amplitudes of Surface Waves and Magnitudes of Shallow Earthquakes, Bull. Seis. Soc. Am. v. 35, n. 1.

Gutenberg, B., 1945b: Amplitudes of P, PP, and S and Magnitudes of Shallow Earthquakes, Bull. Seis. Soc. Am., v. 35, n. 2.

Gutenberg, B., 1945c: Magnitude Determination for Deep-Focus Earthquakes, Bull. Seis. Soc. Am., v. 35, n. 3.

Gutenberg, B., 1948: On the Layer of Relatively Low Wave Velocity at a Depth of about 80 Kilometers, Bull. Seis. Soc. Am., v. 38, n. 2.

Gutenberg, B. and C. F. Richter, 1942: Earthquake Magnitude, Intensity, Energy and Acceleration, Bull. Seis. Soc. Am. v. 32, n. 3.

Gutenberg, B. and C. F. Richter, 1956, Magnitude and energy of earthquakes: Annali di Geofisica, v. 9, n. 1.

Richter, C. F., 1935: An Instrumental Earthquake Scale, Bull. Seis. Soc. Am., v. 25, n. 1.

Richter, C. F., 1958: Elementary Seismology, W. H. Freeman and Co., San Francisco, Calif.

Texas Instruments Incorporated, 1963: Seismological Bulletin, Blue Mountains Seismological Observatory, Cumberland Plateau Seismological Observatory, and Uinta Basin Seismological Observatory, Seis. Bull., Jan.

Texas Instruments Incorporated, 1964a: Final Rpt. on Evaluation of 1960 Seismicity, Contract AF 19(604)-8517, 15 Jan.

Texas Instruments Incorporated, 1964b: Final Rpt. on Evaluation of 1963 Seismicity, Contract AF 19(604)-8517, 18 Nov.

Texas Instruments Incorporated, 1965a: Semiannual Tech. Rpt. No. I, Contract C-104-65, 28 Apr.

Texas Instruments Incorporated, 1965b, Semiannual Tech. Rpt. No. II, Contract C-104-65, 28 Oct.

Texas Instruments Incorporated, 1966, Semiannual Tech. Rpt. No. III, Contract C-104-65, 28 Apr.

United States Coast and Geodetic Survey, 1963. Notes on Magnitude Determination.

United States Coast and Geodetic Survey, 1963-64: Earthquake Data Reports, 11 Mar.-10 Feb.

APPENDIX A

REVISED HYPOCENTERS, JANUARY 1964

BLANK PAGE

APPENDIX A

REVISED HYPOCENTERS, JANUARY 1964

A total of 344 hypocenter locations published by the USC&GS for January 1964 were input to the Texas Instruments Incorporated hypocenter program. Of these, 333 revisions are presented. Six locations cannot be determined from the data supplied, and five revisions yield results which are incompatible with observations of earthquake occurrences. It had been planned to reprocess these 11 events, but circumstances did not allow it.

The computer program used by Texas Instruments (described in Technical Report No. III, 1966) was written for the CDC 6600.

The following are the column headings for the data presented:

EVENT	Chronological number assigned to each event located by the USC&GS
SOURCE	TI and PDE for Texas Instruments revised hypocenter and input preliminary hypocenters located by the USC&GS, respectively
HR, MIN, SEC	Origin time (GCT) in hours, minutes, seconds, and tenths of seconds
LAT.	Geographical latitude in degrees
LONG.	Geographical longitude in degrees
DEPTH	Depth of earthquake foci in km; (*depth restrained to 33 km after negative depth encountered iteration process)
N	Number of stations used for each location
SD	Standard deviation for each location in seconds (shown for TI data only)
A, B, and C	Semiminor axis, semimajor axis, and inclination of the 70-percent confidence ellipses (shown for TI data only)
MB and MS	Magnitudes computed on m_b and M_s scales, respectively
REG	Seismic region based on Gutenberg and Richter's (1954) region as modified by Flinn and Engdahl (1964)

EVENT	SOURCE	HR	MIN	SEC	LAT	LONG	DEPTH	N	SD	A	B	C	MB	MS	REG	
1 JANUARY 1964																
1	TT	04	22	13.4	43.7N	126.3W	33*	7	1.9	13	20	38	3.8		3	
	PDE	04	22	13.4	43.7N	126.3W	33	6					3.7		3	
2	TT	05	14	25.3	37.7N	142.8E	17	19	0.6	3	5	-20	4.3		19	
	PDE	05	14	26.5	37.4N	142.7E	33	10					4.1		19	
3	TT	09	14	02.1	19.1S	169.6E	247	10	0.9	6	7	6	4.4		14	
	PDE	09	14	01.8	19.1S	169.5E	247	10					4.4		14	
4	TT	09	43	59.5	18.2N	105.9W	33*	19	2.5	13	44	5	4.5		5	
	PDE	09	43	59.5	18.2N	105.9W	33	16					4.4		5	
5	TT	09	45	29.5	23.8S	67.5W	203	8	0.8	5	9	18	4.2		8	
	PDE	09	45	28.7	23.9S	67.4W	220	7					4.1		8	
6	TT	12	21	56.6	6.8S	129.8E	103	66	1.5	4	9	35	5.5		24	
	PDE	12	21	55.4	6.8S	129.8E	96	23					5.7		24	
7	TT	14	16	27.6	41.4S	74.4W	33*	7	1.0	29	138	-1	4.6		9	
	PDE	14	16	27.6	41.4S	74.4W	33	5					4.7		9	
8	TT	14	19	1.8	4.3S	106.1W	180	27	1.2	5	20	6	4.2	6.5	44	
	PDE	14	18	53.9	4.3S	105.9W	33	18					4.6		44	
9	TT	15	49	52.5	55.9S	27.1W	84	16	1.4	11	29	18	5.2		10	
	PDE	15	49	47.0	55.8S	27.1W	33	12					5.4		10	
10	TT	16	43	13.3	37.8N	112.7W	41	9	5.4	23	37	6	3.1		34	
	PDE	16	43	08.0	37.7N	112.5W	15	6							34	
11	TT	17	26	39.2	45.5N	151.8E	13	155	1.8	4	6	-5	5.4	5.0	19	
	PDE	17	26	43.5	45.4N	151.9E	45	55					5.6		19	
12	TT	19	45	11.0	19.6N	106.0W	105	9	2.7	12	50	13	3.7		5	
	PDE	19	45	45.1	23.9N	105.9W	33	6					4.0		34	
13	TT	20	02	28.1	3.2S	139.7E	4	35	1.2	5	7	40	5.1	3.7	16	
	PDE	20	02	32.5	3.2S	139.7E	33	15					6.3		16	
14	TT	21	04	25.0	45.6N	151.6E	10	18	1.5	10	16	-23	4.5		19	
	PDE	21	04	28.5	45.5N	151.8E	40	10					4.2		19	
15	TT	22	42	22.6	45.6N	151.8E	13	48	0.9	4	6	12	4.9		19	
	PDE	22	42	27.0	45.5N	151.7E	45	23					4.7		19	
16	TT	23	40	40.8	45.5N	151.9E	34	38	1.3	7	9	9	4.6		19	
	PDE	23	40	44.1	45.5N	151.9E	60	20					4.5		19	
2 JANUARY 1964																
17	TT	00	11	14.9	6.1S	105.1W	33*	10	1.4	23	191	7	4.3		44	
	PDE	00	11	14.9	6.1S	105.1W	33	7					4.4		44	
18	TT	05	01	53.9	53.1N	159.8E	45	71	1.4	5	9	-10	5.0		19	
	PDE	05	01	53.5	53.0N	159.6E	40	32					4.9		19	
19	TT	05	21	03.1	54.6N	161.6E	60	49	1.1	4	8	-15	4.8	5.9	19	
	PDE	05	21	00.5	54.6N	161.5E	33	28					4.9		19	
20	TT	06	32	59.5	21.6S	68.1W	120	40	1.5	6	17	24	4.9		8	
	PDE	06	32	58.9	21.6S	68.2W	110	26					5.1		8	
21	TT	17	28	35.1	36.4N	71.1E	237	29	0.9	3	5	13	4.5		48	
	PDE	17	28	35.5	36.4N	71.1E	233	12					4.8		48	
22	TT	18	16	12.3	3.1S	130.0E	33*	7	9.2	60	109	33			23	
	PDE	18	16	12.3	3.1S	130.0E	33	6					4.3		23	
23	TT	19	15	22.5	8.3S	157.1E	12	50	2.0	7	9	41	5.3	3.9	15	
	PDE	19	15	23.9	8.4S	157.1E	33	21					5.5		15	
24	TT	19	48	39.4	35.0N	118.4W	29	15	1.4	6	7	-43	4.5		3	
	PDE	19	48	37.9	35.0N	118.4W	14	14					4.4		3	
3 JANUARY 1964																
25	TT	00	45	20.4	5.9S	146.7E	34	8	2.3	14	21	0	4.5		16	
	PDE	00	45	20.4	5.9S	146.7E	34	7					4.6		16	
26	TT	00	59	34.3	8.6S	157.4E	53	20	2.4	11	15	-41	4.7	6.0	15	
			59	33.8	8.5S	157.4E	61	12					4.8		15	
27	TT	03	17	58.0	23.3S	179.7W	432	13	0.6	4	7	8	4.3		12	
	PDE	03	18	02.4	23.4S	180.0	509	11					4.5		12	
28	TT	05	20	33.8	19.5S	69.2W	116	8	6.7	33	73	7	3.6		8	
	PDE	05	20	32.0	19.4S	69.2W	62	6					4.1		8	

EVENT	SOURCE	HR	MIN	SEC	LAT	LONG	DEPTH	N	SD	A	B	C	MB	MS	REG
29	TT	06	14	31.6	7.0S	128.8E	89	12	2.0	12	21	35	5.2		24
	PDE	06	14	24.4	6.9S	129.7E	33	9							24
30	TT	07	14	55.8	7.1S	129.1E	165	26	1.7	7	14	31	4.6		24
	PDE	07	14	54.2	7.1S	130.0E	157	11							24
31	TT	13	27	44.6	5.0S	77.3W	33*	12	8.4	43	201	20	4.2		8
	PDE	13	27	44.6	5.0S	77.3W	9	6					4.2		8
32	TT	14	41	46.7	44.8N	151.5E	33*	9	7.0	52	131	41	4.0		19
	PDE	14	41	46.7	44.9N	151.5E	33	5					4.0		19
33	TT	16	37	15.9	36.2N	71.3E	78	58	1.5	4	9	17	4.7		48
	PDE	16	37	12.4	36.0N	71.3E	123	10					4.5		48
34	TT	17	21	02.1	53.0N	173.1E	110	69	1.0	4	7	-3	4.8	5.7	1
	PDE	17	20	54.0	52.9N	173.1E	33	22					4.9		1
35	TT	21	24	57.2	20.2S	178.3W	559	47	1.1	5	6	34	5.0		12
	PDE	21	24	56.3	20.4S	178.2W	520	28					5.3		12
36	TT	21	48	05.6	53.0S	21.2E	33*	9	2.0	21	41	-6	7.3		33
	PDE	21	48	05.6	53.0S	21.2E	33	7							33
37	TT	22	12	09.7	1.5S	79.3W	33*	7	1.0	12	72	26	4.2		8
	PDE	22	12	09.1	1.5S	79.3W	33	5					4.4		8
4 JANUARY 1964															
38	TT	03	41	22.2	3.5S	148.9E	2	14	5.3	29	37	24	4.4	4.9	16
	PDE	03	41	22.6	3.4S	149.2E	33	9					4.3		16
39	TT	10	38	58.6	21.7N	121.7E	34	44	1.8	6	10	24	5.1		21
	PDE	10	38	58.8	21.6N	121.8E	33	20					4.7		21
40	TT	16	17	16.2	44.5N	150.7E	51	49	4.9	23	28	2	4.8		19
	PDE	16	17	16.5	44.4N	150.8E	38	20					4.7		19
41	TT	16	44	18.5	21.8N	121.8E	38	32	2.1	8	11	27	4.8		21
	PDE	16	44	16.9	21.7N	121.8E	33	8							21
42	TT	17	40	27.4	5.6S	150.4E	146	12	2.6	13	26	-18	5.2		15
	PDE	17	40	23.3	5.5S	150.0E	117	8					5.2		15
43	TT	21	12	09.1	52.8S	20.8E	34	7	1.7	14	43	-6	5.0	4.2	33
	PDE	21	12	09.3	52.9S	20.9E	33	5							33
44	PDE	22	45	46.6	1.9S	102.3E	33	5							46
5 JANUARY 1964															
45	TT	01	31	27.3	61.9N	149.9W	89	18	1.2	6	12	-5	4.2	5.8	1
	PDE	01	31	27.0	61.9N	149.5W	72	11					4.6		1
46	PDE	03	05	44.1	20.6S	179.0W	650	13					4.6		12
47	TT	07	06	51.2	54.9N	160.4W	109	12	0.9	6	11	-30	4.0	5.8	1
	PDE	07	06	40.2	54.6N	161.2W	33	10					4.1		1
48	TT	07	11	26.3	37.5S	72.6W	62	14	5.5	28	103	4	4.2		8
	PDE	07	11	26.5	37.6S	72.5W	61	11					4.3		8
49	TT	08	57	22.1	32.6N	141.6E	34	44	4.6	20	33	1	4.9		18
	PDE	08	57	22.3	32.5N	141.7E	33	20					4.8		18
50	TT	09	08	16.0	17.1N	60.7W	34	20	7.7	36	46	30	4.1	3.5	7
	PDE	09	08	15.2	17.2N	60.6W	33	9					4.2		7
51	TT	10	11	52.8	26.9S	175.8W	32	47	9.4	37	64	-36	5.5	4.9	12
	PDE	10	11	53.0	26.6S	175.7W	31	25					5.1		12
52	TT	12	00	05.1	53.8N	165.2W	66	63	1.0	4	6	-14	4.7	5.8	1
	PDE	12	00	05.0	53.8N	165.3W	63	27					4.8		1
53	TT	13	57	23.5	41.3N	109.6W	67	8	4.9	25	31	-12	3.5		34
	PDE	13	57	18.3	41.1N	109.3W	15	7					3.9		34
54	TT	15	17	40.7	43.5N	144.4E	76	13	2.0	17	28	-42	4.6		19
	PDE	15	17	43.6	43.1N	144.4E	110	9					4.3		19
55	TT	15	49	15.7	0.4N	78.2W	60	12	1.4	7	21	30	4.2		8
	PDE	15	49	12.7	0.4N	78.2W	33	11					4.1		8
56	TT	16	25	49.9	61.3S	155.5E	1	23	5.0	20	89	-4	5.0	4.7	45
	PDE	16	25	52.6	61.4S	154.9E	33	10							45
57	TT	17	15	14.2	29.8S	105.2E	33*	9	2.1	230	688	2	4.4		43
	PDE	17	15	14.2	29.8S	105.2E	33	7					4.5		43
58	TT	17	50	52.6	51.3N	179.5E	102	13	0.7	5	9	44	4.5	6.4	1
	PDE	17	50	45.3	51.1N	179.6E	33	11					4.3		1

EVENT	SOURCE	HR	MIN	SEC	LAT	LONG	DEPTH	N	SD	A	B	C	MB	MS	REG
59	TT	18	33	54.7	8.9S	74.5W	147	99	1.2	3	7	14	5.1		8
	[illegible]	18	33	54.7	8.9S	74.5W	110	48					5.2		8
60	TT	20	25	50.2	21.6S	69.8W	71	13	1.4	6	16	2	4.3		8
	PDE	20	25	52.4	21.5S	69.8W	70	9					4.2		8
61	TT	23	46	1[illegible].7	53.2S	28.6E	33*	61	3.4	15	37	1	5.8	5.5	33
	PDE	23	46	1 .7	53.2S	28.6E	33	28							33
6 JANUARY 1964															
62	TT	05	54	44.1	27.3N	127.3E	124	138	1.6	4	5	19	5.4		20
	PDE	05	54	42.7	27.2N	127.3E	110	35					5.7		20
63	TT	15	07	08.5	44.5N	82.4E	23	41	1.1	4	6	1	4.4		28
	PDE	15	07	09.6	44.2N	82.6E	33	19					4.5		28
64	TT	16	06	39.7	3 .4N	138.4E	450	12	0.8	6	10	-13	4.1		18
	PDE	16	06	35.3	30.4N	138.4E	426	9					4.1		18
65	TT	16	12	46.4	22.7S	67.8W	206	12	0.8	4	9	19	4.2		8
	PDE	16	12	45.5	22.8S	67.7W	206	9					4.4		8
66	TT	19	35	10.7	44.5N	114.2W	25	18	4.2	13	29	0	4.4		3
	PDE	19	35	09.8	44.3N	114.7W	33	10					4.7		3
67	TT	23	06	39.2	6.8N	73.1W	124	9	0.7	4	7	16	4.2		7
	PDE	23	06	32.1	6.9N	73.6W	36	6					4.5		7
68	TT	23	37	52.6	19.3N	108.3W	33*	10	12.4	55	240	4	4.0	6.1	5
	PDE	23	37	52.6	19.3N	108.3W	33	7					4.1		5
69	TT	23	45	27.1	50.9N	157.3E	73	164	1.5	3	6	-7	5.4	6.7	19
	PDE	23	45	23.4	50.9N	157.3E	33	48					5.6		19
70	TT	23	47	09.2	33.8N	116.6W	25	14	2.8	12	14	16	4.4		3
	PDE	23	47	11.4	34.4N	116.5W	14	13							3
7 JANUARY 1964															
71	TT	01	50	11.1	19.2S	169.2E	146	6	2.3	12	15	-44	4.0		14
	PDE	01	50	08.5	19.2S	169.4E	150	5							14
72	TT	02	08	19.4	56.9S	146.0E	66	7	4.1	20	196	1			45
	PDE	02	08	19.1	56.8S	147.7E	33	6							45
73	TT	02	14	59.5	17.8S	178.0W	509	17	1.2	6	15	20	4.4		12
	PDE	02	15	00.6	18.0S	178.0W	593	9					5.0		12
74	TT	03	22	07.3	6.8N	73.1W	140	7	0.5	3	4	32	4.1		7
	PDE	03	21	59.6	7.0N	73.6W	33	5					4.2		7
75	TT	04	41	53.0	18.6N	105.4W	33*	12	3.2	13	42	1	3.7		5
	PDE	04	41	53.0	18.6N	105.4W	33	5					3.8		5
76	TT	04	50	37.0	30.0N	98.8E	33	26	2.3	10	11	-17	4.9		26
	PDE	04	50	37.4	29.8N	98.7E	46	7					5.0		26
77	TT	05	18	30.0	58.8S	149.4E	85	16	4.0	17	56	-3	4.8	6.5	45
	PDE	05	18	24.5	58.8S	149.4E	33	8							45
78	TT	08	46	48.7	54.0N	165.4W	90	44	1.0	5	7	-17	4.8		1
	PDE	08	46	48.0	54.0N	165.4W	80	21					4.7		1
79	TT	10	40	42.9	2.9S	139.0E	43	24	2.6	11	17	37	4.8		16
	PDE	10	40	42.9	3.0S	139.0E	47	15					5.0		16
80	TT	11	06	21.3	18.6N	155.9W	33*	14	5.7	58	76	-21	4.4	3.6	39
	PDE	11	06	21.3	18.6N	155.9W	33	9					4.4		39
81	TT	11	55	34.2	39.2N	114.2W	39	12	7.9	34	47	21	3.9		3
	PDE	11	55	34.2	39.2N	114.2W	39	6					3.6		3
82	TT	12	32	54.9	56.6S	25.2W	61	12	1.6	13	24	10	6.7	6.7	10
	PDE	12	32	54.5	56.8S	26.1W	33	6					5.6		10
83	TT	12	53	47.8	39.1N	114.2W	33*	12	12.7	57	71	13	3.6		3
	PDE	12	53	47.8	39.1N	114.2W	33	7					3.5		3
84	TT	14	00	23.5	2.5N	73.1W	46	5	19.2	99	295	18	4.2		8
	PDE	14	00	23.5	2.5N	73.1W	46	5					4.1		8
85	PDE	15	06	47.1	15.2S	167.2E	99	5							14
86	TT	17	22	27.8	6.9N	73.0W	153	7	0.7	4	5	0	3.9		7
	PDE	17	22	27.3	6.2N	72.5W	213	5					3.7		7
87	TT	20	04	37.8	39.5N	73.8E	44	30	3.3	12	16	0	4.4		48
	PDE	20	04	35.8	39.3N	73.8E	33	7					4.5		48

EVENT	SOURCE	HR	MIN	SEC	LAT	LONG	DEPTH	N	GP	A	B	C	MB	MS	REG
88	TT	20	52	04.0	4.7S	103.2E	81	28	0.9	3	9	-42	5.2		24
	PDE	20	52	04.9	4.6S	103.3E	80	14					5.0		24
89	TT	22	12	30.4	18.4S	173.3W	7	12	1.0	7	20	-35	4.7	3.8	12
	PDE	22	12	33.4	18.3S	173.4W	33	12					4.7		12
9 JANUARY 1964															
90	TT	00	16	20.0	3.2N	101.1W	265	9	1.3	8	33	9	3.9	5.8	44
	PDE	00	15	55.7	3.0N	101.1W	33	7					4.3		44
91	TT	02	11	18.4	51.4N	179.0W	33*	6	1.2	11	29	37	4.2		1
	PDE	02	11	18.4	51.4N	179.0W	33	5					4.2		1
92	TT	04	23	47.8	5.2S	144.4E	73	16	2.0	11	16	33	4.6		16
	PDE	04	23	46.3	5.0S	144.3E	72	8					5.1		16
93	TT	05	47	31.8	54.4N	161.8E	33*	14	5.5	42	63	-27	4.5		19
	PDE	05	47	31.8	54.4N	161.8E	33	9					4.3		19
94	TT	10	04	30.2	46.3N	77.9W	12	38	3.8	12	18	-21	3.8		34
	PDE	10	04	31.6	46.1N	77.7W	33	27					3.8		34
95	TT	11	58	38.9	19.3S	173.4W	3	20	2.4	12	23	-36	4.9	4.1	12
	PDE	11	58	42.5	18.8S	173.8W	33	11					4.8		12
96	TT	13	42	48.9	52.5N	173.6E	101	23	0.8	4	10	-19	4.3		1
	PDE	13	42	41.3	52.3N	173.5E	33	12					4.5		1
97	TT	14	34	51.5	19.2S	69.8W	165	6	0.4	2	4	12	3.9		8
	PDE	14	34	52.5	19.3S	69.0W	199	5					3.9		8
98	TT	16	02	36.2	6.9S	129.5E	166	13	1.1	6	10	44	4.7		24
	PDE	16	02	30.0	6.9S	129.4E	108	6							24
99	PDE	18	46	50.4	44.1N	127.5W	33	5					4.2		3
100	TT	19	44	09.5	68.8N	14.6W	3	7	11.2	98	511	21	4.1		40
	PDE	19	44	13.1	69.3N	15.0W	33	5					4.7		40
101	TT	22	30	50.2	3.7S	119.5E	90	83	1.3	6	31		5.8	6.5	23
	PDE	22	30	49.7	3.7S	119.4E	90	30					5.2		23
102	TT	23	13	50.4	7.2S	155.7E	33	7	1.9	12	18	14	4.6		15
	PDE	23	13	56.1	6.9S	155.3E	101	5					4.2		15
9 JANUARY 1964															
103	TT	02	59	23.3	41.7N	141.8E	66	94	2.0	6	10	-6	5.0		19
	PDE	02	59	21.6	41.7N	141.9E	50	29					5.0		19
104	TT	03	10	59.1	44.3N	114.3W	44	16	2.7	10	20	2	4.1		3
	PDE	03	10	58.3	44.3N	114.6W	33	9					4.5		3
105	TT	11	11	52.0	43.7N	114.4W	3	7	6.3	28	49	-1	3.5		3
	PDE	11	11	55.6	44.2N	114.8W	33	6					3.6		3
106	TT	11	47	57.3	30.7S	65.4W	190	14	0.4	2	5	23	4.3		8
	PDE	11	47	45.0	31.1S	64.4W	119	10					4.3		8
107	TT	18	31	52.6	45.6N	150.9E	40	200	1.5	3	5	-7	5.7	5.0	19
	PDE	18	31	52.4	45.5N	150.9E	40	16					5.6		19
108	TT	18	38	10.8	14.9N	87.9W	33*	7	2.9	51	71	-13	3.5		6
	PDE	18	38	10.8	14.9N	87.9W	33	5					4.7		6
109	TT	20	56	59.2	48.7N	153.1E	124	21	0.6	3	11	-36	4.7		19
	PDE	20	57	01.6	48.6N	153.1E	148	10					4.8		19
110	TT	21	19	38.4	1.2S	89.9W	33*	5	1.9	9	27	29	4.0		44
	PDE	21	19	38.4	1.2S	89.9W	33	6					4.0		44
111	TT	21	23	00.4	20.0S	177.7W	497	9	0.4	3	6	42	3.8		12
	PDE	21	23	08.1	20.0S	178.3W	649	7					4.0		12
112	TT	21	47	11.3	42.3S	174.3E	47	17	2.4	9	18	-21	5.4		11
	PDE	21	47	08.6	42.6S	174.8E	61	9					5.5		11
10 JANUARY 1964															
113	TT	03	34	18.8	38.2N	20.7E	25	16	4.1	17	35	34	4.7		30
	PDE	03	34	20.2	39.0N	21.1E	16	8					4.3		30
114	TT	04	50	53.4	42.0N	142.6E	38	188	1.6	3	5	-8	5.6	4.8	19
	PDE	04	50	53.4	42.0N	142.6E	33	23					5.5		19
115	TT	05	37	05.0	17.4S	69.8W	167	15	0.9	5	8	-43	4.2		8
	PDE	05	37	22.5	15.8S	70.3W	234	8					4.2		8
116	TT	10	52	46.4	44.9N	150.0E	48	45	1.8	8	10	8	4.7	5.8	19
	PDE	10	52	45.6	44.8N	149.6E	33	12					4.5		19

EVENT	SOURCE	HR	MIN	SEC	LAT	LONG	DEPTH	N	SD	A	B	C	MB	MS	REG
117	TT	11	08	20.4	8.0S	120.0E	198	9	2.2	13	23	-34	4.1		24
	PDE	11	08	03.6	7.1S	119.1E	126	6							24
118	TT	11	56	32.7	44.6N	150.5E	34	25	1.3	7	9	29	4.8		19
	PDE	11	56	33.4	44.1N	150.8E	58	9					4.1		19
119	TT	16	52	35.4	14.5S	175.4W	11	32	3.7	18	43	32	5.3	4.6	12
	PDE	16	52	36.2	15.4S	175.0W	33	19					5.0		12
120	TT	16	57	26.3	45.5N	149.9E	53	130	1.1	3	4	-5	5.4	6.1	19
	PDE	16	57	26.5	45.4N	150.0E	50	27					5.4		19
121	TT	19	21	56.9	3.7N	126.6E	11	17	3.0	18	38	34	5.1		23
	PDE	19	21	57.7	2.8N	127.0E	33	7							23
122	TT	21	52	53.1	7.0S	129.5E	168	35	1.6	6	11	43	5.3		24
	PDE	21	52	47.6	6.9S	129.4E	117	10					5.5		24
11 JANUARY 1964															
123	TT	00	40	24.8	16.3N	98.2W	83	28	1.3	4	10	6	4.[illegible]		5
	PDE	00	40	21.2	16.4N	98.2W	33	12					4.5		5
124	TT	06	39	55.7	15.3S	172.8W	39	10	5.4	37	114	-40	4.4	3.8	12
	PDE	06	39	55.4	15.1S	172.9W	33	7					4.5		12
125	TT	07	34	18.3	3.6N	32.6W	57	11	0.6	3	20	28	4.3	5.7	6
	PDE	07	34	15.2	3.6N	82.7W	33	6					4.1		6
126	TT	09	24	14.5	14.1S	169.6E	8	12	2.5	14	27	40	4.5	4.4	14
	PDE	09	24	15.6	14.1S	169.6E	33	8					4.9		14
127	TT	10	23	09.2	11.4S	90.8E	26	22	1.3	7	11	26	5.1		33
	PDE	10	23	10.9	11.4S	90.9E	33	8							33
128	TT	14	09	22.6	32.3N	141.3E	183	10	0.6	4	7	-12	4.4		18
	PDE	14	09	16.3	32.3N	142.0E	109	8					4.3		18
129	TT	21	23	53.1	40.4S	72.6W	8	15	6.6	37	164	0	5.1		9
	PDE	21	23	54.2	40.4S	72.6W	33	6					4.5		9
130	TT	22	02	04.2	8.7S	123.5E	76	50	1.5	5	11	43	5.2		24
	PDE	22	02	02.8	8.6S	123.4E	70	16					5.5		24
12 JANUARY 1964															
131	TT	06	00	12.4	53.2N	166.3W	35	185	1.3	3	4	-5	5.5	4.7	1
	PDE	06	00	13.2	53.2N	166.3W	33	76					5.5		1
132	TT	06	40	34.3	3.5N	82.9W	33*	14	1.1	4	10	21	4.4		6
	PDE	06	40	34.1	3.5N	82.9W	33*	11					4.2		6
133	TT	08	37	51.7	44.7N	149.3E	43	11	2.3	17	36	-38	4.2		19
	PDE	08	37	48.8	44.1N	149.5E	40	5					4.3		19
134	PDE	11	06	03.6	38.8N	118.0W	15	6							3
135	TT	11	13	19.9	5.4S	146.7E	226	60	0.9	2	4	25	5.0		16
	PDE	11	13	19.6	5.4S	146.7E	229	44					5.6		16
136	TT	12	36	29.3	56.1S	27.8W	132	17	0.8	6	15	10	5.2		10
	PDE	12	36	18.7	56.0S	27.6W	33	12					5.5		10
137	TT	12	45	50.6	31.6N	49.2E	60	74	1.5	3	5	19	5.0		29
	PDE	12	45	50.6	31.5N	49.2E	33	6					5.2		29
138	TT	14	21	50.4	10.9S	74.6W	69	12	1.9	10	15	29	4.3		8
	PDE	14	21	51.5	10.9S	74.6W	94	8					4.2		8
139	TT	14	28	20.0	4.4S	137.3E	22	15	1.4	7	10	-31	4.3		16
	PDE	14	28	20.0	4.4S	137.3E	22	9					5.4		16
140	TT	23	33	38.7	19.6S	69.3W	194	8	0.2	1	3	19	4.2		8
	PDE	23	33	40.9	19.3S	69.3W	204	8					4.2		8
13 JANUARY 1964															
141	TT	04	00	53.9	28.8S	65.9W	87	28	1.2	4	13	19	4.6		8
	PDE	04	00	48.3	28.9S	66.2W	33	18					4.8		8
142	TT	06	04	48.2	28.7S	178.0W	33*	7	1.2	10	12	-8	4.0		12
	PDE	06	04	48.2	28.7S	178.0W	3	5					3.9		12
143	TT	13	25	03.5	46.2N	152.0E	54	46	1.6	7	10	-22	4.9		19
	PDE	13	25	01.9	46.6N	152.1E	20	18					4.9		19
144	TT	13	33	01.9	19.7S	175.7W	211	11	0.6	4	8	-39	4.2		12
	PDE	13	32	59.2	19.8S	175.6W	190	9					4.1		12
145	TT	17	23	40.0	2.3N	101.8W	139	21	1.6	7	17	15	4.9	6.1	44
	PDE	17	23	30.1	2.3N	102.0W	33	11					4.9		44

EVENT	SOURCE	HR	MIN	SEC	LAT	LONG	DEPTH	N	SD	A	B	C	MB	MS	REG
146	TT	18	49	12.7	11.6S	166.1E	70	48	1.9	8	8	-10	5.0	6.4	14
	PDE	18	49	09.8	11.6S	166.2E	59	22					5.2		14
14 JANUARY 1964															
147	TT	01	11	18.0	53.0N	159.6E	101	60	0.9	3	6	-2	4.9		19
	PDE	01	11	12.6	52.9N	159.6E	50	16					4.9		19
148	TT	04	17	52.4	28.2S	176.7W	72	21	1.3	7	11	38	5.0	6.4	12
	PDE	04	17	50.5	28.8S	176.2W	89	11					4.7		12
149	TT	08	24	47.2	3.0S	104.3E	349	11	1.4	7	14	24	4.8		24
	PDE	08	24	46.6	3.1S	104.5E	344	6					4.9		24
150	TT	08	53	09.8	48.2N	145.6E	506	32	2.5	12	19	4	4.4		41
	PDE	08	53	09.9	47.9N	145.6E	565	12					4.1		41
151	TT	10	10	44.7	15.9S	173.0W	33*	14	5.3	33	90	44	4.5		12
	PDE	10	10	44.7	15.9S	173.0W	33*	10					4.5		12
152	TT	10	20	11.0	28.3S	178.1W	203	13	1.4	10	14	-41	4.5		12
	PDE	10	20	10.3	28.1S	178.1W	195	13					4.5		12
153	TT	15	06	42.4	14.1N	120.4E	85	26	0.9	4	7	13	4.4		22
	PDE	15	06	35.3	13.6N	120.5E	44	10					4.5		22
154	TT	15	38	13.7	5.2S	150.9E	160	85	1.3	3	5	25	5.7	6.6	15
	PDE	15	38	13.8	5.2S	150.8E	169	39					5.6		15
15 JANUARY 1964															
155	PDE	01	00	02.5	39.0N	117.9W	15	5							3
156	TT	02	23	47.9	45.5N	150.7E	46	70	1.0	3	5	-9	5.2		19
	PDE	02	23	47.4	45.3N	150.6E	45	12					5.3		19
157	TT	07	37	24.2	8.7S	109.3W	141	8	0.6	4	9	-2	4.2		44
	PDE	07	37	22.2	7.6S	108.6W	33	5					4.4		44
158	TT	08	10	57.2	21.3N	143.4E	25	10	8.8	66	126	-17	4.7		18
	PDE	08	10	57.2	21.3N	143.4E	25	10					4.8		18
159	TT	08	25	37.7	7.1S	154.8E	83	10	4.5	24	36	-15	4.6		15
	PDE	08	25	32.1	7.1S	154.8E	55	6					4.9		15
160	TT	17	40	01.4	25.2N	95.5E	78	7	3.4	23	34	2	4.1		25
	PDE	17	40	01.4	25.2N	95.5E	78	5					4.0		25
161	TT	18	46	32.6	28.5S	178.2W	211	39	1.6	8	8	10	5.0		12
	PDE	18	46	32.9	28.4S	178.4W	211	23					4.7		12
162	TT	21	26	43.2	23.7N	45.0W	33*	45	1.7	8	9	-14	5.2	4.5	32
	PDE	21	26	43.2	23.7N	45.0W	33	27					4.7		32
163	TT	21	36	03.9	29.2N	140.9E	59	192	1.5	3	4	18	6.1	6.6	18
	PDE	21	36	05.0	29.1N	140.8E	70	23					6.4		18
164	TT	22	43	13.9	14.6S	167.0E	58	8	4.1	23	45	40	5.5		14
	PDE	22	43	14.3	14.6S	166.8E	55	7					4.5		14
165	TT	23	05	13.8	17.3S	179.7E	643	14	1.9	12	37	36	4.7		13
	PDE	23	05	02.0	17.4S	179.7E	599	16					4.3		13
166	TT	23	06	35.5	45.8N	119.9W	31	7	13.4	59	165	30	4.4		2
	PDE	23	06	35.5	45.8N	119.9W	31	6					4.2		2
16 JANUARY 1966															
167	TT	05	09	57.8	36.8N	89.5W	18	14	10.8	59	68	-15	4.2		34
	PDE	05	09	57.8	36.8N	89.5W	18	12					4.5		34
168	TT	10	50	35.3	50.6N	154.1E	201	37	0.8	4	8	-19	4.7		19
	PDE	10	50	35.7	50.5N	154.0E	203	18					4.8		19
169	TT	11	44	49.3	21.4S	179.1W	601	13	0.9	6	9	20	4.7		12
	PDE	11	44	41.8	21.5S	179.1W	609	10					4.4		12
170	TT	14	37	44.6	30.1S	71.6W	48	20	3.3	13	57	5	4.3	5.9	8
	PDE	14	37	37.3	30.4S	69.5W	33	11					4.0		8
171	TT	17	10	41.1	52.5N	162.9E	33*	10	4.9	46	127	42	4.4		19
	PDE	17	10	41.1	52.5N	162.9E	33	5					4.2		19
172	TT	17	53	39.7	55.3N	160.1E	33*	11	1.2	13	35	-27	4.8		19
	PDE	17	53	39.7	55.3N	160.1E	33	6					4.4		19
173	TT	20	56	57.2	17.6N	61.6W	50	29	1.3	5	8	21	4.6	5.8	7
	PDE	20	56	56.4	17.6N	61.8W	45	8							7
174	TT	23	10	37.3	37.7N	134.8E	384	11	0.4	3	3	-29	4.1		41
	PDE	23	10	34.4	37.3N	134.8E	380	5					4.1		41

EVENT	SOURCE	HR	MIN	SEC	LAT	LONG	DEPTH	N	SD	A	B	C	MB	MS	REG
17 JANUARY 1964															
175	TT	00	15	06.5	38.2N	112.7W	33*	9	9.6	39	67	9	3.1		34
	PDE	00	15	06.5	38.2N	112.7W	33	9							34
176	TT	00	15	37.6	38.2N	112.7W	33*	6	16.5	76	112	-7	3.2		34
	PDE	00	15	37.6	38.2N	112.7W	33	5							34
177	TT	00	24	50.0	17.9N	99.9W	91	15	1.5	6	15	11	3.9		5
	PDE	00	24	40.8	17.5N	99.8W	33	8					4.0		5
178	TT	02	54	21.0	45.6N	151.3E	38	123	1.2	3	4	-7	5.3	4.0	19
	PDE	02	54	22.6	45.5N	151.3E	55	48					5.1		19
179	TT	02	54	26.0	21.7S	169.9E	13	42	2.0	8	8	29	5.7	5.0	14
	PDE	02	54	26.8	21.6S	169.9E	33	16							14
180	TT	03	13	58.5	12.2S	167.0E	246	19	4.1	25	35	2	5.3		14
	PDE	03	13	56.3	12.3S	167.1E	230	15					4.7		14
181	TT	03	25	00.3	36.9N	71.4E	95	47	1.1	3	5	15	5.2		48
	PDE	03	25	00.6	36.8N	71.4E	94	19					5.2		48
182	TT	06	02	19.8	40.4N	124.5W	22	14	1.2	4	9	-26	4.2		3
	PDE	06	02	19.9	40.4N	124.6W	33	7					4.3		3
183	PDE	07	08	27.9	31.1N	114.2W	14						4.3		4
184	TT	09	32	48.8	11.3S	162.4E	14	13	1.6	8	10	-31	4.6		15
	PDE	09	32	51.6	11.4S	162.4E	33	8					4.7		15
185	TT	12	14	26.7	23.9S	177.2W	136	12	0.4	3	6	44	4.7		12
	PDE	12	14	25.8	24.3S	177.0W	51	9					4.7		12
186	TT	13	27	21.0	3.5S	77.5W	13	7	1.8	9	46	16	4.1		8
	PDE	13	27	21.8	3.4S	77.5W	33	6					4.1		8
187	TT	17	13	30.3	10.8S	167.7E	114	8	6.9	111	121	-17			14
	PDE	17	13	30.3	10.8S	167.7E	114	6							14
188	TT	20	15	17.6	39.2N	114.3W	55	7	4.3	20	29	11	3.2		3
	PDE	20	15	17.6	39.1N	114.2W	33	7							3
189	TT	22	18	33.0	17.7N	98.7W	160	14	1.0	4	14	15	4.1		5
	PDE	22	18	12.9	16.6N	98.7W	33	6					4.2		5
18 JANUARY 1964															
190	TT	00	10	56.6	21.3S	68.9W	128	7	1.2	7	17	3	4.1		8
	PDE	00	10	51.0	21.7S	67.8W	130	7					3.8		8
191	TT	04	14	37.7	30.0S	177.9W	47	6	2.3	17	29	-12	4.2		12
	PDE	04	14	37.7	30.0S	177.9W	47	6					4.1		12
192	TT	06	53	01.3	17.9S	69.5W	157	6	2.3	11	18	33	3.8		8
	PDE	06	53	01.3	17.9S	69.5W	157	6					3.8		8
193	TT	07	10	12.8	34.3S	104.1W	27	14	3.6	27	50	-6	4.3		43
	PDE	07	10	21.9	34.5S	103.7W	33	8					4.5		43
194	TT	12	04	39.3	23.2N	120.6E	28	165	1.2	2	3	28	5.9	5.3	21
	PDE	12	04	40.0	23.1N	120.5E	33	47					5.9		21
195	TT	12	32	33.9	23.6N	122.9E	8	25	2.0	11	17	4	4.6		21
	PDE	12	32	36.3	23.5N	122.9E	33	14					4.8		21
196	TT	13	43	05.5	23.4N	120.8E	29	17	3.9	19	27	-10	4.8		21
	PDE	13	43	05.6	23.1N	120.8E	31	8					4.5		21
197	TT	14	40	56.1	15.1N	94.2W	57	26	0.9	3	6	28	4.5		5
	PDE	14	40	54.6	15.2N	94.2W	33	18					4.6		5
198	TT	14	45	38.3	20.5N	122.1E	16	19	1.6	8	13	5	4.4		22
	PDE			39.4	20.6N	122.1E	18	10					4.9		22
199	TT	15	17	48.0	13.6N	143.8E	33*	8	0.9	6	10	12	4.0		17
	PDE	15	17	47.5	13.5N	143.8E	33	9					4.8		17
200	TT	16	45	52.6	6.9S	129.3E	75	9	1.5	8	16	38	4.9		24
	PDE	16	45	53.6	6.9S	129.3E	84	5							24
201	TT	18	44	02.4	25.0S	176.9W	6	20	1.9	10	20	-35	4.8	3.5	12
	PDE	18	44	05.0	25.1S	176.9W	33	12					4.6		12
202	TT	21	57	11.8	16.2N	89.3W	6	9	4.0	19	74	18	3.9		5
	PDE	21	57	14.4	16.1N	89.3W	33	7					3.8		5
203	TT	22	36	18.4	18.8N	69.4W	104	113	1.9	4	7	25	5.3		7
	PDE	22	36	17.6	18.8N	69.4W	95	35					5.3		7

EVENT	SOURCE	HR	MIN	SEC	LAT	LONG	DEPTH	N	SD	A	B	C	MB	MS	REG
19 JANUARY 1964															
204	TI	1	59	47.7	18.4S	179.4W	321	7	.6	5	11	21	4.0		12
	PDE	1	58	23.8	18.5S	178.3W	600	7					4.1		12
205	TI	2	27	04.0	39.0S	72.4W	6	13	5.7	34	141	1	4.4	4.0	8
	PDE	2	27	06.6	39.1S	72.4W	33	6					4.5		8
206	TI	6	50	02.5	58.7S	25.5W	90	12	1.2	10	19	8	5.8	6.4	10
	PDE	6	49	55.9	58.6S	25.1W	33	11							10
207	TI	7	00	04.1	9.2S	158.3E	35	18	1.1	6	8	-9	5.1	3.7	15
	PDE	7	00	03.3	9.2S	158.2E	32	11					5.7		15
208	PDE	7	55	09.4	5.9S	134.1E	33	5							16
209	TI	8	47	10.7	21.8N	121.0E	21	19	7.2	38	62	-3	4.9		21
	PDE	8	47	9.9	21.8N	120.9E	18	9					4.6		21
210	TI	9	13	54.3	26.9N	54.0E	37	91	1.0	2	3	19	5.2	4.4	29
	PDE	9	13	53.5	26.9N	54.0E	33	28					5.6		29
211	TI	9	34	12.6	4.3S	152.9E	41	11	1.7	10	11	-17	4.7		15
	PDE	9	34	11.1	4.2S	152.8E	33	6					5.1		15
212	TI	16	12	54.0	23.3N	120.7E	57	36	2.3	8	11	27	4.6		21
	PDE	16	12	50.0	23.0N	120.4E	33	11					4.8		21
213	TI	17	01	17.0	45.2N	141.5E	139	11	11.8	91	242	-22	4.5		22
	PDE	17	01	16.2	45.2N	141.5E	136	7					4.0		22
214	TI	17	10	46.9	44.1N	145.1E	36	24	1.9	11	20	-20	4.6		19
	PDE	17	10	46.1	44.1N	145.0E	33	13					4.6		19
215	TI	23	05	36.7	45.8N	150.0E	43	11	0.5	3	9	-41	4.2		19
	PDE	23	05	38.1	45.9N	149.9E	50	5					4.1		19
216	TI	23	23	18.2	18.4S	177.9W	592	19	2.0	12	24	33	4.0		12
	PDE	23	22	19.1	18.3S	176.9W	48	9					4.5		12
20 JANUARY 1964															
217	TI	00	16	01.6	30.3S	178.0W	155	10	0.7	5	9	39	4.3		12
	PDE	00	15	48.4	30.2S	177.8W	35	10					4.4		12
218	TI	2	28	32.6	20.9S	179.1W	157	11	0.7	6	11	30	4.3		12
	PDE	2	27	26.4	20.7S	178.4W	600	9					4.3		12
219	TI	04	47	00.0	8.3N	126.7E	108	18	0.8	5	10	11	5.0		22
	PDE	04	46	59.7	8.2N	126.6E	110	18					4.9		22
220	TI	13	46	16.7	1.0N	126.1E	100	6	4.0	27	44	26	5.6		22
	PDE	13	46	08.3	0.9N	126.2E	33	6					4.3		22
221	TI	15	39	43.8	23.1N	120.5E	46	23	3.8	18	24	-3	4.9		21
	PDE	15	39	41.5	23.2N	120.3E	49	10					5.1		21
222	TI	17	08	36.0	20.7S	170.0E	127	97	1.3	4	5	0	6.4	6.9	14
	PDE	17	08	37.4	20.7S	169.9E	141	45					6.1		14
223	TI	20	30	15.3	16.6N	98.5W	72	33	1.4	4	9	12	4.5		5
	PDE	20	30	12.6	16.8N	98.5W	33	12					4.3		5
224	TI	20	38	16.9	18.8N	120.7E	52	55	1.7	5	9	23	4.8		22
	PDE	20	38	16.5	18.8N	120.7E	53	18					4.8		22
225	TI	23	06	27.0	30.0S	177.8W	47	20	7.0	39	62	-27	5.1		12
	PDE	23	06	26.2	30.0S	177.9W	44	15					5.1		12
21 JANUARY 1964															
226	TI	12	34	48.6	20.6S	68.8W	111	10	1.7	8	25	20	4.2		8
	PDE	12	35	00.1	19.7S	69.1W	161	7					4.1		8
227	TI	15	43	50.6	16.6N	86.3W	36	7	6.0	43	64	6	3.9		7
	PDE	15	43	49.8	16.6N	86.4W	33	6					3.8		7
228	TI	16	14	23.5	15.0N	60.6W	66	20	0.9	3	5	21	4.4		7
	PDE	16	14	25.6	15.0N	60.8W	82	11					4.1		7
229	PDE	18	57	47.3	41.4S	87.8W	33	5					4.5		43
230	TI	21	02	39.5	52.6N	172.8E	198	18	0.7	4	11	-35	4.2		1
	PDE	21	02	20.0	52.2N	172.4E	33	11					4.6		1
231	TI	22	18	13.9	10.5N	125.3E	54	54	1.3	4	7	31	5.1	6.2	22
	PDE	22	18	13.0	10.6N	125.3E	53	20					5.2		22
232	TI	23	31	43.1	39.2N	114.1W	36	9	8.1	38	49	14	3.6		3
	PDE	23	31	42.3	39.2N	114.2W	33	11					3.9		3

EVENT	SOURCE	HR	MIN	SEC	LAT	LONG	DEPTH	N	SD	A	B	C	MB	MS	REG
22 JANUARY 1964															
233	TT	02	15	29.9	45.8S	75.1W	36	11	2.0	14	71	-2	4.6	3.7	9
	PDE	02	15	29.1	45.8S	75.2W	33	11					4.7		9
234	TT	06	46	36.6	30.7S	177.9W	169	7	0.3	2	3	42	4.0		12
	PDE	06	46	36.4	30.6S	178.0W	166	7					4.0		12
235	TT	08	19	58.5	21.6S	169.8E	36	8	4.9	30	44	-18	4.4		14
	PDE	08	19	57.7	21.6S	169.7E	33	6					4.3		14
236	TT	09	11	57.6	4.0S	136.2E	15	17	1.0	5	7	36	5.1	3.5	16
	PDE	09	12	03.4	4.2S	136.2E	71	13					5.1		16
237	TT	13	44	20.3	47.7N	152.9E	36	9	13.6	96	277	-37	4.1		19
	PDE	13	44	19.5	47.7N	152.8E	33	5					4.2		19
238	TT	15	58	45.0	22.4N	93.6E	72	120	1.4	3	4	44	6.4	6.0	25
	PDE	15	58	46.5	22.4N	93.6E	88	41					6.1		25
239	TT	17	41	57.7	4.7S	134.1E	63	10	4.5	27	45	36	4.6		16
	PDE	17	41	50.0	4.0S	133.9E	33	6							16
240	TT	17	58	14.3	20.2N	147.1E	22	46	1.1	4	7	-2	5.0	3.7	18
	PDE	17	58	16.3	20.2N	147.1E	39	23					5.1		18
241	TT	18	48	30.7	7.6N	126.9E	136	16	1.1	6	12	30	5.0		22
	PDE	18	48	30.9	7.6N	126.9E	144	14					4.2		22
242	TT	20	03	07.7	20.6S	178.8W	109	6	0.2	2	5	35	4.0		12
	PDE	20	01	32.6	20.0S	177.6W	220	7					3.9		12
243	TT	21	10	56.8	44.5N	114.4W	50	6	9.4	38	88	7	3.7		34
	PDE	21	10	56.0	44.5N	114.5W	47	6							34
244	TT	21	28	30.0	19.4N	72.9W	36	7	2.6	13	40	-37	3.7		7
	PDE	21	28	25.7	19.0N	73.1W	19	5					3.8		7
245	TT	21	40	38.1	50.5N	173.4W	36	13	1.3	9	20	-35	4.3	3.4	1
	PDE	21	40	37.3	50.5N	173.5W	33	7					4.3		1
246	TT	22	19	50.8	15.6S	175.1W	356	10	0.8	5	11	28	4.2		12
	PDE	22	19	44.1	15.8S	175.1W	307	8					4.1		12
247	TT	22	37	59.6	27.2N	44.3W	7	10	0.4	3	5	32	4.3	3.4	32
	PDE	22	38	03.4	27.1N	44.1W	33	9					4.2		32
248	TT	23	59	50.1	13.7S	165.9E	93	89	2.9	9	11	10	5.8	6.8	14
	PDE	23	59	43.6	13.7S	165.9E	33	51					6.0		14
23 JANUARY 1964															
249	TT	01	42	31.3	18.2N	107.6W	27	14	2.2	8	31	6	3.9		5
	PDE	01	42	34.7	18.5N	107.4W	33	11					3.8		5
250	TT	02	49	33.2	17.0S	179.0W	575	10	1.5	9	36	29	3.7		12
	PDE	02	49	22.2	17.7S	178.6W	520	8					3.6		12
251	TT	03	04	46.3	44.1N	114.7W	27	6	8.9	38	76	2	3.5		3
	PDE	03	04	49.7	44.4N	114.5W	33	5					4.1		3
252	TT	05	17	32.3	30.6N	137.5E	509	17	1.0	6	12	-4	4.1		18
	PDE	05	17	26.1	30.6N	137.3E	478	11					4.0		18
253	TT	05	56	34.0	8.4S	13.3W	33*	6	1.5	15	23	28	5.0	4.0	32
	PDE	05	56	34.0	8.4S	13.3W	33	7					4.0		32
254	TT	09	12	54.1	53.6N	158.2E	33*	13	6.7	51	113	-12	3.7		19
	PDE	09	12	54.1	53.6N	158.2E	33	7					3.9		19
255	TT	10	03	53.9	19.3N	147.1E	249	9	2.6	23	44	-10	4.3		18
	PDE	10	03	21.5	17.8N	147.0E	33	6					4.2		18
256	TT	11	38	49.8	2.6S	80.1W	377	11	6.1	34	68	23	3.5		8
	PDE	11	38	51.9	2.5S	80.1W	418	6					3.6		8
257	TT	13	43	51.6	28.8N	139.4E	441	23	0.8	5	9	-7	4.3		18
	PDE	13	43	46.7	28.7N	139.4E	417	14					4.0		18
258	TT	15	19	30.1	36.6N	71.1E	22	60	2.8	7	11	12	5.2		48
	PDE	15	19	31.6	36.9N	71.2E	28	17					4.4		48
259	TT	16	08	55.0	11.4N	122.6E	43	33	2.1	8	16	30	4.8	5.8	22
	PDE	16	08	55.5	11.5N	122.5E	47	10					4.5		22
24 JANUARY 1964															
260	TT	02	40	02.9	4.2S	154.1E	427	20	1.1	5	6	20	4.5		15
	PDE	02	40	00.1	4.2S	154.2E	416	16					4.3		15

EVENT	SOURCE	HR	MIN	SEC	LAT	LONG	DEPTH	N	SD	A	B	C	MB	MS	REG
261	TT	03	35	36.4	78.4N	19.5W	33*	13	2.4	14	78	5	4.0		40
	PDE	03	35	36.4	78.4N	19.5W	33	8					4.2		40
262	TT	03	52	29.2	5.9S	154.0E	80	9	1.1	7	11	16	4.5		15
	PDE	03	52	29.3	5.9S	154.0E	85	7							15
263	TT	05	31	31.2	64.4N	126.5W	33*	20	3.0	11	35	4	4.3		42
	PDE	05	31	31.2	64.4N	126.5W	33	11					3.9		42
264	TT	06	43	04.5	60.8N	148.0W	150	12	6.1	39	74	-5	3.8	5.8	1
	PDE	06	42	53.9	60.4N	146.5W	33	6					3.7		1
265	TT	10	00	47.4	36.3N	73.9E	188	6	0.4	2	3	-23	4.0		48
	PDE	10	00	47.4	35.6N	74.4E	215	5							48
266	TT	10	34	29.1	23.8S	179.2E	112	11	0.6	5	17	36	4.6		12
	PDE	10	33	24.5	23.5S	179.9E	550	7					4.3		12
267	PDE	13	33	55.2	5.6S	146.7E	141	5							15
268	TT	15	17	03.0	15.0S	173.1W	33*	12	1.3	29	105	-34	4.5	3.8	12
	PDE	15	17	03.0	15.0S	173.1W	33	9					4.5		12
269	TT	17	17	53.4	38.8N	129.5E	579	172	1.9	4	6	9	5.2		41
	PDE	17	17	45.5	38.7N	129.4E	542	50					5.3		41
270	TT	19	53	33.8	17.5S	178.6W	598	20	1.2	6	14	27	4.4		12
	PDE	19	53	25.7	17.8S	178.5W	584	14					4.4		12
271	TT	21	12	23.1	22.1S	175.9W	33	26	1.9	10	18	40	4.8		12
	PDE	21	12	23.2	21.7S	176.2W	32	16					4.8		12
272	TT	21	31	23.6	44.7N	150.4E	28	87	0.9	3	4	3	5.0	4.3	19
	PDE	21	31	24.2	44.5N	150.3E	33	27					4.7		19
273	TT	21	44	54.1	23.4S	180.0E	569	14	0.8	5	11	38	4.3		12
	PDE	21	44	46.1	23.6S	179.9E	535	10					4.5		12
274	TT	22	44	02.0	6.9S	106.2E	102	42	1.4	14	26	38	5.3		24
	PDE	22	44	00.6	7.1S	106.0E	94	12					5.5		24
25 JANUARY 1964															
275	TT	02	00	06.0	6.3S	145.6E	134	5	7.8	41	72	39			16
	PDE	02	00	06.0	6.3S	145.6E	134	5							16
276	TT	03	40	34.9	16.1S	173.8W	33*	12	6.2	42	304	-42	4.4		12
	PDE	03	40	34.9	16.1S	173.8W	33	10					4.3		12
277	TT	03	46	41.4	1.2N	85.3W	46	10	2.0	9	17	25	4.2		8
	PDE	03	46	35.9	1.2N	85.3W	33	7					3.7		8
278	TT	04	09	20.3	20.7N	143.8E	74	10	0.5	4	10	-40	4.3		18
	PDE	04	09	13.5	20.2N	143.8E	33	9					4.4		18
279	TT	07	04	36.5	22.8S	179.3W	578	20	1.2	6	14	39	4.4		12
	PDE	07	04	32.8	22.6S	179.7W	600	13					5.1		12
280	TT	07	13	32.5	28.3N	86.6E	69	26	3.1	11	18	37	4.6		26
	PDE	07	13	30.8	28.5N	86.8E	44	8					4.5		26
281	TT	12	09	12.9	28.5S	176.5W	63	13	3.3	25	31	42	4.8	6.1	12
	PDE	12	09	08.8	28.3S	176.5W	17	10					4.5		12
282	TT	15	09	14.5	5.1S	153.5E	34	6	2.1	13	18	18			15
	PDE	15	09	17.3	5.2S	153.1E	64	7					4.6		15
283	TT	17	35	04.8	16.3N	86.8W	86	12	3.8	20	26	-14	3.8		7
	PDE	17	35	04.9	17.0N	86.9W	33	10					3.9		7
284	TT	18	43	27.3	16.5N	86.8W	101	12	2.4	13	18	-2	3.9		7
	PDE	18		26.8	17.1N	87.2W	33	6					3.8		7
285	TT	19	48	51.2	9.9N	69.1W	56	15	4.7	26	36	28	4.4		7
	PDE	19	48	49.1	10.1N	69.4W	41	9					4.5		7
286	TT	21	42	16.8	53.4N	157.5E	171	18	0.8	5	16	-32	4.6		19
	PDE		41	59.9	52.7N	157.3E	33	13					4.7		19
287	TT	21	47	10.9	23.4S	179.7W	495	14	0.7	4	10	42	4.1		12
	PDE	21	46	55.6	22.6S	179.9W	350	12					4.4		12
288	TT	22	09	03.1	5.2S	152.9E	53	14	2.8	15	24	39	4.4		15
	PDE	22	09	00.8	5.3S	153.2E	42	11					4.8		15
289	TT	22	46	17.5	16.5N	86.4W	66	11	2.5	13	18	-16	3.9		7
	PDE	22	46	18.4	17.0N	86.6W	33	5					3.9		7
290	TT	23	07	35.5	21.0S	178.6W	583	17	0.7	4	9	-36	4.3		12
	PDE	23	07	29.3	20.8S	178.8W	580	12					4.5		12

EVENT	SOURCE	HR	MIN	SEC	LAT	LONG	DEPTH	N	SD	A	B	C	MB	MS	REG
26 JANUARY 1964															
291	TT	09	09	35.5	16.3S	71.7W	128	117	1.8	4	9	16	5.8	6.8	8
	PDE	09	09	33.9	16.3S	71.7W	116	77					6.1		8
292	TT	10	02	16.5	23.2N	120.4E	47	46	1.4	5	7	18	4.8		21
	PDE	10	02	15.0	23.1N	120.4E	37	18					4.9		21
293	TT	12	05	51.8	40.9N	140.6E	123	25	1.0	5	12	-14	4.5		19
	PDE	12	05	54.3	40.8N	140.1E	160	16					4.4		19
294	TT	19	53	19.0	6.8N	73.0W	163	8	0.5	3	4	1	3.8		7
	PDE	19	53	18.8	6.9N	73.0W	160	6					3.8		7
295	TT	20	55	04.4	16.5N	86.3W	42	11	0.7	3	5	9	4.0		7
	PDE	20	55	07.8	17.2N	86.1W	33	9					3.8		7
27 JANUARY 1964															
296	TT	01	12	23.5	00.0N	17.9W	33*	100	3.6	12	15	-26	5.2	4.8	32
	PDE	01	12	23.5	00.0N	17.9W	33	45					5.3		32
297	TT	02	46	35.2	60.7S	155.0E	37	9	2.2	10	59	2	8.3		11
	PDE	02	46	33.4	60.9S	155.2E	33	8							11
298	TT	05	07	00.3	13.1S	166.5E	46	14	2.9	13	21	-8	4.3		14
	PDE	05	07	00.3	13.1S	166.5E	46	13					4.2		14
299	TT	05	29	27.3	29.2N	97.2E	33*	7	1.7	11	12	30	4.3		26
	PDE	05	29	27.3	29.2N	97.2E	33	5					4.9		26
300	TT	06	19	19.0	47.3N	152.1E	33*	10	8.6	75	189	-35	4.6		19
	PDE	06	19	19.0	47.3N	152.1E	33	8					4.4		19
301	TT	10	32	13.4	19.9S	115.4W	33*	8	12.6	95	230	-6	4.5		43
	PDE	10	32	13.4	19.9S	115.4W	33	6					4.2		43
302	TT	11	21	14.3	16.5N	86.8W	85	9	2.8	15	21	-22	4.0		7
	PDE	11	21	14.4	17.0N	87.0W	33	6					3.8		7
303	TT	15	36	57.9	10.8S	166.2E	183	12	0.8	5	6	30	4.0		14
	PDE	15	36	56.2	10.6S	166.1E	165	9					4.3		14
304	TT	17	51	51.3	52.7N	160.5E	69	9	1.3	11	22	-20	4.6		19
	PDE	17	51	47.3	52.5N	160.8E	33	7					4.1		19
305	TT	20	19	47.9	20.4S	178.7E	600	5	0.9	5	22	31	4.1		12
	PDE	20	19	30.6	23.1S	179.4E	526	5					4.1		12
28 JANUARY 1964															
306	TT	00	02	30.0	40.8N	141.1E	90	14	1.3	6	26	-25	4.4		19
	PDE	00	02	25.7	41.0N	141.5E	33	10					4.3		19
307	TT	04	56	48.6	43.3N	125.9W	17	5	15.1	205	279	-29	4.3		3
	PDE	04	56	48.6	43.3N	125.9W	17	6					4.5		3
308	TT	05	43	22.5	6.2S	148.8E	32	48	2.1	7	11	12	4.9	4.9	15
	PDE	05	43	22.1	6.3S	148.7E	33	18					5.1		15
309	TT	06	17	15.4	20.4S	177.7W	502	10	1.1	7	18	34	4.1		12
	PDE	06	17	09.3	20.5S	177.8W	473	9					4.0		12
310	TT	07	29	39.0	17.2S	176.2W	477	8	1.9	15	54	42	3.9		12
	PDE	07	29	28.3	17.7S	176.7W	417	7					4.1		12
311	TT	09	00	46.9	21.7N	121.6E	33*	13	3.0	39	51	10	4.5		21
	E	09	00	46.9	21.7N	121.6E	33	6							21
312	TT	12	57	07.9	43.2N	111.4W	41	10	8.3	32	75	9	3.3		34
	PDE	12	57	07.9	43.2N	111.4W	41	8					4.2		34
313	TT	13	03	41.5	14.2S	72.1W	21	8	8.6	62	172	43	4.2		8
	PDE	13	03	41.5	14.2S	72.1W	21	5					4.1		8
314	TT	14	09	15.7	36.5N	70.9E	195	181	1.5	2	4	32	6.5	6.9	48
	PDE	14	09	17.1	36.5N	70.9E	207	74					6.1		48
315	TT	16	26	04.6	7.2S	124.2E	361	13	4.5	25	64	-43	4.8		24
	PDE	16	26	05.6	7.0S	124.5E	407	8					5.1		24
316	TT	17	46	20.3	45.5N	149.9E	64	14	1.1	7	16	-37	4.6		19
	PDE	17	46	16.2	45.3N	149.8E	33	8					4.4		19
317	TT	18	30	43.9	61.2N	147.8W	172	8	5.1	67	188	-1	4.1		1
	PDE	18	30	43.9	61.2N	147.8W	172	7					4.0		1
318	TT	19	11	06.2	55.8N	166.3E	138	7	0.6	5	23	-40	4.0		1
	PDE	19	10	53.9	55.8N	165.7E	33	6					4.3		1

EVENT	SOURCE	HR	MIN	SEC	LAT	LONG	DEPTH	N	SD	A	B	C	MB	MS	REG
29 JANUARY 1964															
319	TT	02	30	00.1	21.4S	68.9W	133	11	1.3	6	16	13	4.3		8
	PDE	02	29	59.8	21.5S	68.8W	136	7					4.0		8
320	TT	05	45	36.2	39.5N	72.6E	51	14	1.6	6	13	-17	4.6		48
	PDE	05	45	48.0	38.7N	73.2E	187	5					3.8		48
321	TT	08	47	34.0	3.0N	125.7E	172	26	1.0	4	10	30	4.9		23
	PDE	08	47	29.9	3.0N	125.7E	133	18					4.9		23
322	TT	13	07	26.0	2.3S	139.5E	94	11	0.9	6	12	30	4.9		16
	PDE	13	07	18.4	2.2S	139.5E	33	9					4.4		16
323	TT	17	29	08.0	55.1N	161.7E	78	9	1.2	10	62	-44	4.6		19
	PDE	17	29	08.0	55.1N	161.7E	78	8					4.6		19
324	TT	18	37	30.5	6.9S	130.7E	35	7	0.8	5	19	36	4.6		24
	PDE	18	37	29.3	6.8S	130.7E	33	5							24
325	TT	22	32	19.6	41.8N	141.9E	44	24	0.7	3	7	-19	4.7		19
	PDE	22	32	20.9	41.7N	141.9E	56	16					4.5		19
30 JANUARY 1964															
326	TT	01	11	17.0	7.0N	72.7W	129	8	1.9	12	15	3	4.0		7
	PDE	01	11	16.6	6.9N	72.6W	151	8					3.9		7
327	TT	02	33	55.3	20.1S	69.5W	33*	9	2.4	87	202	11	4.3		8
	PDE	02	33	53.3	20.1S	69.5W	33	9					4.2		8
328	TT	05	39	44.1	24.5N	108.6W	41	33	1.9	5	12	7	4.5	5.8	4
	PDE	05	39	44.6	24.5N	108.6W	49	24					4.5		4
329	TT	07	37	01.3	24.6S	176.8W	33*	5	8.1	47	107	-39	4.5		12
	PDE	07	37	01.3	24.6S	176.8W	33	5					3.9		12
330	TT	09	05	59.2	11.6N	121.7E	3	12	2.4	13	32	25	4.7		22
	PDE	09	06	01.9	11.4N	121.6E	33	8					4.2		22
331	TT	12	23	23.5	32.9N	48.7E	139	14	6.7	33	48	-2	4.1		29
	PDE	12	23	10.3	32.7N	47.8E	33	5							29
332	TT	12	39	29.2	1.8N	99.7E	179	24	0.9	4	10	29	4.6		46
	PDE	12	39	23.8	1.7N	99.6E	133	12					5.4		46
333	TT	17	20	10.7	23.6N	143.4E	3	41	4.9	24	36	20	4.9		18
	PDE	17	20	13.4	23.4N	143.3E	33	16					4.7		18
334	TT	17	45	56.5	37.4N	29.9E	59	115	1.7	3	5	22	5.0	6.4	30
	PDE	17	45	54.6	37.3N	29.9E	41	40					5.3		30
335	TT	21	23	58.3	48.9N	151.3E	307	13	2.8	17	70	-29	3.7		19
	PDE	21	23	58.2	49.2N	150.6E	292	5					4.1		19
31 JANUARY 1964															
336	TT	00	14	58.2	36.4N	71.5E	122	16	1.7	7	14	9	4.2		48
	PDE	00	14	58.4	36.3N	71.4E	127	6					4.2		48
337	TT	04	17	12.9	61.5N	151.8W	45	65	1.6	6	9	7	4.6	6.0	1
	PDE	04	17	12.4	61.5N	151.9W	33	38					4.9		1
338	TT	06	46	14.4	17.2N	99.0W	107	12	1.8	7	27	10	3.9	5.8	5
	PDE	06	46	06.9	16.9N	99.0W	56	10					3.9		5
339	PDE	08	06	38.5	47.0N	138.8E	433	6					3.8		41
340	TT	09	23	16.6	37.5N	22.6E	32	18	1.9	8	16		4.5		30
	PDE	09	23	20.6	37.5N	23.2E	75	11					4.3		30
341	TT	12	30	30.8	23.8N	121.0E	33*	12	9.3	61	78	15	4.4		21
	PDE	12	30	30.8	23.8N	121.0E	33	5					4.5		21
342	TT	16	40	10.4	43.2N	141.7E	48	10	7.7	49	94	-23	4.5		19
	PDE	16	40	09.8	42.2N	142.1E	49	6					4.2		19
343	TT	17	07	36.1	51.7N	126.3W	44	15	6.5	26	79	25	3.9		2
	PDE	17	07	43.1	51.3N	124.7W	14	8					4.2		2
344	TT	21	46	36.0	00.3S	77.8W	83	23	1.4	6	15	24	4.4		8
	PDE	21	46	31.7	00.2S	77.9W	33	24					4.6		8

APPENDIX B

ANALYSIS OF HYPOCENTER REVISION

APPENDIX B

ANALYSIS OF HYPOCENTER REVISION

The most striking single result of the hypocenter revision performed by Texas Instruments Incorporated is the difference in depth distribution of the located hypocenters. Texas Instruments results indicate that less than 60 percent of the earthquakes located in January 1964 occurred at depths of 70 km and shallower and that less than 50 percent occurred at depths of 50 km and shallower. The preliminary results published by USC&GS, however, indicate that more than two-thirds of the earthquakes occurred at depths of 70 km and shallower and more than 60 percent occurred at depths of 50 km and shallower. This result is primarily due to the decrease in the number of events with depths restrained to 33 km by Texas Instruments.

As shown in Table B-1, 151 of the USC&GS hypocenters were restrained to depths of 33 km (about 45 percent of the total) while TI results show only 43 events so restrained. Of the 108 events restrained to 33 km by USC&GS but not by Texas Instruments, 33 depths were placed shallower than 33 km and 75 deeper than 33 km. These changes in depths resulted in 47 events placed at depths greater than 50 km and 35 events at depths greater than 70 km rather than at 33 km.

Since the USC&GS usually places the accuracy of its published depth determination at ±25 km, this figure is used to establish the number of depths determined by Texas Instruments, which differs significantly from that determined by the USC&GS. Using this criterion, 109 of the TI depth determinations are found to differ appreciably from the USC&GS depths.

The results discussed here should not be construed to imply that 109 of the USC&GS depth determinations are incorrect. Due to lack of time and funds, Texas Instruments results could not be subjected to as rigorous and extensive quality control as the USC&GS routinely applies to their data.

Table B-1

DEPTH DISTRIBUTION

Depth (km)	Number of Events TI	CGS
1 to 10	17	--
11 to 20	14	12
21 to 30	18	5
31 to 40	76*	166**
41 to 50	30	27
51 to 60	20	10
61 to 70	14	9
71 to 100	35	20
101 to 150	42	25
151 to 200	26	17
201 to 250	11	12
251 to 300	1	1
301 to 350	3	3
351 to 400	4	1
401 to 450	4	6
451 to 500	3	2
501 to 550	5	7
551 to 600	8	8
601 to 650	2	2
Total	333	333

*43 events restrained to 33-km depth

**151 events restrained to 33-km depth

To say that one set of results is "better" than another is a rather dubious statement. To further illustrate this, a comparison with the International Seismological Center (ISC) results shows both agreement and disparity with USC&GS and Texas Instruments results. The observed differences in depth determination illustrate the extent of the depth-determination problem. Considerable study of this problem is strongly recommended. Data of all types should be used, and overconfidence in computer processing and preconceived ideas should be avoided in such studies.

The significance of epicenter shifts is somewhat more difficult to assess. Only 90 of the 333 epicenters are unchanged in the revision process. A total of 109 epicenters are shifted 0.1° latitude and/or longitude and 134 epicenter shifts exceed 0.1° latitude and/or longitude.

Another indication of the degree of changes in epicenter locations is that 165 of the TI epicenters do not include the USC&GS location within the 70-percent confidence region. In other words, probably about 115 of the TI epicenters do differ from USC&GS epicenters.

When changes are considered in either epicenter location and focal depth, or both, appreciable changes are found to have been made in half (a total of 168) of the input hypocenters processed. Criteria for significance are epicenter-location changes exceeding 0.1° latitude and/or longitude and focal-depth changes exceeding 25 km, or both.

In evaluating the differences in the results, two factors must be considered: differences in the methods and the data used. With regard to method, the Texas Instruments hypocenter program differs in two principal ways from the USC&GS program:

- Travel-time corrections are applied to observed times for nearly 100 stations, and these corrections depend on areas in which the events occurred
- Larger time residuals are allowed than in the USC&GS program

Table B-2

AVERAGE NUMBER OF STATIONS IN EACH QUADRANT FOR VARIOUS SEISMIC REGIONS

Region	Quadrant (TI)				Quadrant (PDE)				No. of nts
	1	2	3	4	1	2	3	4	
1	18	7	2	9	10	5	1	3	15
3	4	4	1	3	3	2	1	2	13
5	4	1	0	12	2	1	0	8	11
7	4	1	2	11	2	0	1	6	16
8	4	1	1	13	2	1	1	8	31
10	1	5	3	6	0	5	1	4	4
12, 13	9	0	3	2	6	0	3	1	43
14	10	4	5	10	6	2	5	4	13
15	6	5	5	7	4	2	4	2	14
16	4	7	3	6	3	5	2	2	11
17, 18	16	3	2	15	8	2	0	3	12
19	20	2	5	20	10	0	2	4	42
20, 21	13	6	4	25	6	4	1	5	12
22	7	3	2	13	4	4	1	5	9
23, 24	3	8	1	14	1	6	1	3	17
25, 26	8	6	3	21	2	4	2	6	5
29, 30	14	2	1	37	2	1	0	13	6
34	2	3	4	3	1	2	4	3	8
44	2	1	0	8	2	0	0	7	6
48	11	5	3	24	4	3	2	8	9

The first of these two differences probably has the greater effect on hypocenter determinations.

Data used by Texas Instruments differ in both quantity and quality. In locating 333 hypocenters, TI used more than 9000 station readings compared to 4270 used by the USC&GS. Of course, the use of more data does not necessarily improve the accuracy of hypocenter determinations. An important factor is the distribution of these data. Table B-2 compares quadrant distribution of data used by Texas Instruments to determine hypocenter locations in various seismic regions. Quadrant 1 refers to epicenter-to-station azimuths ranging from 0° to 90°; quadrant 2, from 90° to 180°; quadrant 3, from 180° to 270°; and quadrant 4, from 270° to 360°.

Based on the average number of stations used in each quadrant, the quadrant distribution of data used by Texas Instruments is somewhat improved over that used by the USC&GS in regions 1, 5, 7, 8, 10, 15, 16, 17, 18, 19, 29, 30, 34, and 44. The proportions of additional data used for hypocenter determinations in regions 20 through 26 and in 48 which are in the fourth, or northwest, quadrant — result in considerably greater weight on data to the northwest in the TI determinations than in the USC&GS determinations.

Comparing the quantity of data on a regional basis, it may be seen that TI uses approximately three times as much data as does the USC&GS for determinations in regions 17, 18, 19, 20, 21, 22, 25, 26, 29, and 30; approximately twice as much data is used for determinations in regions 1, 7, 22, and 48. At least 40 percent more data is used in the regions listed in Table B-2, except in regions 34 and 44. Thus, the quantity and/or quadrant distributions of data are considerably enhanced in nearly all regions.

The quality, or accuracy, of arrival times of most data used was probably somewhat improved over that supplied to the USC&GS since, in a considerable number of cases, data analysis was performed after the USC&GS preliminary hypocenter locations were published.

In summary, appreciable changes in about half of the preliminary hypocenters for January 1964 are effected through use of the Texas Instruments hypocenter program. A portion of this result stems from the application of station/source-region travel-time corrections and another portion from the use of considerably more data, which are generally better distributed and somewhat improved in overall quality or accuracy. Probably the most significant results are the sharp decrease in the number of events with depths restrained to 33 km and the increase in the proportion of events with intermediate focal depths. However, these results require further investigation as does the depth problem in general.

Further improvement in hypocenter determination accuracy requires

- Considerably more knowledge of variations in travel times resulting from effects near both source and station
- Availability of more high-quality data (particularly in the Southern Hemisphere)
- Development of methods for weighting data on the basis of quality and distribution

It is also recommended that alternatives to the least-mean-squares method of hypocenter determination be explored.

APPENDIX C

LOCAL SEISMICITY

BLANK PAGE

APPENDIX C

LOCAL SEISMICITY

The number and density of seismograph stations in the Middle East and in Southern Asia precludes the location of many earthquakes of small or even moderate magnitudes. Consequently, in the area south of the USSR and China, most seismicity evaluations are based on relatively large events.

In this report, an alternative method has been used. Rather than evaluating the seismicity of the entire region, the seismicity of an area included by a radius of 1000 km around the more capable seismograph stations has been evaluated. The following are the procedures:

- Determine the perceptibility limits for values of m_b from 2.0 to 5.5 in increments of 0.5 units
- Determine the epicentral distances and magnitudes of all events within 1000 km of the station
- Count the number of events with magnitudes of 2.0 $\pm$ 0.25, 2.5 $\pm$ 0.25, etc., which occur within the calculated limits of perceptibility for m_b = 2.0, 2.5, etc.
- Normalize this number to a radius of 1000 km in each case; i.e., multiply by 10^6 km^2 and divide by r^2 where r is the calculated perceptibility limit
- Plot the logarithms (base 10) of these numbers vs magnitude
- Fit a straight line to the plotted points by the least-squares

Data obtained from the analyses of short-period vertical seismograms recorded in 1963 at Istanbul, Turkey; Shiraz, Iran; Quetta, Pakistan; and Shillong, India were used to accomplish the study. Results are shown in Figures C-1 through C-4.

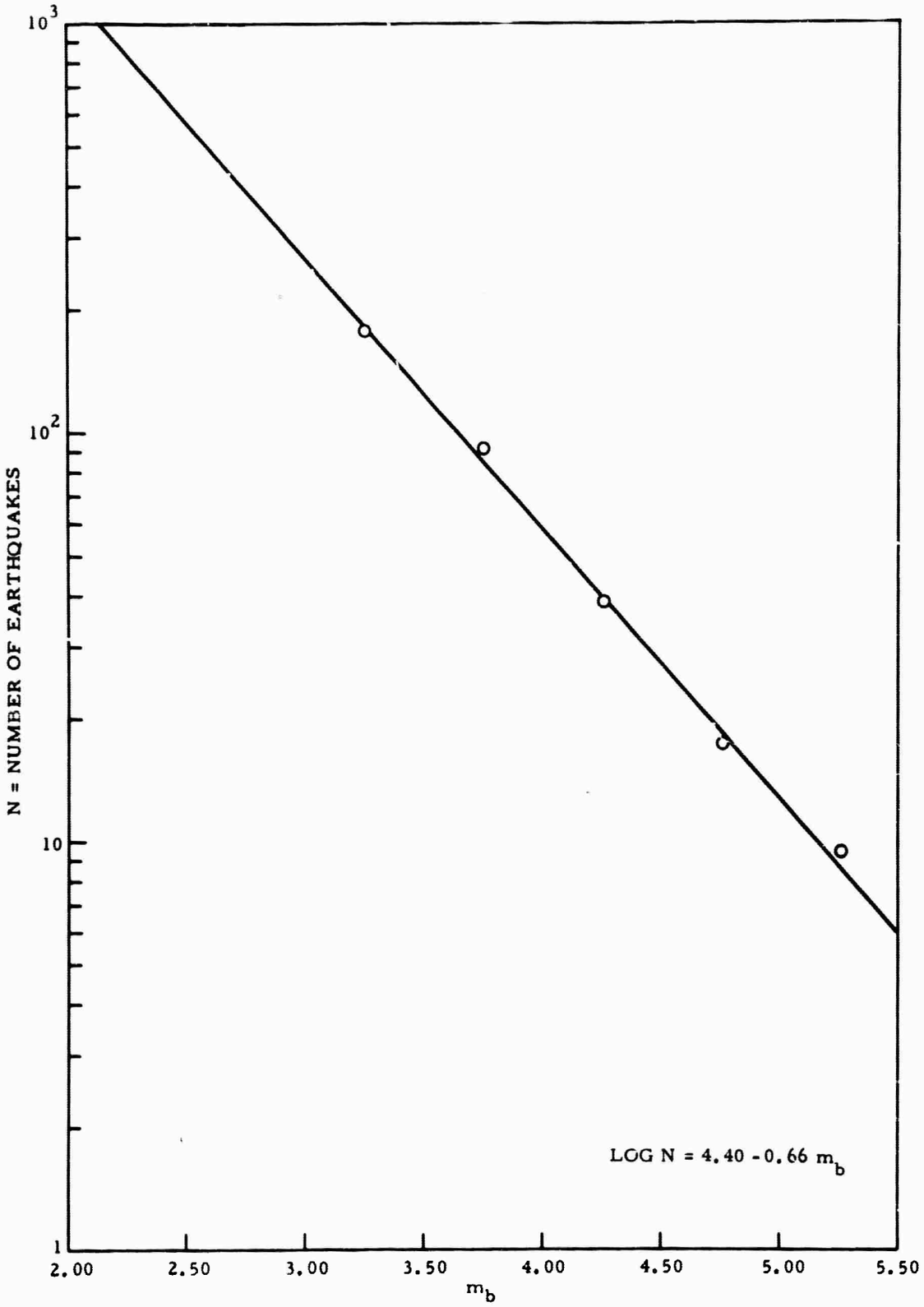

Figure C-1. Earthquake Frequency in Vicinity of Istanbul, Turkey

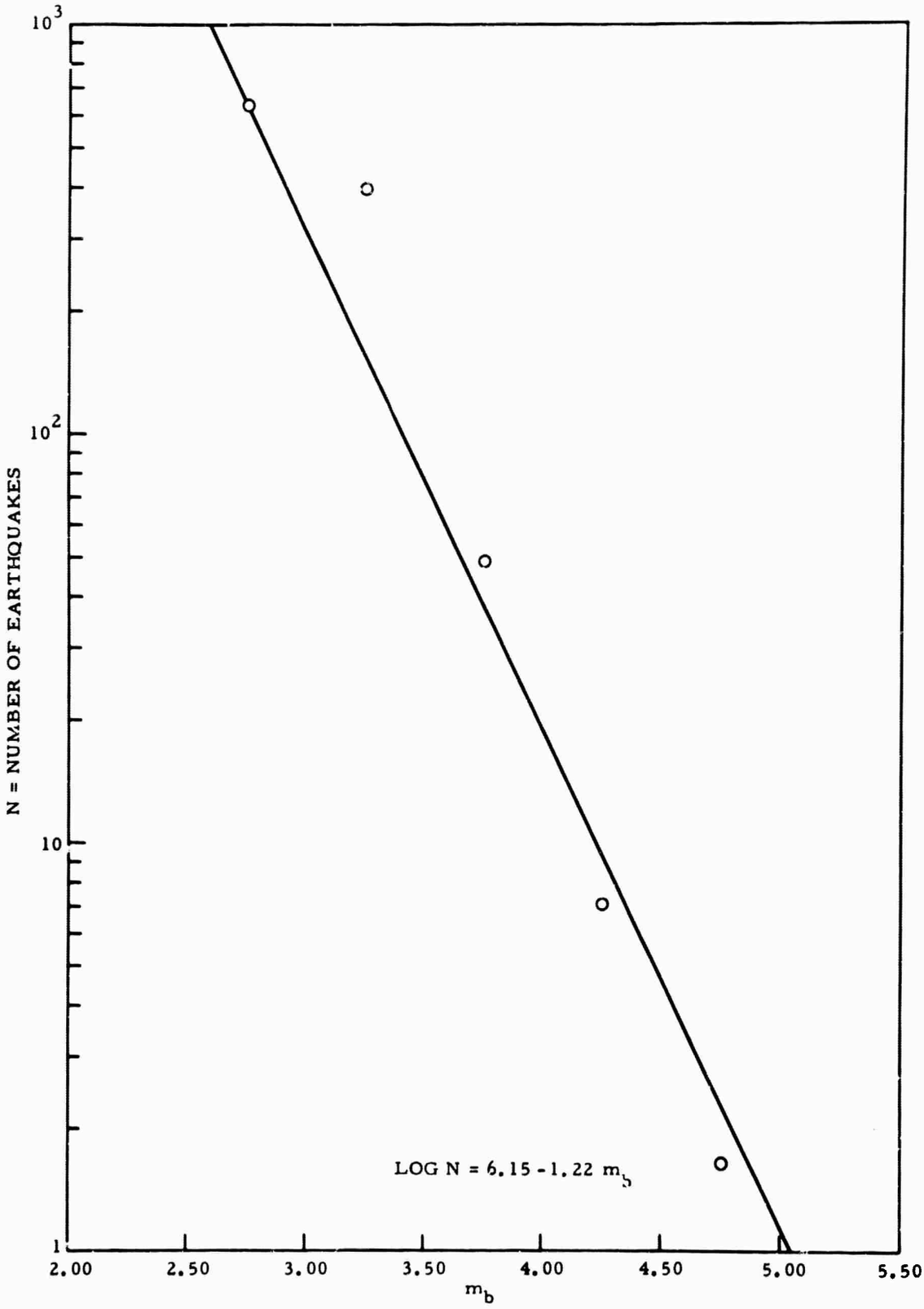

Figure C-2. Earthquake Frequency in Vicinity of Shiraz, Iran

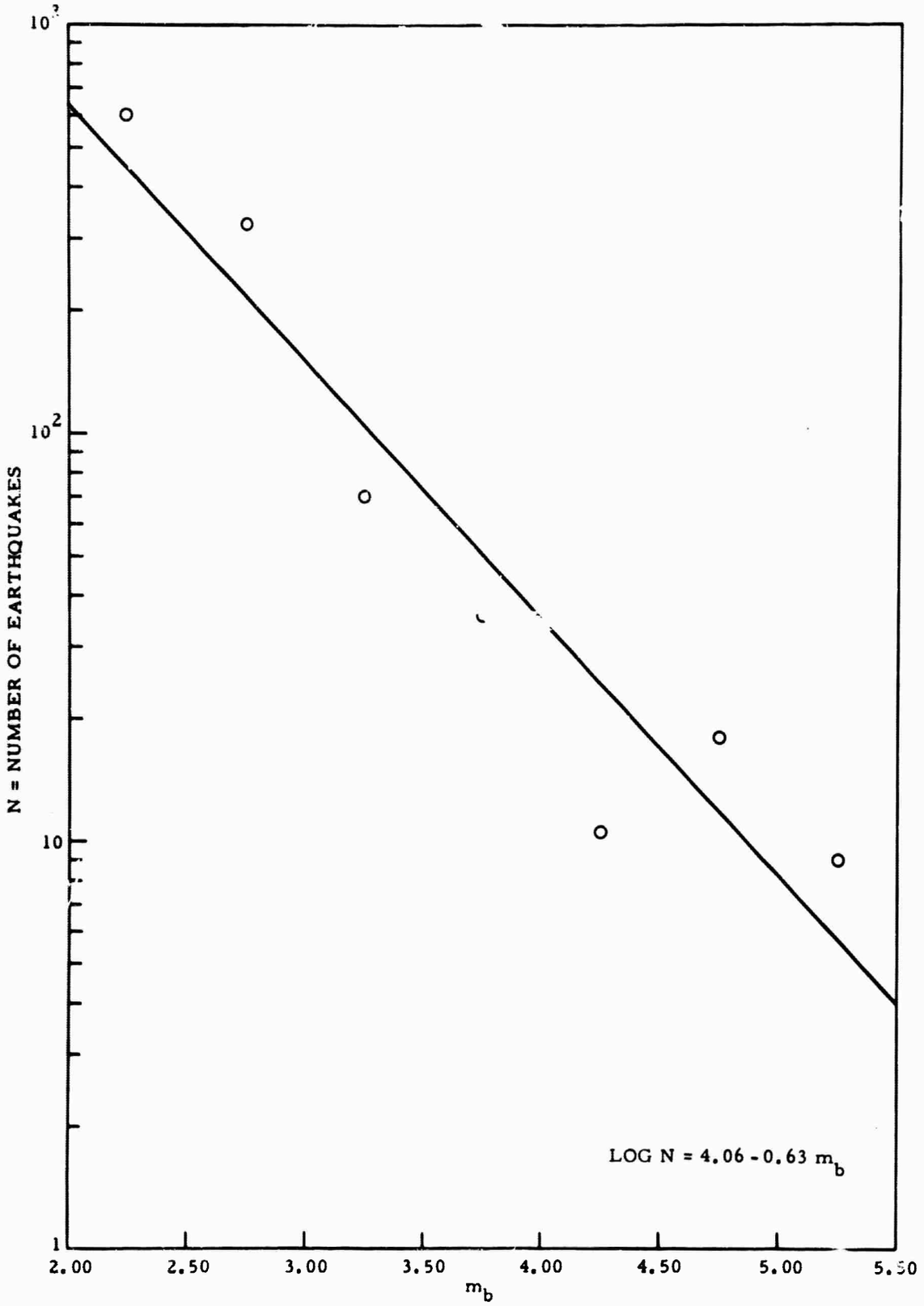

Figure C-3. Earthquake Frequency in Vicinity of Quetta, Pakistan

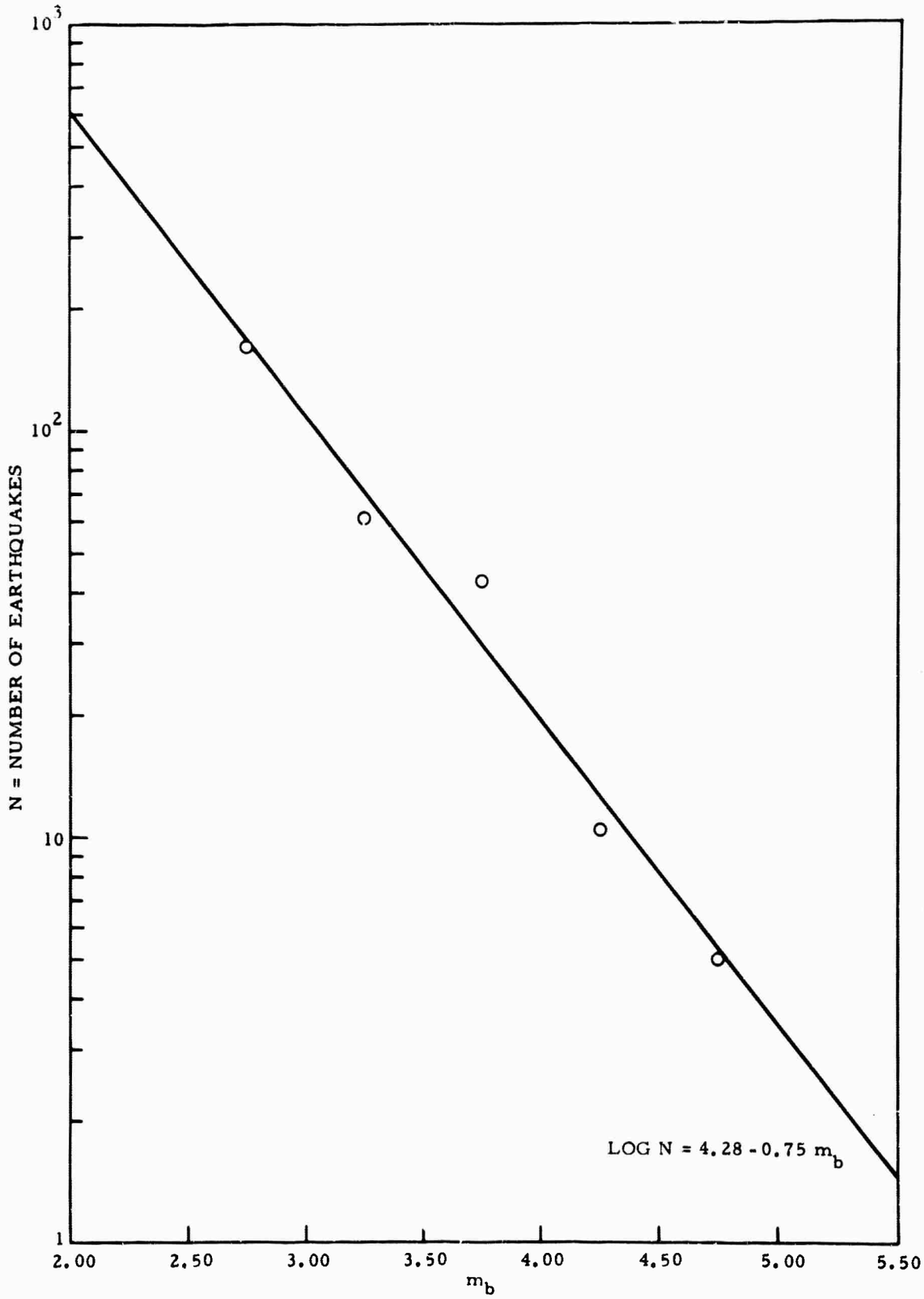

Figure C-4. Earthquake Frequency in Vicinity of Shillong, India

On the basis of the results obtained, the rates of earthquake recurrence in the vicinities of Istanbul and Quetta are nearly the same and only slightly larger near Shillong. However, the recurrence rate for earthquakes near Shiraz is nearly twice that for Quetta. Thus, in 1963, the numbers of earthquakes with magnitudes of $m_b = 5.0 \pm 0.25$ within 1000 km of the stations are

Istanbul	13
Shiraz	1
Quetta	8
Shillong	3

At magnitudes of $m_b = 3.0 \pm 0.25$, however, the estimated numbers are

Istanbul	263
Shiraz	309
Quetta	148
Shillong	108

Thus, if seismicity were based on only numbers of events, the Shiraz area would be considered the most seismic; however, since more larger events occur near Istanbul, the total seismic energy release in this area is highest. The conclusion reached is that the area surrounding Istanbul is the most seismic of those studied.

APPENDIX D

WORLDWIDE ARRAY PROCESSING

BLANK PAGE

APPENDIX D

WORLDWIDE ARRAY PROCESSING

A. INTRODUCTION AND SUMMARY OF RESULTS

Digital processing of records from stations forming a worldwide array (as reported by Texas Instruments Incorporated in Special Report No. 4) was initially undertaken as a possible means of enhancing depth-phase identification. The present study is a continuation of the investigation into the problem of energy propagation and magnitude determination. In the previous study, errors may have been present in the data because of hand-digitizing from paper records; this difficulty has been overcome in the present study since data were recorded on magnetic tape and computer-digitized.

Worldwide array processing techniques have been applied to data from a selected suite of five Kurile Islands events and the LONGSHOT nuclear explosion in the Aleutian Islands. Table D-1 presents the U.S. Coast and Geodetic Survey hypocenter information on these six events.

Table D-1

EVENTS ANALYZED BY WORLDWIDE ARRAY PROCESSING

Date	H	Lat.	Long.	h	m_b	No. Sta.	Location	Assigned No.
1/15/64	02 23 47.4	45.3N	150.6E	45	5.3	10	Kurile Islands	15
3/16/66	08 44 32.8	44.8N	146.8E	140	5.7	12	Kurile Islands	76
7/1/64	09 46 49.6	45.2N	150.3E	75	4.8	10	Kurile Islands	183
11/12/64	05 16 26.2	47.1N	146.6E	328	4.8	8	Kurile Islands	317
12/17/64	05 18 34.8	45.4N	150.1E	17	5.3	10	Kurile Islands	352
10/26/65	21 00 00.1	51.4N	179.2E	0	6.0	33	Aleutian Islands	LS

The processing sequence shown in Figure D-1 was applied to all data. Then, the processed data were studied for information relevant to four areas of special interest.

1. Depth-Phase Identification

Short-period vertical traces from each station were gathered and composited to form a single record with individual, equalized traces displayed side by side in the order of increasing epicentral distance; 41 pP phases could be identified on the composite record as compared to 12 pP phases reported by the individual stations. Stacked traces from three of the five earthquake events clearly showed a pP phase.

2. Digital Filtering Techniques

In previous worldwide array processing, most filtering was analog filtering accomplished electrically on playback. Digital filtering is generally superior to analog filtering because digital filters are stronger and more selective and the filtered output can be input into further processing. Development of digital filtering capabilities, therefore, was considered important to further progress in worldwide array processing.

Each of 10 filters designed was applied to 16 selected traces, and the results were displayed side by side on a single record. Results of the study were twofold:

- A library of 10 assorted filters is stored on magnetic tape for future use
- There is visual evidence of each filter's effectiveness on various types of traces

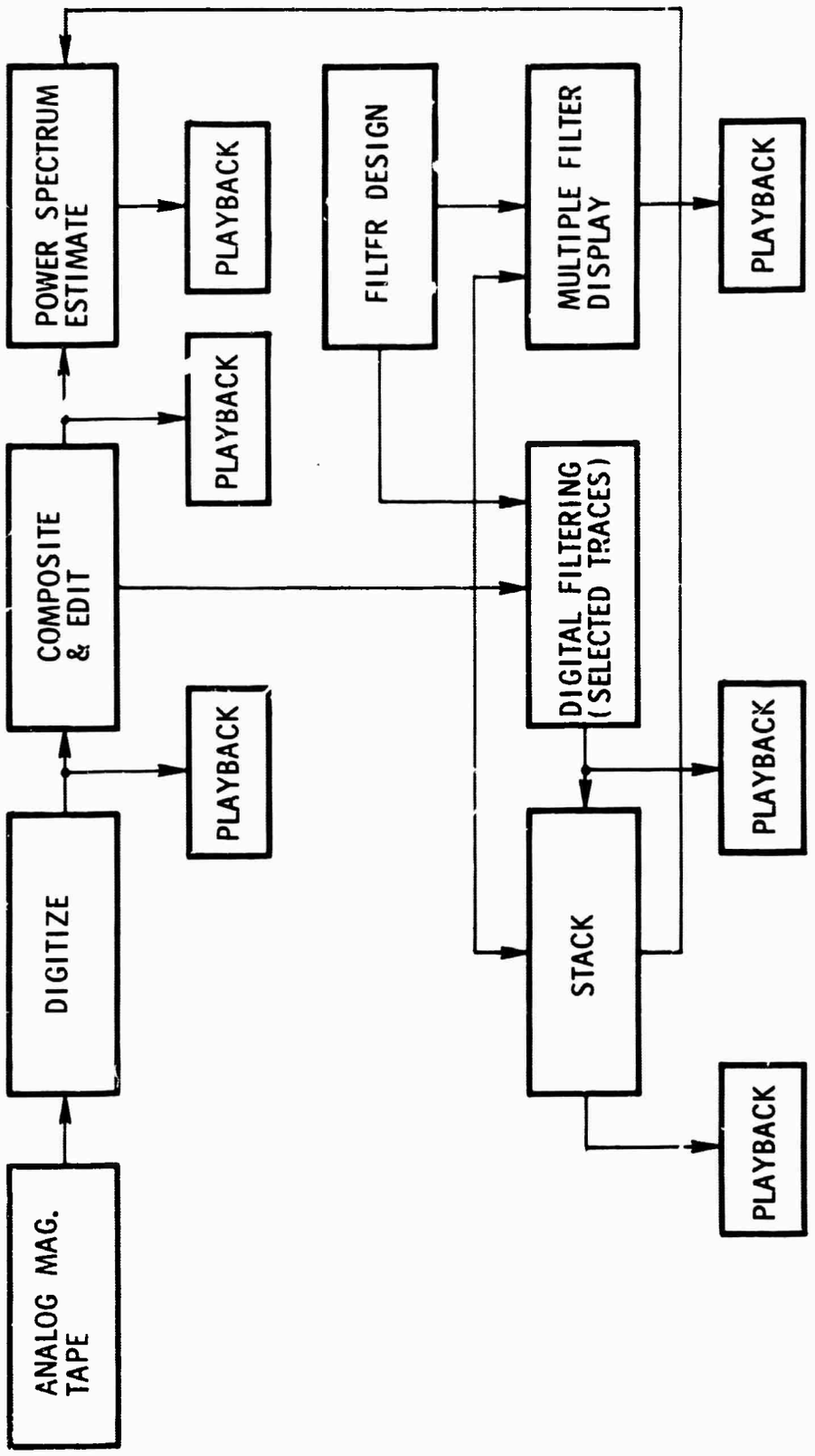

Figure D-1. Array Processing

3. Power Density Spectrum Studies

The power density spectrum of the short-period vertical trace was computed for each station. The differences in power spectra recorded by different stations for the same event appear to depend only on the local crustal structure at the stations. Power spectrum results, therefore, have been used to compute magnitude corrections for nine stations.

4. Energy Attenuation

Energy attenuation curves were plotted from average P energy in the first minute after the P-phase arrival at 10 stations recording LONGSHOT at nearly the same azimuth. Comparison of these results with presently used Q curves shows discrepancies as large as one m_b unit; as a result, the need for Q-curve revision is obvious. The results of this study also indicate that energy attenuation, when average power is considered, may not be as irregular as would be expected considering the large standard deviations obtained for magnitudes calculated from a single cycle.

The energy-vs-distance curve may be approximated by $\frac{e^{-2Kr}}{r^2}$ for $\Delta > 56^\circ$. For $\Delta < 56^\circ$, the increasing energy with increasing distance behavior needs further investigation; the cause may possibly be diffraction effects at the Mohorovicic discontinuity.

B. DIGITAL PROCESSING TECHNIQUES

All data used in this study were originally recorded in analog form on magnetic tape by Long-Range Seismic Measurement Vans. Digitizing was done by a Texas Instruments DARC* (Data Analysis and Reduction Computer) directly from composite analog magnetic tapes supplied by the Seismic Data Laboratory in Alexandria, Virginia. This procedure eliminated any

*Trademark of Texas Instruments Incorporated

errors which might have been present in previous studies (Special Report No. 4) as a result of hand-digitizing. The digitized records were in a format compatible with TIAC* (Texas Instruments Automatic Computer), which was used to accomplish all data processing.

A TIAC trace-gather routine transferred the short-period vertical trace from each station onto a composite record for each event. Other routines were then used to edit the composite records. Editing included the shifting of traces to line up the first peak of the P-arrival trace, zeroing to remove spikes or other bad segments from the traces, and trace polarity reversal to make the direction of the first motion of all of the traces the same.

The records were then equalized over the first minute after the P arrival by

- Computing the average trace amplitude for the first minute
- Obtaining the ratio of the desired average amplitude to the computed average amplitude
- Multiplying every point on the original trace by this amplitude ratio and output

The output records from equalization have the same average amplitude and, consequently, the same power over the first minute.

Power spectra were computed by taking the Fourier transform of the autocorrelation of the trace:

$$\text{autocorrelation} = \sum_{t = T_o}^{T_{max}} tr(t) \cdot tr(t \cdots \tau) \qquad (1)$$

*Trademark of Texas Instruments Incorporated

where

τ = 0, $\Delta\tau$, $2\Delta\tau$, ..., τ_{max}

$\Delta\tau$ = sample rate of the correlation

tr(t) = value of trace at time t

tr(t-τ) = value of trace at t-τ

Therefore, power spectrum = $\int_{-\infty}^{\infty}$ autocorrelation $e^{-if\tau}\, d\tau$ (2)

The term "stacking" refers to a simple algebraic sum of N traces. The theory behind stacking is that the noise in each of the N traces is different. Therefore, the total noise in all traces is randomly out of phase and tends to cancel in the algebraic sum. Signals such as pP which arrive at all stations at a nearly constant interval from the P phase, however, tend to be in phase on all traces and, therefore, will add in the sum. The pP amplitude-to-noise ratio on the stacked trace, then, is improved by a factor of $N^{1/2}$.

The digital filters designed in the study were computed by TIAC. The computer reads in the parameters describing the desired filter and outputs the filter onto magnetic tape ready for use. This filter is fed into the computer against the data trace, resulting in a filtered output trace. The main advantage of a digital filter over an analog filter is that the output from the digital filtering process can be input into later processing steps. Another advantage is that the digital filter can be designed to be much "sharper" than the analog filter. Figure D-2 shows typical power spectra for both types of filters.

C. DEPTH-PHASE IDENTIFICATION

The application of worldwide array processing techniques to depth-phase identification has been reported in Special Report No. 4. The

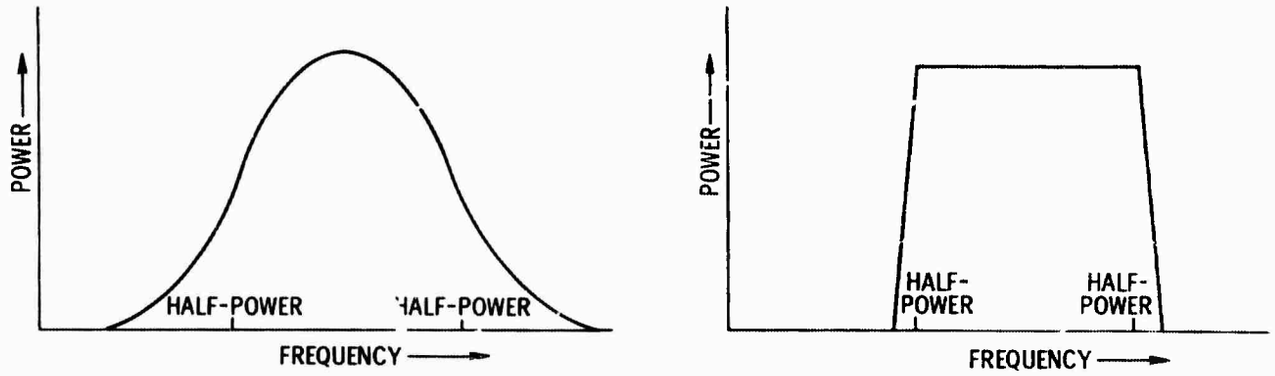

Figure D-2. Power Spectra of Typical Analog and Digital Filters

present effort has limited the work in this area to two processes to avoid duplication; i.e.,

- Composite records are edited, equalized, and displayed in the order of increasing epicentral distance on a single record
- All of the traces for each event aligned on the P arrival are stacked together, forming a single trace

Figures D-3 through D-8 show results of the first process. Depth-phase identification is considerably improved by forming these arrays. Table D-2 lists the number of traces on which pP and PcP can be identified from the array as compared to the number of these phases reported by individual stations.

Table D-2

DEPTH-PHASE IDENTIFICATION—
SINGLE TRACE VS WORLDWIDE ARRAY

Event	pP		PcP	
	Individual Trace	Array	Individual Trace	Array
15	1	9	0	0
76	6	7	0	0
183	3	9	0	0
317	1	6	0	1
352	1	10	0	1
LS	0	0	28	21

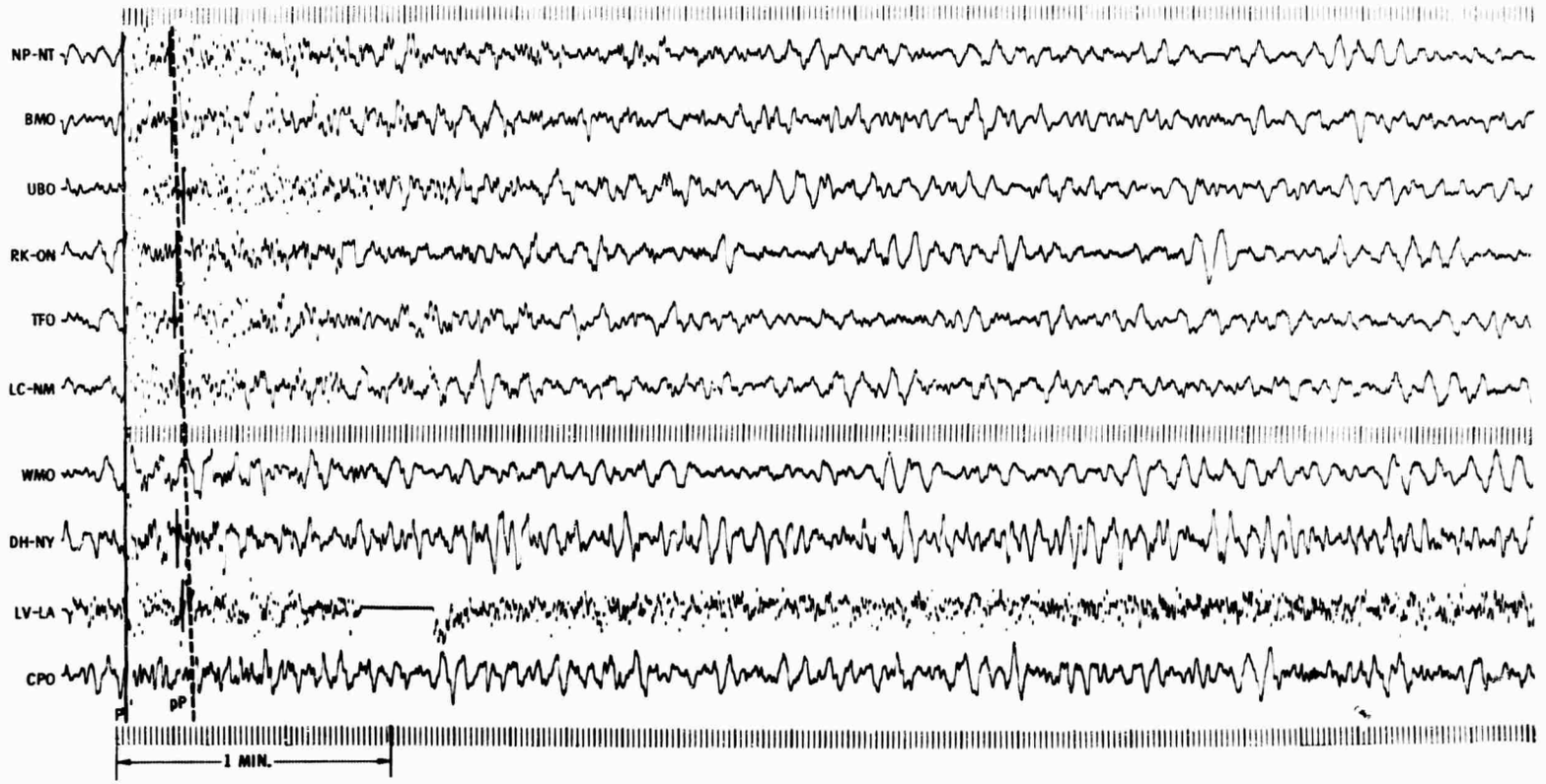

Figure D-3. Earthquake Event 15

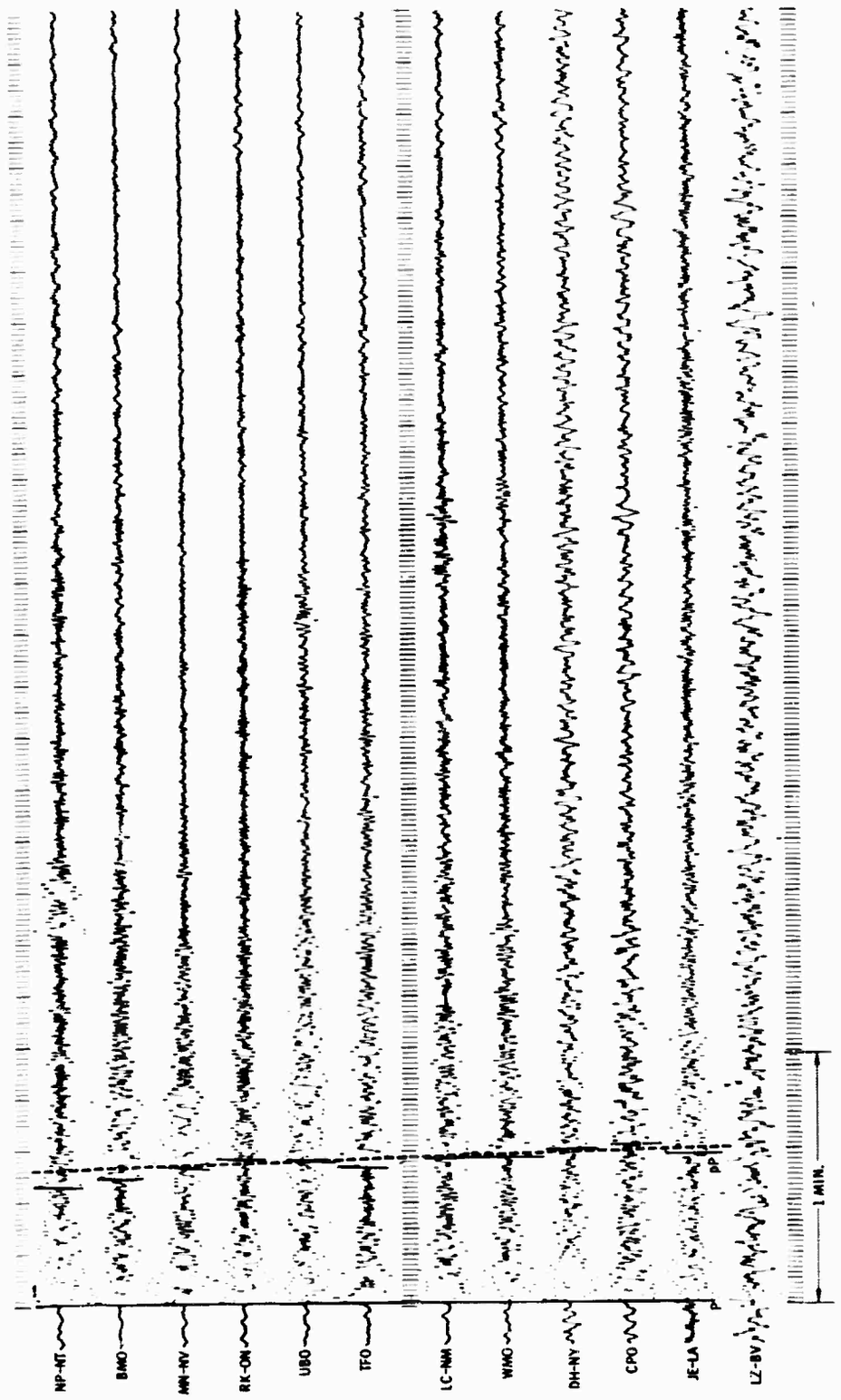

Figure D-4. Earthquake Event 76

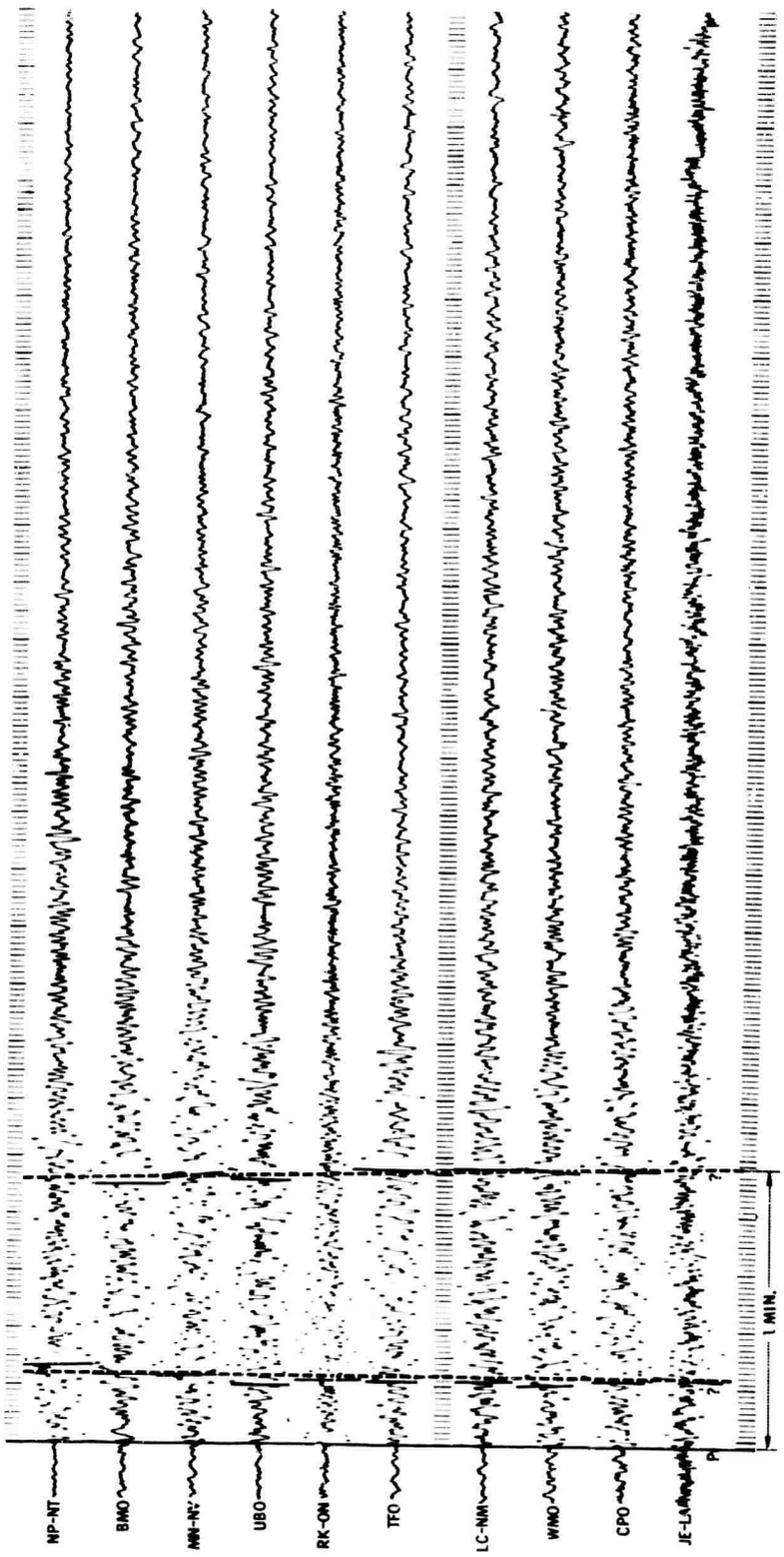

Figure D-5. Earthquake Event 183

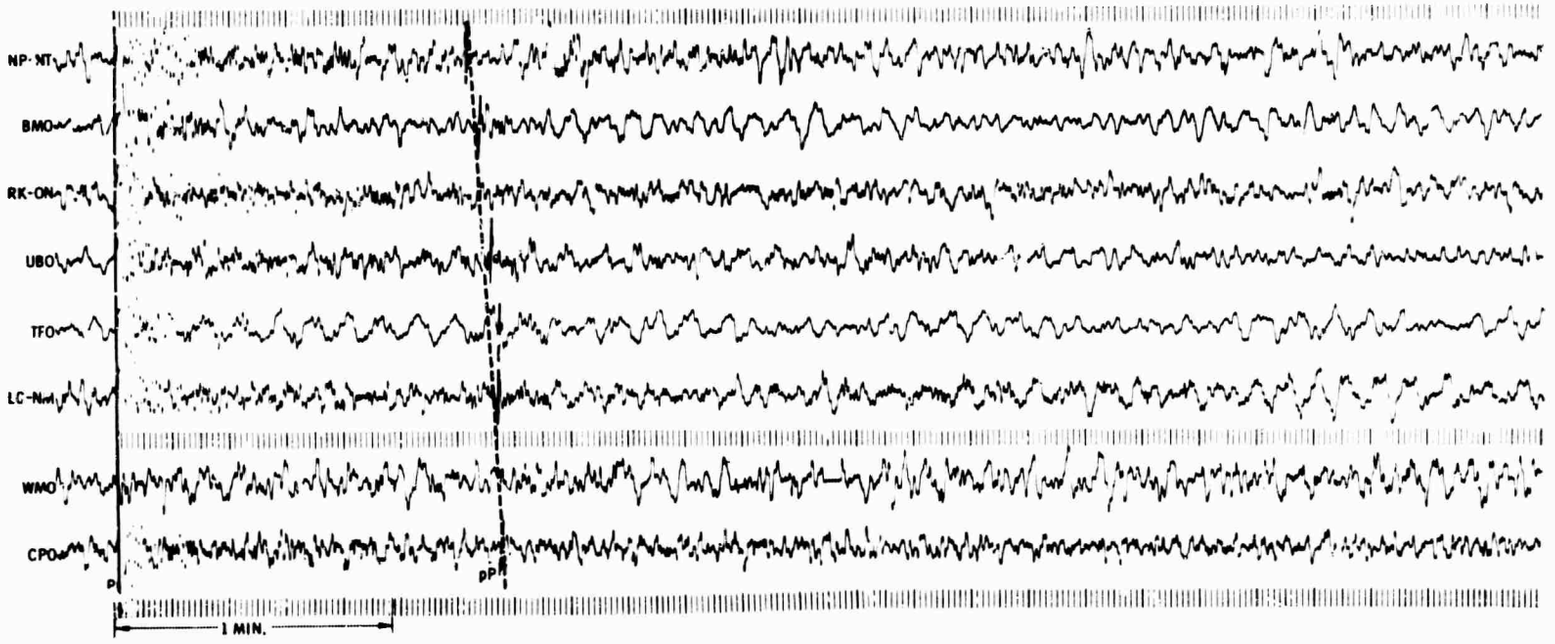

Figure D-6. Earthquake Event 317

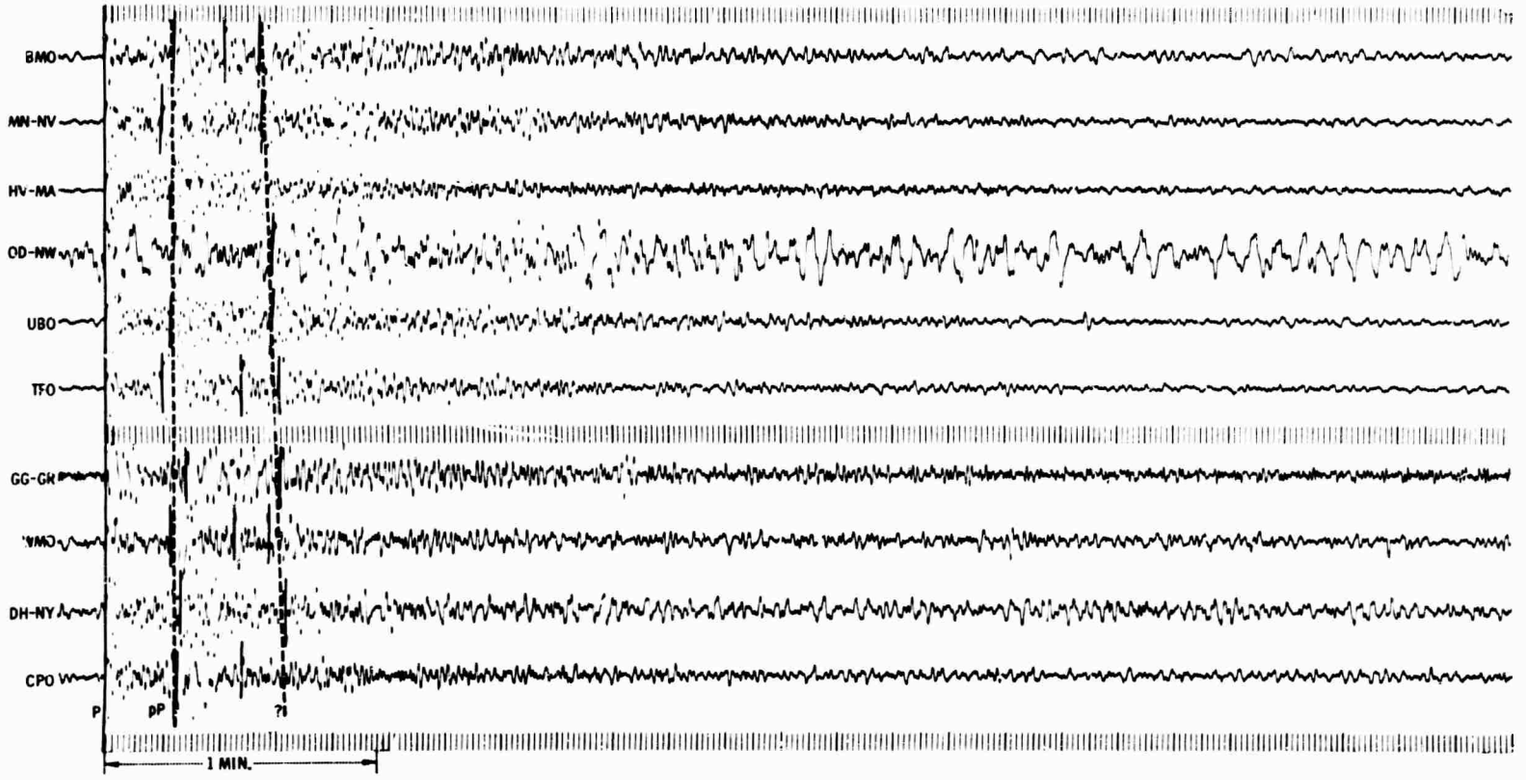

Figure D-7. Earthquake Event 352

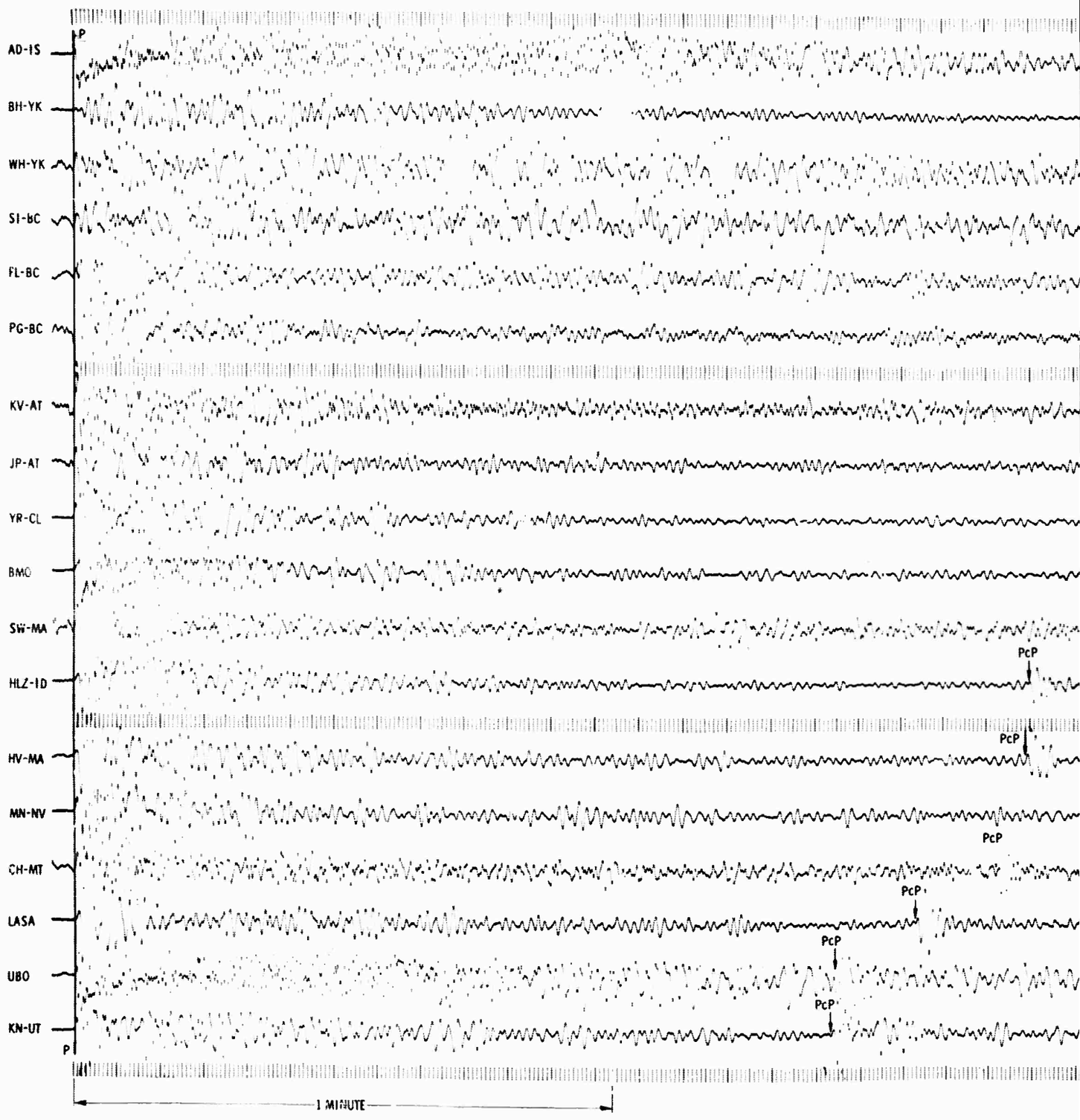
AD-IS
BH-YK
WH-YK
SI-BC
FL-BC
PG-BC
KV-AT
JP-AT
YR-CL
BMO
SW-MA
HLZ-ID
HV-MA
MN-NV
CH-MT
LASA
UBO
KN-UT
P
PcP
PcP
PcP
PcP
PcP
1 MINUTE

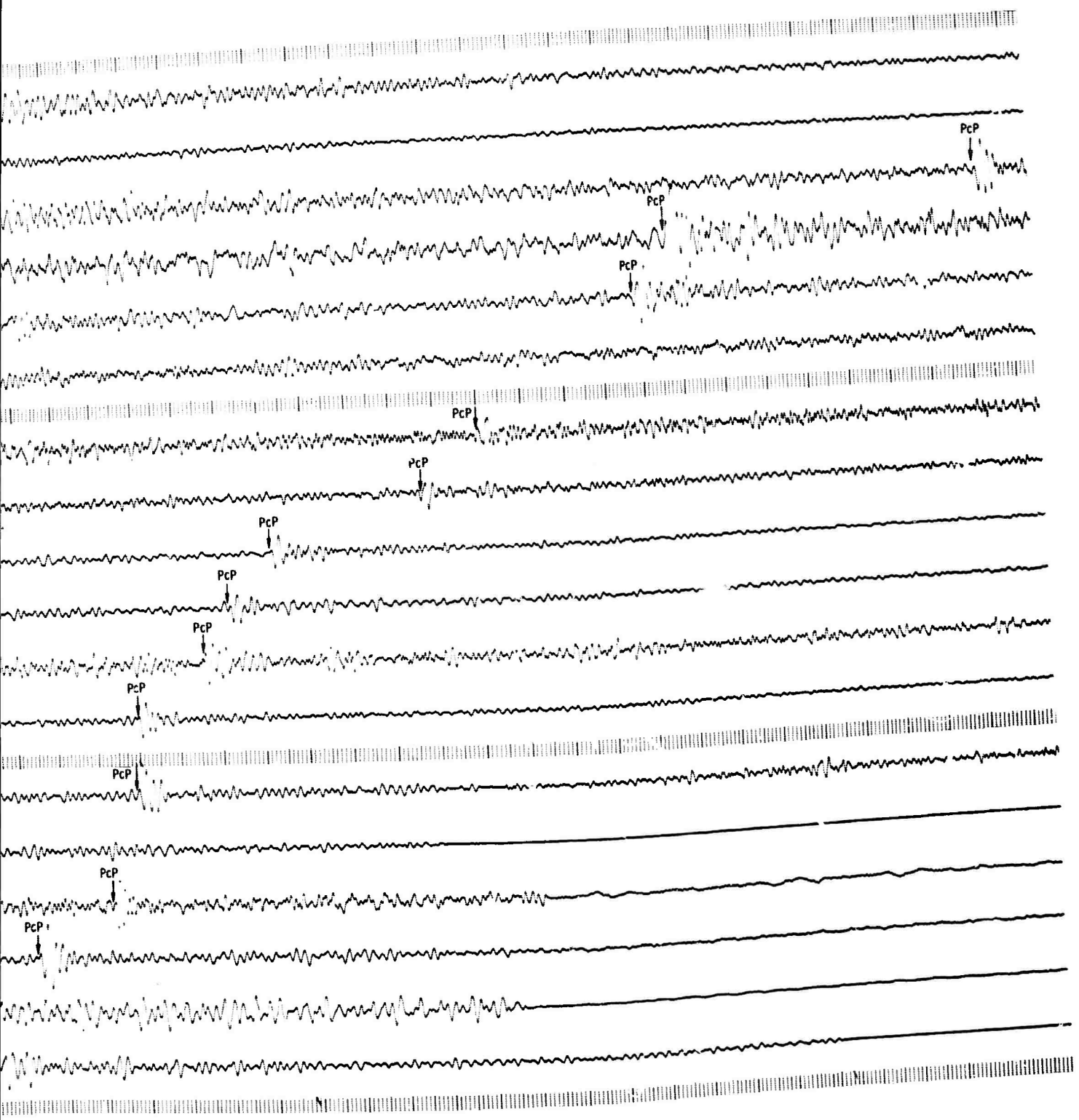

Figure D-8. Array Ensemble Presentation of LONGSHOT Recording (1 of 2)

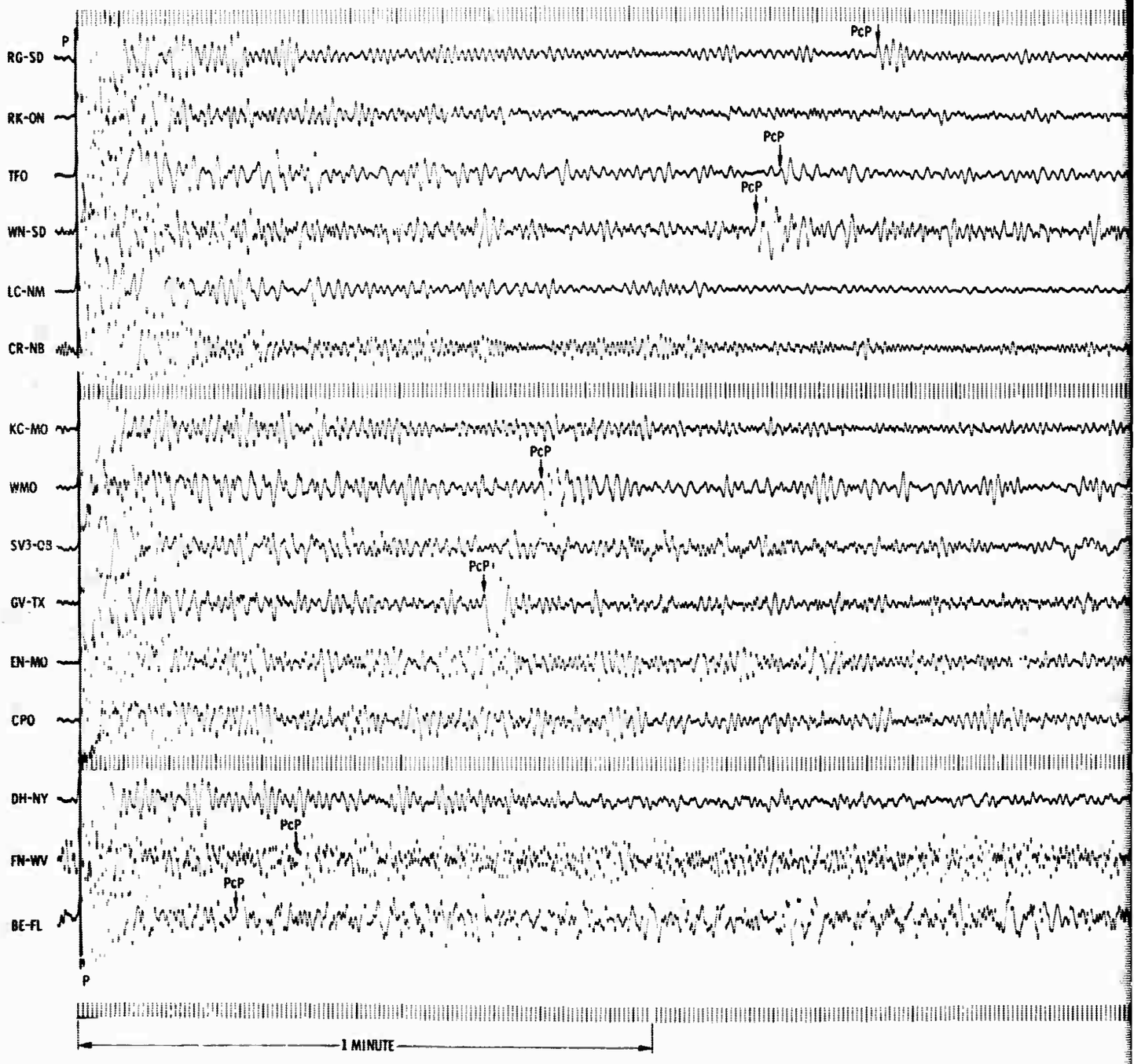
P
RG-SD
RK-ON
TFO
WN-SD
LC-NM
CR-NB
KC-MO
WMO
SV3-OS
GV-TX
EN-MO
CPO
DH-NY
FN-WV
BE-FL
PcP
PcP
PcP
PcP
PcP
PcP
P
1 MINUTE

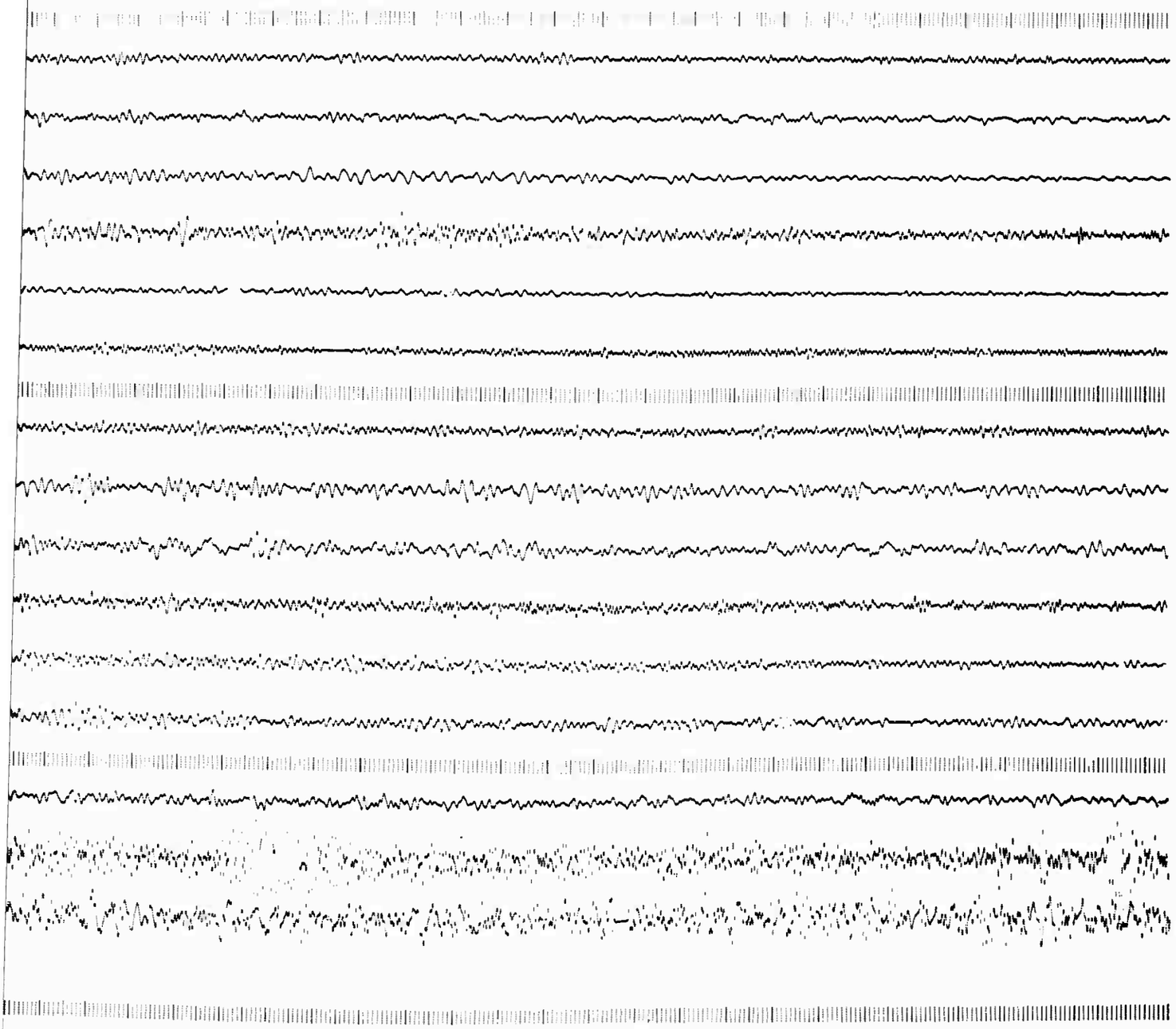

Figure D-8. Array Ensemble Presentation of LONGSHOT Recording (2 of 2)

BLANK PAGE

The second process results in positive pP identification for three of the five processed earthquake events (15, 76, and 352), which indicates that stacking may be developed into a useful tool for depth-phase identification. Figure D-9 shows the stacked traces for the three events of interest.

One interesting discrepancy appeared after study of the stacked traces of event 352. The stacked trace indicates a pP-P interval of 14.75 sec which, at an average distance of 50°, indicates a depth of approximately 60 km as compared with 17 km reported by the USC&GS. For events 15 and 76, the stacked traces indicate depths of 45 km and 140 km, respectively, which exactly agree with the USC&GS value.

D. DIGITAL FILTERING STUDIES

Since previous array processing did not utilize digital filters to any extent, as assortment of high-pass, low-pass, and bandpass digital filters with frequency ranges as listed in Table D-3 were designed and applied to selected traces for the purpose of better determining their usefulness in data processing. Selected from the data were 16 representative traces — two from each earthquake event and six from LONGSHOT. All 10 filters were applied to each of the selected traces. For each input trace, a single output record was received, with the 10 filtered outputs of the same input trace displayed side by side.

These filtered outputs show considerable improvement over the raw data. Here, filtering is definitely superior to the previous analog filtering. Figure D-10 shows two examples.

As a result of this study, a library of 10 filters is stored on magnetic tape ready for immediate use in the future. In addition, there is evidence of the effectiveness of each of the filters on various types of traces.

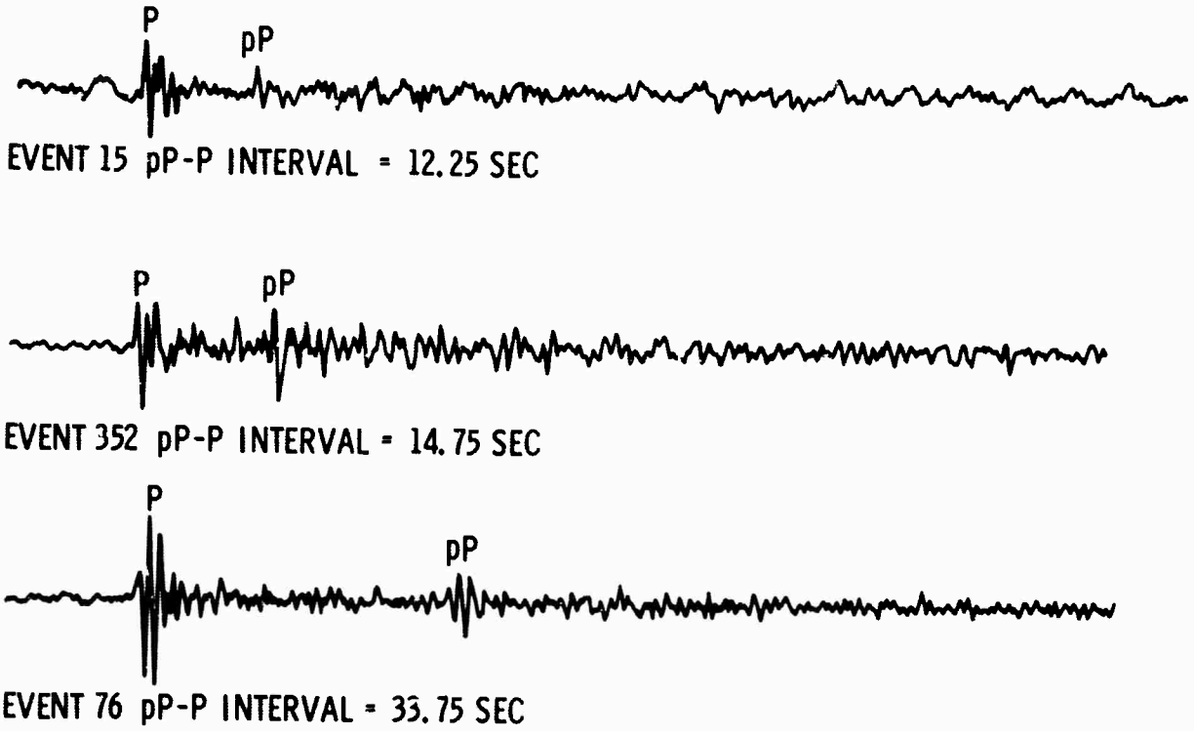

Figure D-9. Stacked Traces Showing Depth Phases

Table D-3

DIGITAL FILTERS

Filter Type	T (sec)
high-pass	0 - 1.5
high-pass	0 - 1.0
high-pass	0 - 2.0
bandpass	0.5 - 1.5
bandpass	1.0 - 1.5
bandpass	0.67 - 2.0
bandpass	1.0 - 2.0
bandpass	0.5 - 1.0
low-pass	0.5 - 00
low-pass	1.0 - 00

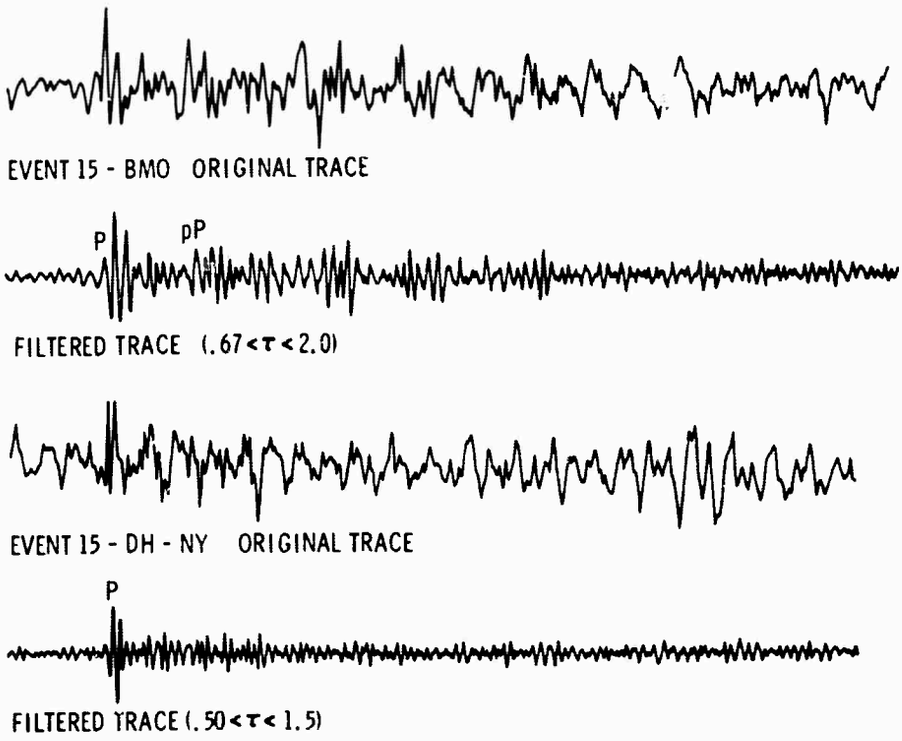

Figure D-10. Typical Results of Digital Filtering Applied to Earthquake Records

E. ENERGY ATTENUATION

The linear position of 10 stations along a single azimuth from the LONGSHOT event (Figure D-11) provides an opportunity to study energy attenuation with distance. The short-period vertical traces from each of the 10 stations selected for this study are equalized over a 1-min time window, beginning with the first P arrival.

The vertical component of the total energy arriving at the station in the first minute is

$$E_V \propto E_{VIE} \left[G^2 \times (IR)^2 \times (EQS)^2\right]^{-1} \qquad (3)$$

where

E_{VIE} = total energy in the first minute of the equalized trace

G = instrument gain
= $\frac{\text{amplitude of calibration signal (peak to peak)}}{\text{equivalent ground motion given in daily tape logs}}$

IR = instrument response of f_{pmax} as calculated in Section II

EQS = equalization scalar
= $\frac{\text{amplitude of chosen peak on equalized trace}}{\text{amplitude of same peak on unequalized trace}}$

As a result of equalization, E_{VIE} is a constant and can be omitted from Equation (3). The vertical component of the energy, then, is given by

$$E_V \propto \left[G^2 \times (IR)^2 \times (EQS)^2\right]^{-1} \tag{4}$$

Figure D-12 shows results of the calculation of the vertical component of P energy for the 10 selected stations as a function of distance. Assuming that energy radiates spherically from the source, the energy per unit area perpendicular to the direction of wave propagation would diminish as follows:

$$E(r) = E_{source} \times \frac{e^{-2K_r}}{r^2} \tag{5}$$

The vertical component of the energy at distance r is

$$E_v(r) = \cos^2(e_o)\, E(r) = \frac{E_{source} \cos^2(e_o)\, e^{-2K_r}}{r^2} \tag{6}$$

where e_o is the angle that the direction of propagation makes with the normal to the earth's surface. The energy-vs-distance curve in Figure D-12 closely follows the expected $\frac{e^{-2Kr}}{r_2}$ curve for $\Delta > 56°$.

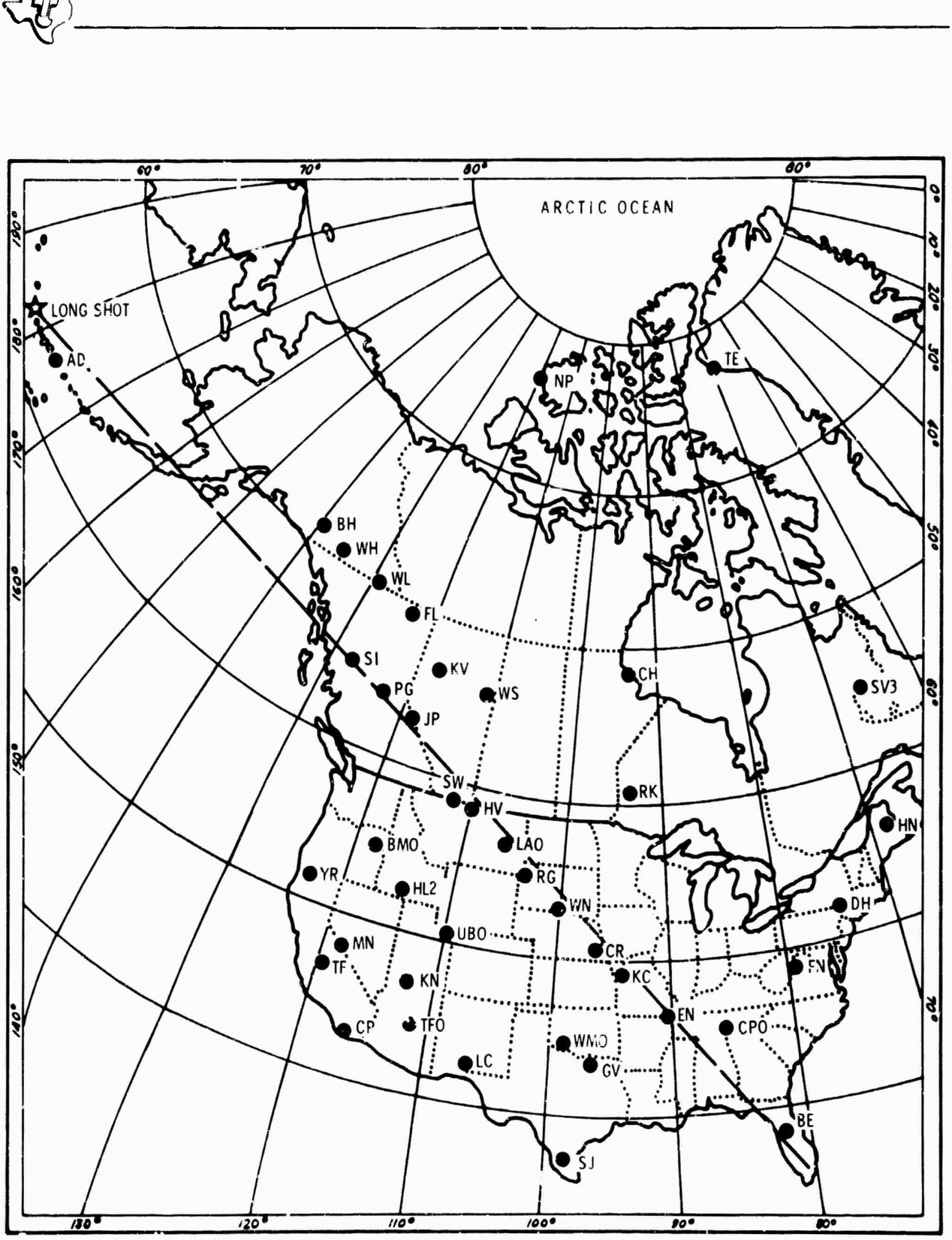

Figure D-11. Recording Stations for LONGSHOT Event

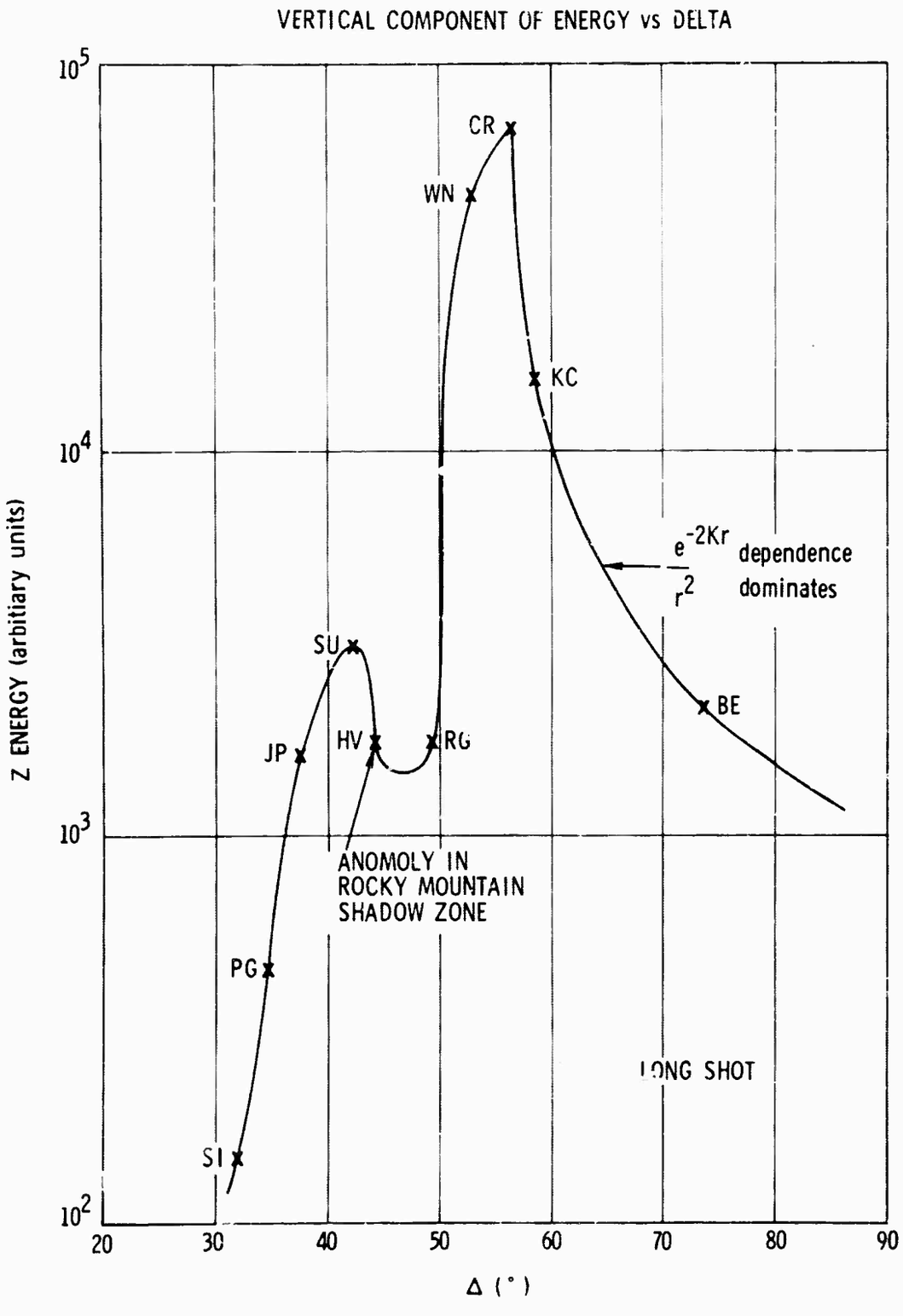

Figure D-12. Vertical Component of Energy Vs Δ

For small distances, the $\cos^2(e_o)$ term would be expected to decrease vertical energy with decreasing distances; however, the effect would be slight and could not account for the large decrease observed.

Further study into this matter is needed; one possible cause might be diffraction at the Mohorovicic discontinuity (Figure D-13). This approach also explains the anomaly in the Rocky Mountain area.

Figure D-14 shows the spherical divergence effect and the possible diffraction effect which, in combination, resemble the LONGSHOT results. The fact that these results are in the form of the simple functions predicted by making the assumption of spherical divergence, which is equivalent to the assumption of homogeneous crust and mantle, indicates that one could expect more consistent energy or magnitude calculations by considering the average P-wave amplitude rather than the amplitude of the maximum cycle.

Figure D-12 has been transformed into a more familiar representation called the Q curve. The unified magnitude m_b is given by

$$m_b = \log \frac{A}{T} + Q \qquad (7)$$

where Q is an empirical correction factor. The Q curve is the plot of this correction factor as a function of distance and depth. The commonly used Q curve for surface-focus events is compared with the Q curve calculated from LONGSHOT data (Figure D-15). The units on the vertical axis and the relative positions of the two curves are arbitrary. The data indicate that present Q curves may introduce errors as large as one magnitude unit into the calculation of m_b. It seems, therefore, that a Q-curve revision is needed for improvement of the m_b scale.

The presence of anomalies in the Q curves, such as the one seen in the LONGSHOT curve, are very dependent on source location. Therefore, it may be necessary to compute sets of Q curves for every source region.

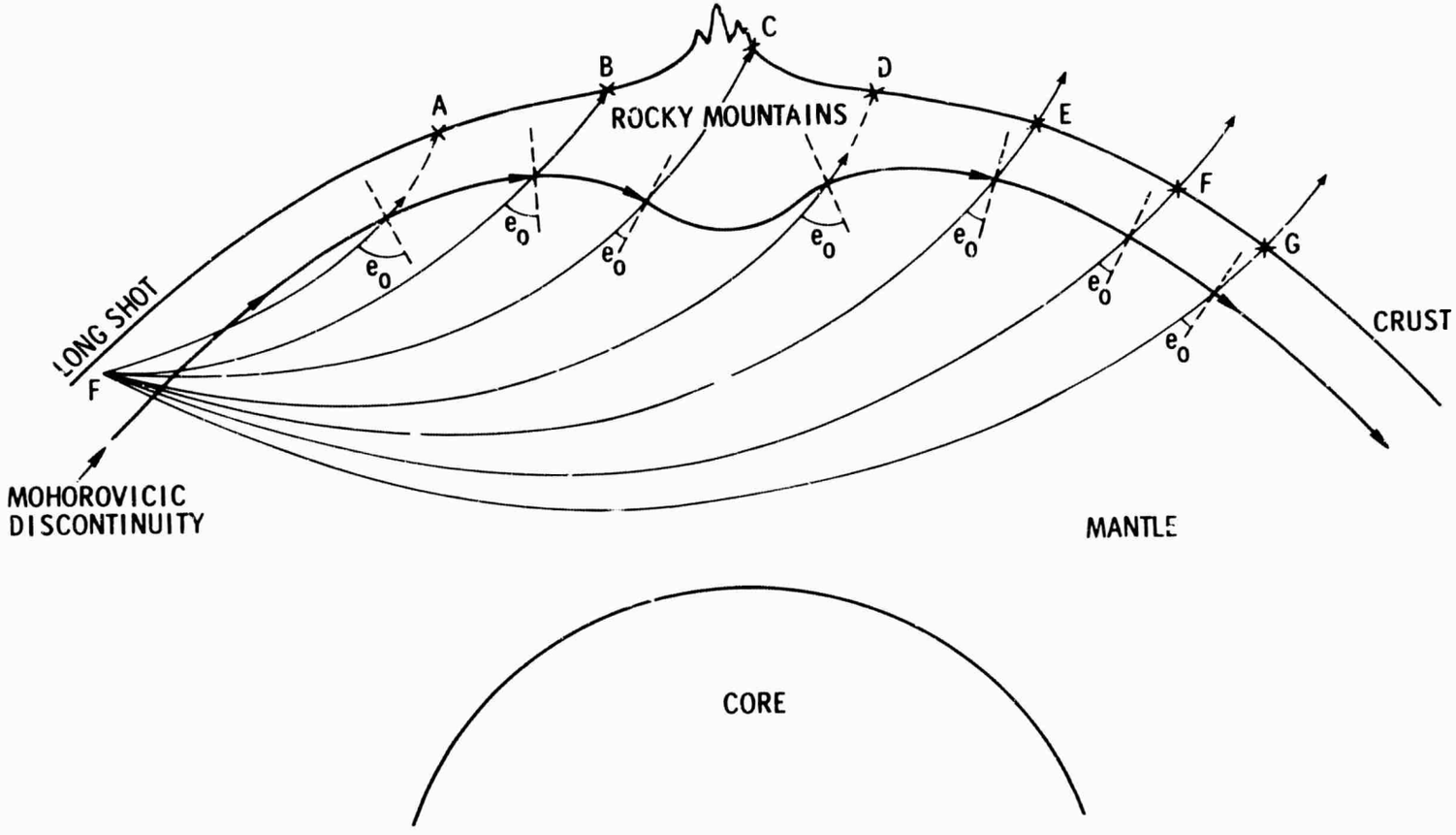

Figure D-13. Diffraction Effect of Moho

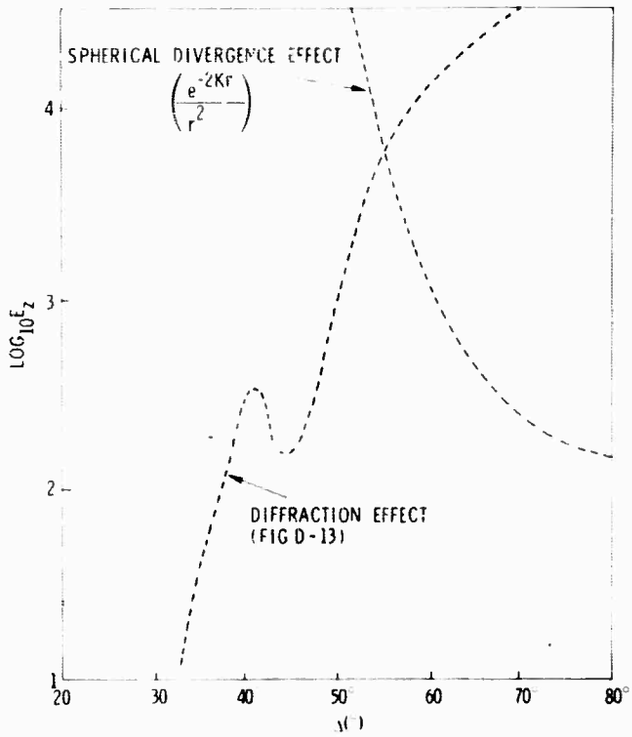

Figure D-14. Two Effects Limiting Energy Arriving at Surface of Earth

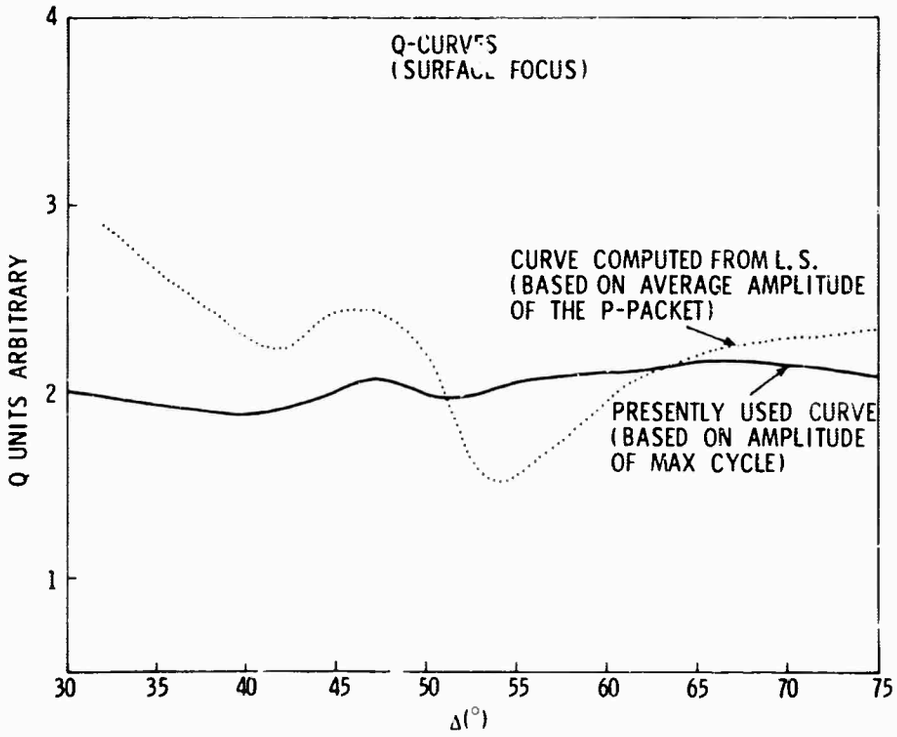

Figure D-15. Q Curves (Surface Focus)

An important result of this study is that a technique has been developed to apply data processing techniques to the precise computation of Q curves, but the method is now somewhat limited because of lack of data recorded on magnetic tape.

F. POWER DENSITY SPECTRA STUDIES

Power density spectra are computed for all stations and all events. The spectra are computed over a 1-min time window, beginning with the P arrival.

Figure D-16 presents power density spectra for all stations recording event 183, and Figure D-17 shows power density spectra for LONGSHOT recorded at stations lying along a single azimuth. For all six events, the power density spectra seem to have the same general appearance. Deviations from this general appearance do not seem to vary in a systematic fashion as distance increases. LeBlanc and Howell (1966) also observed this result.

The frequency of maximum power is calculated from the power density spectrum of each station event and is subtracted from the frequency of maximum power for each station recording each event. Figure D-18 presents the results of this calculation where the frequency of maximum power shows no well-behaved distance dependence.

Figures D-19 and D-20 give magnitude and depth dependence of the average frequency of maximum power for the six events studied. Event focal depth seems to have no effect on energy frequency, although Mohammadioum (1965a and 1965b) has observed this effect for Alaskan earthquakes. A tendency toward higher frequencies for larger events is indicated.

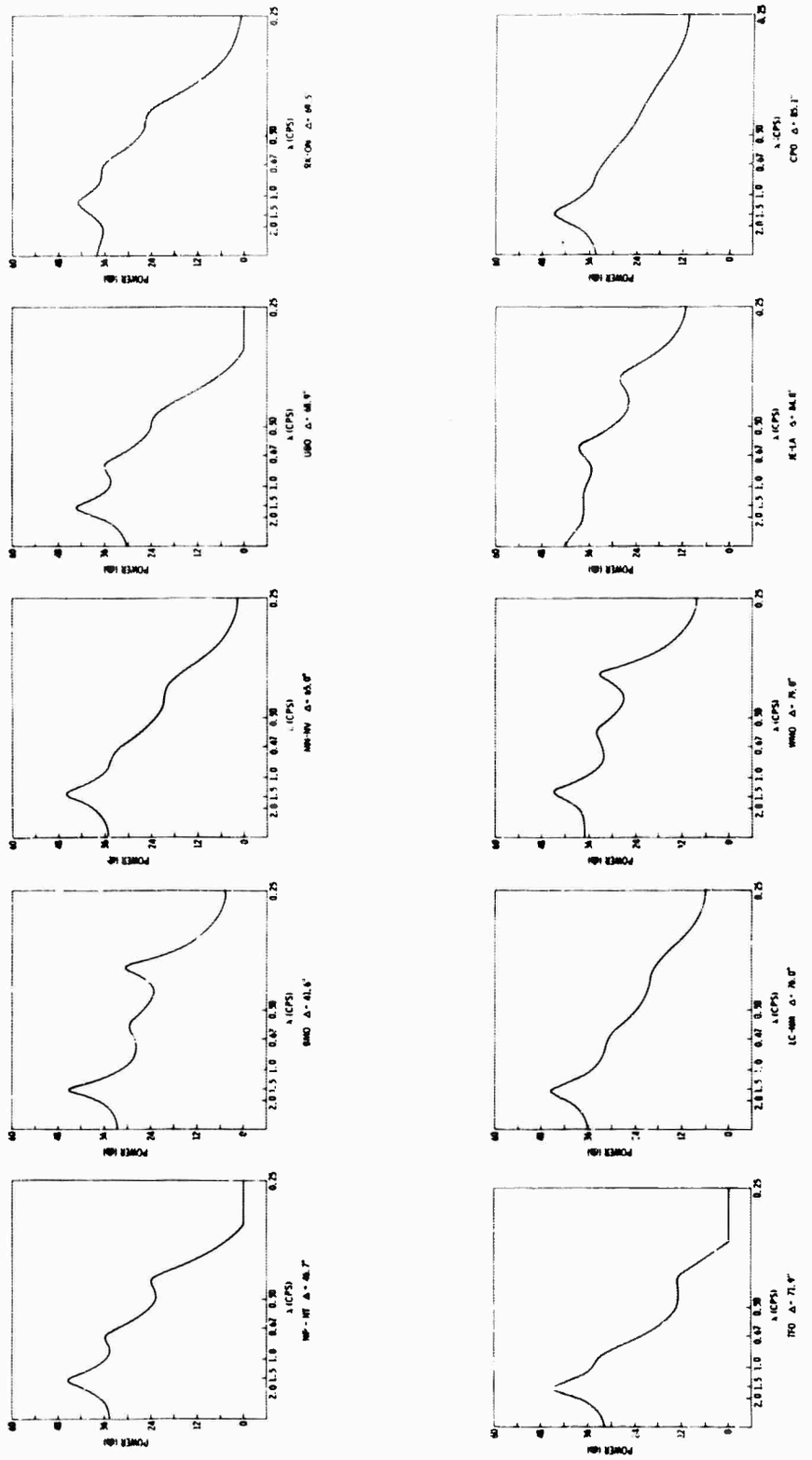

Figure D-16. Power Density Spectra for All Stations Recording Event 183

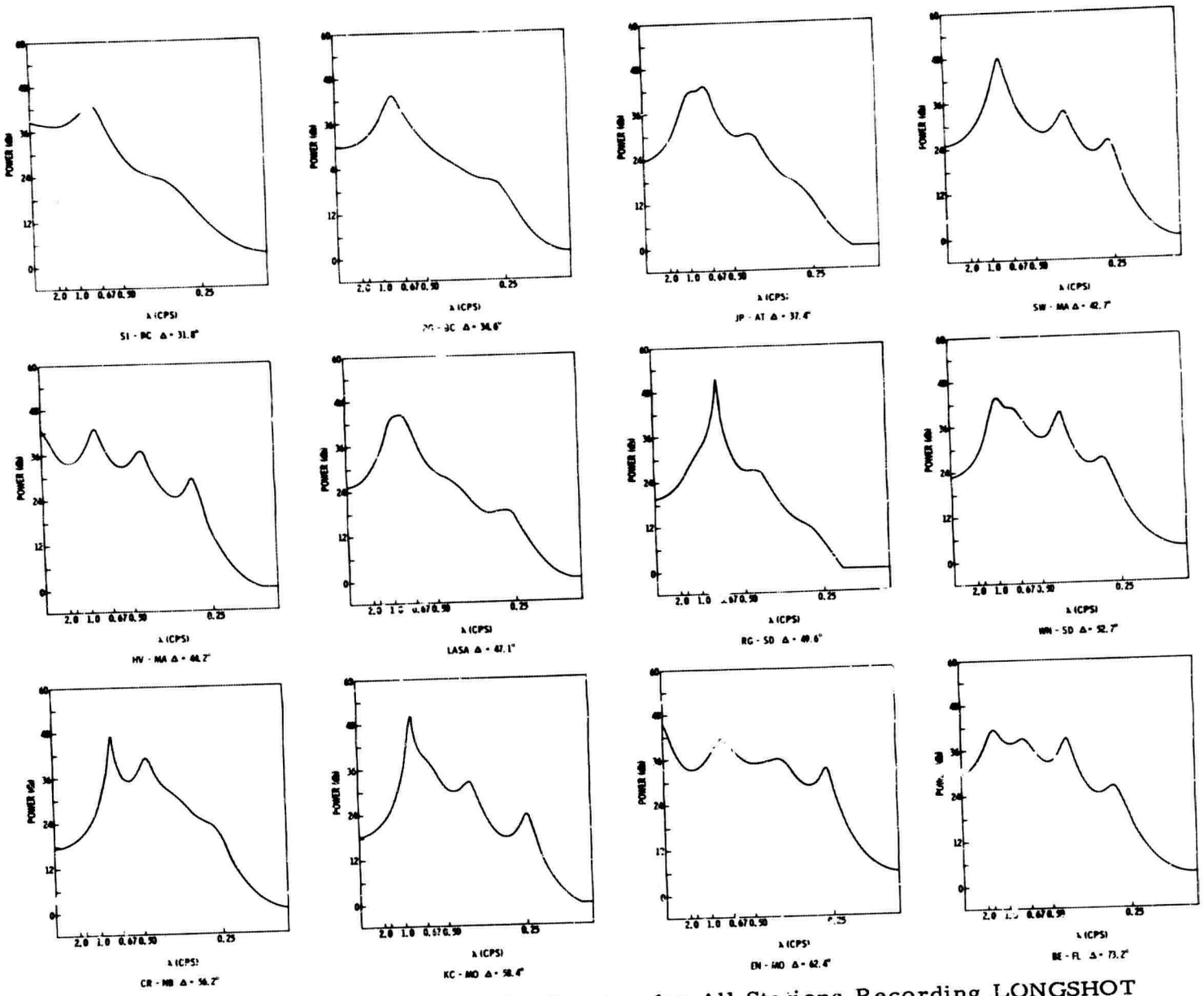

Figure D-17. Power Density Spectra for All Stations Recording LONGSHOT

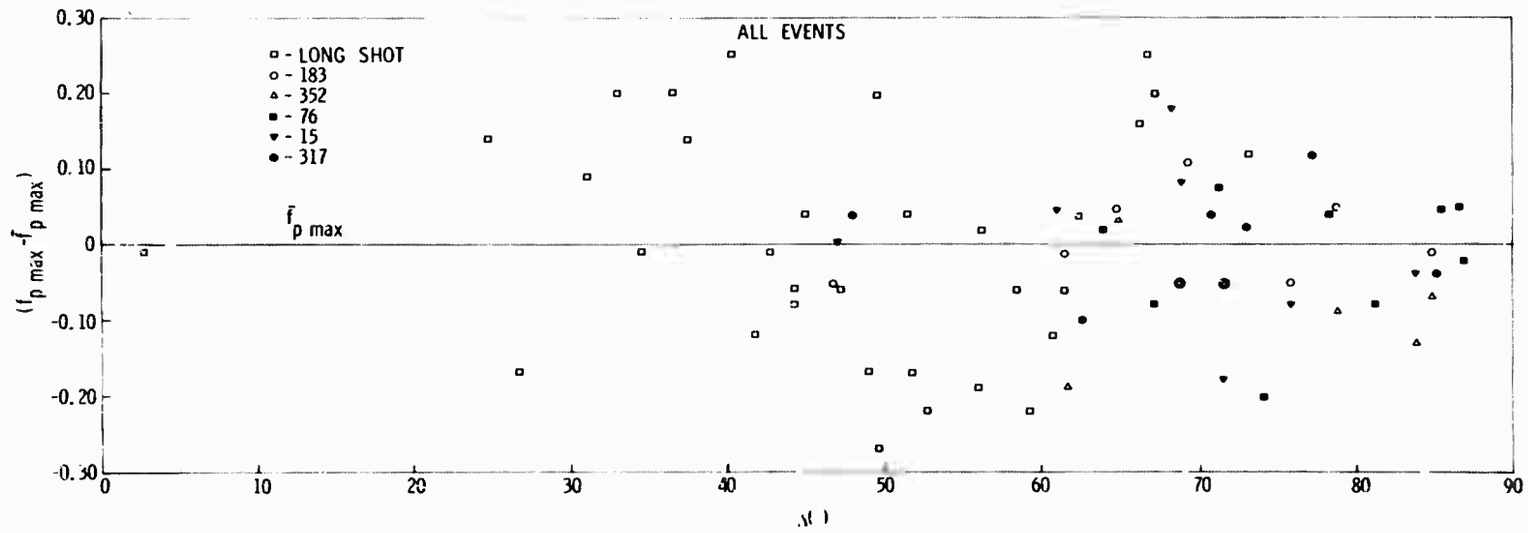

Figure D-18. All Events

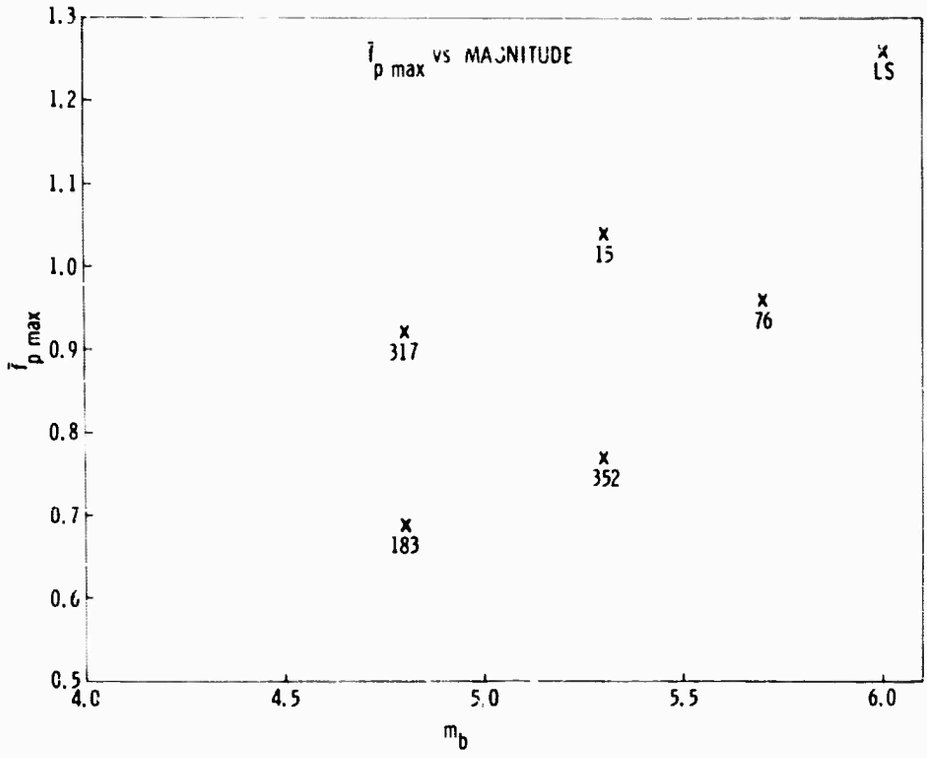

Figure D-19. $\bar{f}_{pmax}$ Vs Magnitude

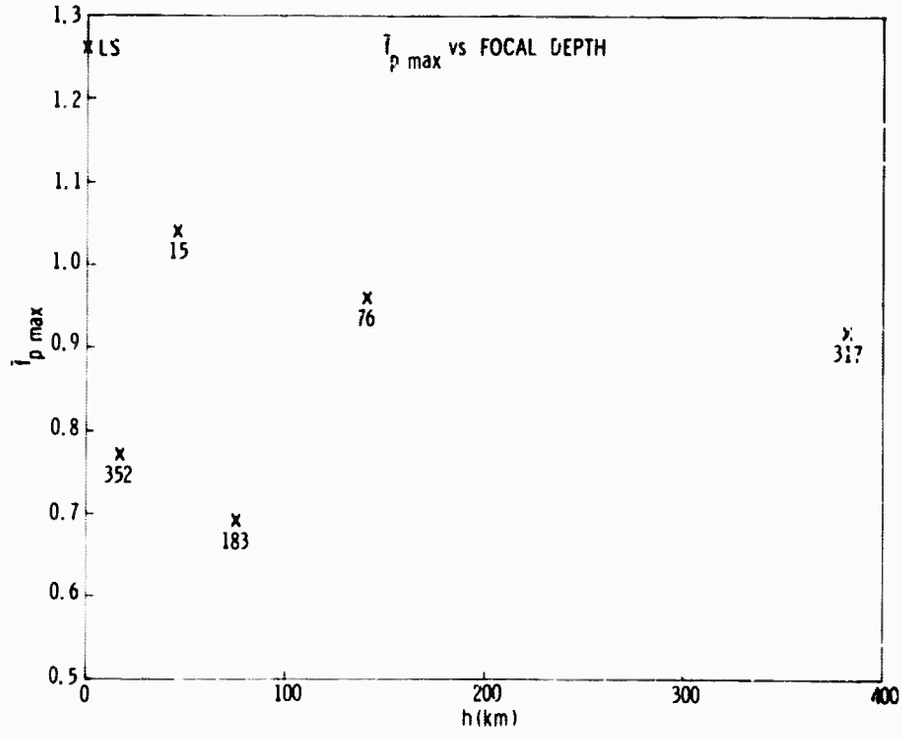

Figure D-20. $\bar{f}_{pmax}$ Vs Focal Depth

Results of TI studies indicate that the power density spectrum of the energy, as it travels through the earth, remains essentially unchanged over the distances studied. The differences in power spectra between different stations for a given event would arise, therefore, from the filtering effect of the complex geology of the crust at the station. If this is true, the power spectra from several events occurring in the same region and recorded at a given station should be similar. Figure D-21 presents the similarity in power spectra for three Kurile Islands events recorded at TFO and BMO.

For every station, then, a crustal operator G may be defined; it operates on the power spectrum Φ of the energy arriving at the bottom of the crust to give Φ' the power spectrum recorded at station i. In general,

$$\Phi = \Phi(f) \quad \Phi \neq \Phi(\lambda) \tag{8}$$

and

$$\Phi_i(f, e_o, \phi) = G_i(f, e_o, \phi)\ \Phi(f) \tag{9}$$

If all events considered are from the same region,

$$G_i(f, e_o, \phi) \cong G_i(f) \equiv g_i(f) \tag{10}$$

Equation (9) for the case where events are in the same region reduces to

$$\Phi_i'(f) = g_i(f)\ \Phi(f) \tag{11}$$

Another subscript is added to Equation (11) to identify the event:

$$\Phi_{ij}'(f) = g_i(f)\ \Phi_j(f) \tag{12}$$

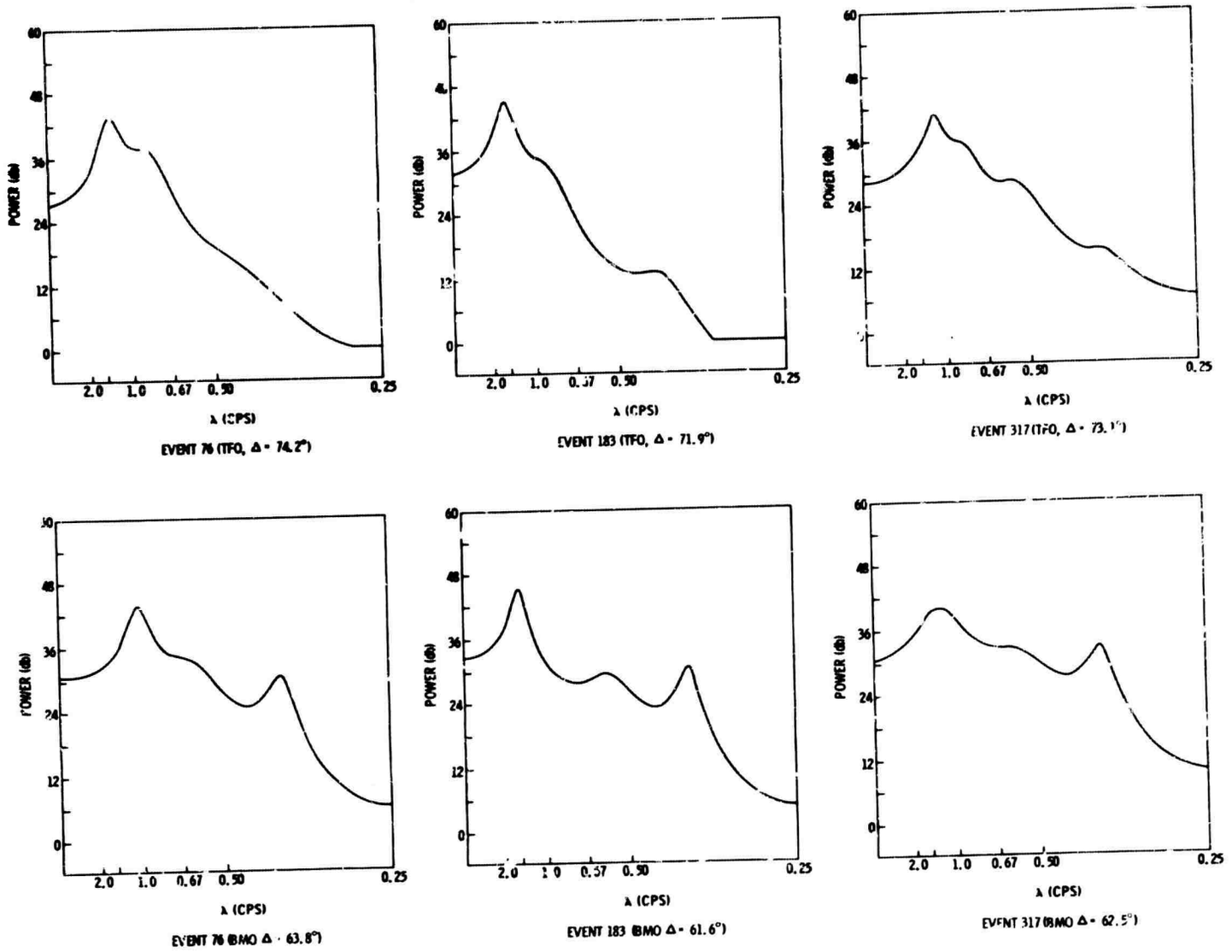

Figure D-21. Power Spectra of Events Recorded at TFO and BMO

Equation (12) represents the crustal operator for station i operating on the power density spectrum of event j, yielding the recorded power density spectrum at station i for event j.

The power density spectrum data may be used from n events to compute the average crustal operator for station i, according to the following equation:

$$g_i(f) = \frac{1}{n} \sum_{j=1}^{n} \frac{\Phi'_{ij}(f)}{\Phi_j(f)} \approx \frac{1}{n} \sum_{j=1}^{n} \frac{\Phi'_{ij}(f)}{\frac{1}{m} \sum_{j=1}^{m} \Phi_{ij}} \tag{13}$$

A third subscript added to Equation (12) to identify source region gives

$$\Phi'_{ijk}(f) = g_{ik}(f)\, \Phi_j(f) \tag{14}$$

Solving for the average crustal operator for station i, given power density spectrum data from n events,

$$\bar{g}_{ik}(f) = \frac{1}{n} \sum_{j=1}^{n} \frac{\Phi'_{ijk}(f)}{\Phi_j(f)} \approx \frac{1}{n} \sum_{j=1}^{n} \frac{\Phi'_{ijk}(f)}{\frac{1}{m} \sum_{i=1}^{m} \Phi'_{ij}} \tag{15}$$

The average crustal operator $\bar{g}_{ik}(f)$, as given in Equation (15), can be used to compute the portion of the energy arriving at the base of the crust at station i from source region k, which will be filtered out.

The average crustal operator, then, is a direct indicator of the errors introduced into magnitude calculations based on the energy arriving at station i and can be used to calculate a station magnitude correction factor.

Power density spectrum data from the six events processed in this study are used to calculate $\bar{g}_{ik}(f)$ for nine stations. The results are presented in Figure D-22. The magnitude calculated from a cycle of frequency f_c recorded at one of these nine stations may be corrected for station effects by being changed by an amount corresponding to the value of the magnitude correction at f_c for that station.

G. RECOMMENDATIONS

The following recommendations for further study are based on results of the present study:

- Digital processing techniques are shown to be of value in many areas of interest to seismology. Further investigation of these areas is severely limited because of lack of data recorded on magnetic tape, so a worldwide ensemble of stations equipped with magnetic tape recording instruments is recommended; such instrumentation would make digital processing techniques readily available for seismological research

- Based on discrepancies between LONGSHOT energy attenuation and the commonly accepted Q curves, revision of Q curves is recommended

- The average energy in the P packet, at least for LONGSHOT, was shown to be a reasonably well-behaved predictable function of distance; therefore, it is the expressed opinion that a magnitude scale based on average P energy would be superior to present scales based on the amplitude of a single cycle

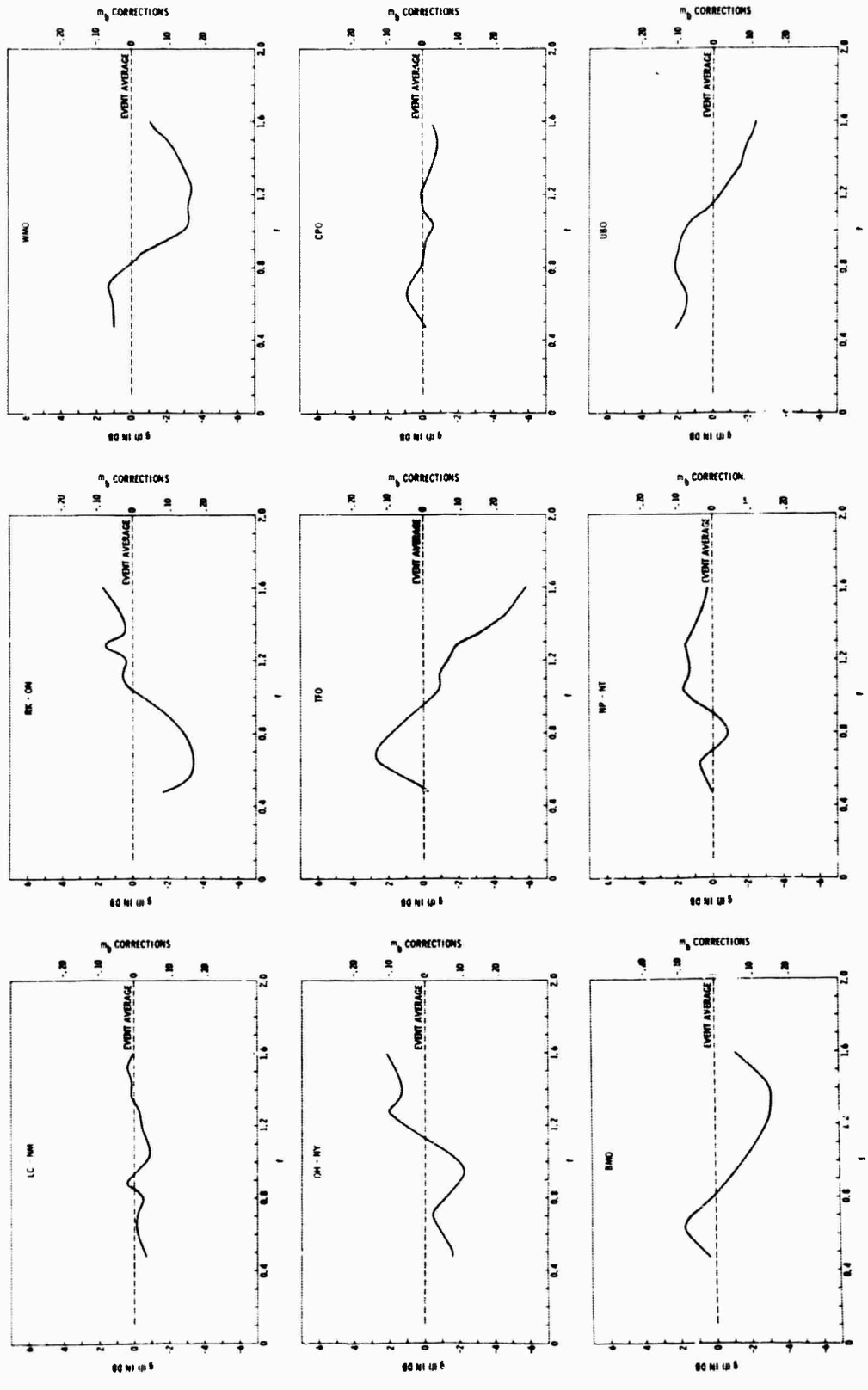

Figure D-22. Crustal Filters

APPENDIX E

REPORTS

APPENDIX E

REPORTS

A. SEMIANNUAL TECHNICAL REPORTS

1. No. I, 28 April 1965

The purpose of this first report is to introduce and establish the background for discussions to be presented in future reports. Since studies have shown there are errors in determining epicenters and depths of focus of seismic events, this report discusses development of techniques to be studied for improvement in determining epicenters, depths of focus, magnitudes, and annual number of seismic events, However, hypocenter determination is emphasized. A discussion of the data necessary for the study is also included.

2. No. II, 28 October 1965

This is a progress report concerning the determination of seismic event parameters such as size, number of occurrences, and accurate locations. Specifically, however, this report presents the accomplishments under Contract C-104-65 following the first semiannual report and observations concerning preliminary findings. Since the first report emphasizes determination, the bulk of this second report deals with hypocenter determination. Discussions of magnitude studies, seismicity evaluation, and two special studies of depth phases are also included.

3. No. III, 28 April 1966

This technical report shows the progress achieved toward accomplishing the objectives initiated in Contract C-104-65, reports the status of various studies, and states plans for completing the contract. Section II describes the data used and the status of data receipt and data reduction and handling. Section III treats the hypocenter determination program

and associated studies. Section IV discusses 1963 magnitude data investigation results and their impact on magnitude determinations for 1964 events, as well as the computer program to be used in calculating magnitudes for 1964 events. Section V discusses future plans and schedules for completing the current contract. The various topics detailed in the body of this report are summarized in Section I.

B. SPECIAL REPORTS

1. No. 1, Revaluation of Seismicity for 1960 and 1963

Included are revisions and corrections to previously published data. Data are prepared for comparison with 1964 seismicity as well as for combination with 1964 data to permit further statistical analysis. Interpretations of the 1960 and 1963 data are modified, revised, and supplemented.

2. No. 2, Correlation of Time Residuals with Magnitude

This report presents the results of an investigation to determine whether an empirical correlation may be observed between time residuals and magnitudes on a station/source-region basis. Results of a study concerning the value of the average time residual as a function of increasing magnitude are given. Included is a study to determine whether station/source-region time correlations expressed as a function of magnitude will increase the accuracy of hypocenter determinations.

3. No. 3, Depth Phases

The objectives of this report are to appraise the likelihood of identifying depth phases from paper seismograms and to evaluate differences in the reliability of various depth-indicator phases.

4. No. 4, Results of Worldwide Array Feasibility Investigation

The object of this report is to enhance the identification of

depth phases by combining single-trace recordings of short-period vertical seismograms (USC&GS Worldwide Standard Stations) in ensemble displays and applying some multichannel computer processing techniques to the ensembles.

5. No. 5, Method for Treating Cumulative Errors in Epicenter Determinations

The method which treats cumulative errors and time-residual patterns is studied to determine a theoretical epicenter shift toward the true location. The method is applied to data from LONGSHOT — a surface event with a computed depth of 57 km.

UNCLASSIFIED
Security Classification

DOCUMENT CONTROL DATA - R&D

(Security classification of title, body of abstract and indexing annotation must be entered when the overall report is classified)

1 ORIGINATING ACTIVITY (Corporate author)
Texas Instruments Incorporated
Science Services Division
P. O. Box 5621, Dallas, Texas 75222

2a REPORT SECURITY CLASSIFICATION
Unclassified

2b GROUP
—

3 REPORT TITLE
WORLDWIDE COLLECTION AND EVALUATION OF EARTHQUAKE DATA — TERMINAL REPORT

4 DESCRIPTIVE NOTES (Type of report and inclusive dates)
Terminal

5 AUTHOR(S) (Last name, first name, initial)
Fisher, Ray L.

6 REPORT DATE	7a TOTAL NO. OF PAGES	7b NO. OF REFS
31 August 1967	136	22

8a CONTRACT OR GRANT NO.	9a ORIGINATOR'S REPORT NUMBER(S)
C-104-65	—
b. PROJECT NO.	
ARPA No. 6207	9b OTHER REPORT NO(S) (Any other numbers that may be assigned this report)
c.	—
d.	

10 AVAILABILITY/LIMITATION NOTICES
—

11 SUPPLEMENTARY NOTES	12 SPONSORING MILITARY ACTIVITY
—	Advanced Research Projects Agency Department of Defense The Pentagon, Washington, D.C. 20301

13 ABSTRACT

This report discusses work performed under Contract C-104-65 from 28 April through 15 October 1966. During that period, the hypocenter and magnitude programs were tested and then used to process January 1964 data.

Results of this processing indicate that the relationship between m_b and M_s, restrained to a slope of 0.63, is given by $m_b = 0.63 M_s + 1.77$. Magnitudes comparable to m_b but based on long-period P amplitudes average approximately 0.7 units higher than m_b, and vertical-component surface-wave magnitudes average about 0.5 units higher than M_s. Analysis of magnitude residuals indicate that patterns of residuals exist and might be used to infer source mechanisms.

The ratio of maximum P to P_n amplitudes is a function of distance, with maxima generally between 300 to 750 km. Considerable variation from station to station leads to the conclusion that m_b is currently unreliable when based on data recorded less than 1000 km from the source.

DD FORM 1 JAN 64 1473

UNCLASSIFIED
Security Classification

14 KEY WORDS	LINK A		LINK B		LINK C	
	ROLE	WT	ROLE	WT	ROLE	WT
Worldwide Collection and Evaluation of Earthquake Data						

INSTRUCTIONS

1. ORIGINATING ACTIVITY: Enter the name and address of the contractor, subcontractor, grantee, Department of Defense activity or other organization *(corporate author)* issuing the report.

2a. REPORT SECURITY CLASSIFICATION: Enter the overall security classification of the report. Indicate whether "Restricted Data" is included. Marking is to be in accordance with appropriate security regulations.

2b. GROUP: Automatic downgrading is specified in DoD Directive 5200.10 and Armed Forces Industrial Manual. Enter the group number. Also, when applicable, show that optional markings have been used for Group 3 and Group 4 as authorized.

3. REPORT TITLE: Enter the complete report title in all capital letters. Titles in all cases should be unclassified. If a meaningful title cannot be selected without classification, show title classification in all capitals in parenthesis immediately following the title.

4. DESCRIPTIVE NOTES: If appropriate, enter the type of report, e.g., interim, progress, summary, annual, or final. Give the inclusive dates when a specific reporting period is covered.

5. AUTHOR(S): Enter the name(s) of author(s) as shown on or in the report. Enter last name, first name, middle initial. If military, show rank and branch of service. The name of the principal author is an absolute minimum requirement.

6. REPORT DATE: Enter the date of the report as day, month, year; or month, year. If more than one date appears on the report, use date of publication.

7a. TOTAL NUMBER OF PAGES: The total page count should follow normal pagination procedures, i.e., enter the number of pages containing information.

7b. NUMBER OF REFERENCES: Enter the total number of references cited in the report.

8a. CONTRACT OR GRANT NUMBER: If appropriate, enter the applicable number of the contract or grant under which the report was written.

8b, 8c, & 8d. PROJECT NUMBER: Enter the appropriate military department identification, such as project number, subproject number, system numbers, task number, etc.

9a. ORIGINATOR'S REPORT NUMBER(S): Enter the official report number by which the document will be identified and controlled by the originating activity. This number must be unique to this report.

9b. OTHER REPORT NUMBER(S): If the report has been assigned any other report numbers *(either by the originator or by the sponsor)*, also enter this number(s).

10. AVAILABILITY/LIMITATION NOTICES: Enter any limitations on further dissemination of the report, other than those imposed by security classification, using standard statements such as:

(1) "Qualified requesters may obtain copies of this report from DDC."

(2) "Foreign announcement and dissemination of this report by DDC is not authorized."

(3) "U. S. Government agencies may obtain copies of this report directly from DDC. Other qualified DDC users shall request through _____."

(4) "U. S. military agencies may obtain copies of this report directly from DDC. Other qualified users shall request through _____."

(5) "All distribution of this report is controlled. Qualified DDC users shall request through _____."

If the report has been furnished to the Office of Technical Services, Department of Commerce, for sale to the public, indicate this fact and enter the price, if known.

11. SUPPLEMENTARY NOTES: Use for additional explanatory notes.

12. SPONSORING MILITARY ACTIVITY: Enter the name of the departmental project office or laboratory sponsoring *(paying for)* the research and development. Include address.

13. ABSTRACT: Enter an abstract giving a brief and factual summary of the document indicative of the report, even though it may also appear elsewhere in the body of the technical report. If additional space is required, a continuation sheet shall be attached.

It is highly desirable that the abstract of classified reports be unclassified. Each paragraph of the abstract shall end with an indication of the military security classification of the information in the paragraph, represented as *(TS), (S), (C), or (U)*.

There is no limitation on the length of the abstract. However, the suggested length is from 150 to 225 words.

14. KEY WORDS: Key words are technically meaningful terms or short phrases that characterize a report and may be used as index entries for cataloging the report. Key words must be selected so that no security classification is required. Identifiers, such as equipment model designation, trade name, military project code name, geographic location, may be used as key words but will be followed by an indication of technical context. The assignment of links, rules, and weights is optional.